REINFORCEMENT OF EPOXIES BY BORON MINERALS

A THESIS SUBMITTED TO
THE GRADUATE SCHOOL OF NATURAL AND APPLIED SCIENCES
OF
MIDDLE EAST TECHNICAL UNIVERSITY

BY

YURDAER BABUÇCUOĞLU

IN PARTIAL FULFILLMENT OF THE REQUIREMENTS
FOR
THE DEGREE OF DOCTOR OF PHILOSOPHY
IN
POLYMER SCIENCE AND TECHNOLOGY

SEPTEMBER 2015

Approval of the thesis:

REINFORCEMENT OF EPOXIES BY BORON MINERALS

submitted by **YURDAER BABUÇCUOĞLU** in partial fulfillment of the requirements for the degree of **Doctor of Philosophy in Polymer Science and Technology Department, Middle East Technical University** by,

Prof. Dr. Gülbin Dural Ünver _____
Director, Graduate School of **Natural and Applied Sciences**
Prof. Dr. Necati Özkan _____
Head of Department, **Polymer Science and Technology**
Prof. Dr. Ali Usanmaz (deceased)
Prof. Dr. Teoman Tinçer _____
Supervisor, **Chemistry Dept., METU**
Assoc. Prof. Dr. Tonguç Özdemir _____
Co-Supervisor, **Chemical Eng. Dept., Mersin University**

Examining Committee Members:

Prof. Dr. Murat Şen _____
Chemistry Dept., Hacettepe University
Prof. Dr. Teoman Tinçer _____
Chemistry Dept., METU
Prof. Dr. Ahmet M. Önal _____
Chemistry Dept., METU
Assoc. Prof. Dr. Ali Çırpan _____
Chemistry Dept., METU
Asst. Prof. Dr. Elif Vargün _____
Chemistry Dept., Muğla Sıtkı Koçman University

Date: 09 / 09 / 2015

ABSTRACT

REINFORCEMENT OF EPOXIES BY BORON MINERALS

Babuçcuoğlu, Yurdaer
Ph.D., Department of Polymer Science and Technology
Supervisor: Prof. Dr. Teoman Tinçer
Co-Supervisor: Assoc. Prof. Dr. Tonguç Özdemir

September 2015, 126 pages

As polymers/fillers have shown much improved mechanical and thermal properties, the subject of epoxy resin reinforcement using boron minerals fillers has become valuable subject to study. The aim of this study is how boron minerals influence epoxy resins' mechanical and thermal properties under gamma irradiation.

The effects of boron on the mechanical and thermal properties of epoxy were studied in terms of mineral type, mineral loading concentration and irradiation dose in air and under vacuum. Bisphenol-A (DGEBA) type epoxy resin (Adriapox Special) was used. Calcined Tincal, Concentrated Tincal, Ground Colemanite, Anhydrous Borax were used as filler which contain B_2O_3 in different percentages.

The highest tensile strength (33 MPa at 2500 kGy by HDR) and the highest Young's modulus (1095 MPa at 500 kGy by LDR) were achieved for ECOL-1 sample. The mechanical behavior of epoxy-boron samples showed a periodical line with three stages as ''increment-decrement-increment' which was related to the competition reaction between chain scission and crosslinking during irradiation by γ –rays.

DMA results revealed that the reinforcement did not affecting the crosslinking process significantly where the increase in the T_g was consistent with the increasing in irradiation dose remarkably.

TGA results showed that the weight loss of the composites was due to the degradation of the epoxy where the decomposition temperature increased about 10 °C because of the boron minerals effects.

The change in the structure of the composites was affected by oxidation reaction and irradiation. The lack of adhesion between epoxy and boron minerals caused formation of weak zones to be cracked.

Keywords: Epoxy, boron minerals, gamma irradiation, crosslinking, chain-scission

ÖZ

EPOKSİLERİN BOR MİNERALLERİ İLE GÜÇLENDİRİLMESİ

Babuçcuoğlu, Yurdaer
Doktora, Polimer Bilimi ve Teknolojisi Bölümü
Tez Yöneticisi: Prof. Dr. Teoman Tinçer
Ortak Tez Yöneticisi: Doç. Dr. Tonguç Özdemir

Eylül 2015, 126 sayfa

Polimerler-katkı malzemeleri çok gelişmiş mekanik ve termal özellikler göstermelerinden dolayı, bor mineralleri takviyeli epoksi reçinelerin güçlendirmeleri konusu çalışılmaya değer bir konu haline gelmiştir. Bu çalışmanın amacı, gama ışınlaması altında bor minerallerinin epoksi reçinelerin mekanik ve termal özelliklerini nasıl etkilediğini görmektedir.

Epoksilerin mekanik ve termal özellikleri üzerine borun etkisi, mineral tipine, mineral yükleme konsantrasyonuna ve hava ile vakum altında ışınlama dozuna bağlı olarak incelenmiştir. Çalışmada, Bisfenol-A (DGEBA) tipi epoksi reçinesi (Adriapox Özel) kullanılmıştır. Farklı yüzdelerde B_2O_3 ihtiva eden Kalsine Tinkal, Konsantre Tinkal, Öğütülmüş Kolemanit ve Susuz Boraks katkı maddesi olarak kullanılmıştır.

En yüksek çekme mukavemeti (HDR tarafından 2500 kGy'de 33 MPa) ve en yüksek Young's modülü (LDR 500 kGy'de 1095 MPa) ECOL-1 numunesi için elde edilmiştir. Epoksi-bor numunelerinin mekanik davranışları γ-ışınlaması süresince oluşan zincir kırılması ve çapraz bağlanma reaksiyonları arasındaki oluşum

rekabetine bağlı olarak 'artan-azalan-artan" şeklinde üç basamaklı bir periyodik davranış göstermektedir.

DMA sonuçlarına göre takviye malzemesinin çapraz bağlanma üzerinde dikkat çekici etkisi olmadığı görülmekle birlikte ışınlama dozundaki artışın Tg artışına etkisi görülmektedir.

TGA sonuçlarına göre kompozitlerin kütle kaybının epoksi bozunmasına bağlı olduğu görülmektedir. Bozunma sıcaklığındaki 10 °C'lik artışın sebebi ise bor mineralleridir.

Kompozitlerin yapısındaki değişiklik oksidasyon reaksiyonu ve ışınlama ile etkilenmektedir. Epoksi ve bor mineralleri ara yüzeyindeki bağlanma eksikliği, kırıklar oluşan zayıf bölgelerin meydana gelmesine neden olmuştur.

Anahtar Kelimeler: Epoksi, bor mineralleri, ışınlama, çapraz bağlanma, kompozit

to my twins: *Cansu* and *Canatan*

(in memory of Prof.Dr.Ali Usanmaz)

ACKNOWLEDGEMENTS

I wish to express my sincere appreciation to my supervisors Prof. Dr. Ali Usanmaz and Prof. Dr. Teoman Tinçer for their guidance, advice, encouragement and insight throughout this study. Their positive approach and politeness always made me focused on my study.

I am also grateful to my co-supervisor Assoc. Prof. Dr. Tonguç Özdemir. He is such a mentor and brother to me and his supports and critiques helped me doing my best in almost every stage of this work. I also give my special thanks to and Asst. Prof. Dr. Elif Vargün for her support, suggestions and critiques. This study found its way by their guidance.

I should mention my laboratory mates Aydın Mert Akgün and Fırat Hacıoğlu from 'Prof. Dr. Ali Usanmaz Research Group' for their help and suggestions. I would like to thank Prof. Dr. Uğur Adnan Sevil from Hitit University for his help in the irradiation procedure of samples. Besides, I would also like to express my acknowledgments to Ümit Tayfun and technician Osman Yaslıtaş in Chemistry Department for their assistance and guidance to me during experimental work.

I am also thankful to staff from Graduate School of Natural and Applied Sciences for their patience and politeness during my study.

Grateful thanks go to my wife Arzu Babuçcuoğlu for her unlimited support, patience and love during this work.

The last but not least, I would like to extend my gratitude to my family for their endless love and support in every step of my life. I could not achieve any of these without their support and belief in me.

TABLE OF CONTENTS

ABSTRACT……...v

ÖZ……....vii

ACKNOWLEDGEMENTS…….....x

TABLE OF CONTENTS……...xi

LIST OF TABLES…….xiv

LIST OF FIGURES……..... xvi

LIST OF SYMBOLS AND ABBREVATIONS……..xx

CHAPTERS

1. INTRODUCTION……..... 1

1.1. Epoxy……..…..……..1

1.2. Reinforcement of Polymers……..…..……6

1.2.1. Literature Survey About Epoxy Reinforcement…… 7

1.3. Irradiation of Polymers……..……9

1.3.1. Literature Survey About Irradiation of Epoxy……11

1.4. Boron and Boron Minerals……..13

1.5. Aim of The Study……..……. 14

2. EXPERIMENTAL…… 17

2.1. Materials…….……..….. 17

2.1.1. Epoxy Resin……...… 17

2.1.2. Boron Minerals……..17

2.1.3. Epoxy-Boron Polymers……18

2.2. Irradiation…….…… 20

2.2.1. Low Dose Rate Irradiation…… 20

2.2.2. High Dose Rate Irradiation……...…… 20

2.2.3. High Dose Rate Irradiation in vacuum……..… 21

2.3. Characterization of samples…...…….……22

2.3.1. Curing Temperature Comparison……..…22

2.3.2. Water Absorption Test……..… 22

2.3.3. Tensile Tests……...23
2.3.4. Attenuated Total Reflection Fourier Transform Infrared (ATR-FTIR)…….……24
2.3.5. Dynamic Mechanical Analysis (DMA)…….…25
2.3.6. Thermogravimetric Analysis (TGA)……..……...… 26
2.3.7. Field Emission Scanning Electron Microscopy (FE-SEM)...…..27
3. RESULTS AND DISCUSSION……..…….…….. 29
3.1. Non-Irradiated Samples…….…….….. 29
3.1.1. Curing Temperature Comparison…….……..… 30
3.1.2. Water Absorption Test…….…….…… 35
3.2. Irradiated Samples…….…….….. 37
3.2.1. Mechanical Test……44
3.2.1.1. Mechanical Tests for Neat Epoxy (EPO)……..…..….44
3.2.1.2. Mechanical Tests for Epoxy-Calcined Tincal (ECAT)..... 53
3.2.1.3. Mechanical Tests for Epoxy-Concentrated Tincal (ECOT)…….….. 59
3.2.1.4. Mechanical Tests for Epoxy-Colomanite (ECOL)……...…… 66
3.2.1.5. Mechanical Tests for Epoxy-Anhydrous Borax (EANB)……..…….71
3.2.1.6. Summary of Mechanical Tests ……..…..77
3.2.2. Attenuated Total Reflection Fourier Transform Infrared (ATR-FTIR)……..……78
3.2.2.1. ATR-FTIR Results of Boron Minerals…….…78
3.2.2.2. ATR-FTIR Results of Neat Epoxy Samples……..…….. 81
3.2.2.3. ATR-FTIR Results of Epoxy-Boron Samples…….….83
3.2.3. Dynamic Mechanical Analysis (DMA)…….…… 88
3.2.4. Thermogravimetric Analysis (TGA)…….…… 90
3.2.5. Scanning Electron Microscopy (SEM)…….…… 93
4. CONCLUSION……..……. 101
REFERENCES…….. 103
APPENDICES A. Chemical Compositions of Epoxy Components……... 121

APPENDICES B. Contents of Boron Minerals Used In This Study……..123
B.1: Contents of Etibor-68 (Anhydrous Borax)……123
B.2: Contents of Calcined Tincal……. 123
B.3: Contents of Concentrated Tincal……...124
B.4: Contents of Ground Colemanite……124
CURRICULUM VITAE……125

LIST OF TABLES

TABLES

Table 2.1: Boron Minerals Used in This Study……18
Table 2.2: Epoxy – Boron Polymer Compositions…….. 19
Table 2.3: Dose rates and absorbed dose (kGy) values for irradiated samples…….21
Table 3.1: Young's Modulus of the epoxy samples cured at different temperatures……..…….. 30
Table 3.2: Water absorption capacity of the non-irradiated epoxy samples with different boron-minerals……..……...36
Table 3.3: Young's Modulus, tensile strength and elongation at break for EPO as a function of absorbed dose ……..47
Table 3.4 Young's Modulus of Non-irradiated EPO samples as a function of curing temperatures……..…. 51
Table 3.5 Young's Modulus, tensile strength and elongation at break for ECAT as a function of absorbed dose ……..54
Table 3.6: Young's Modulus of Non-irradiated ECAT samples as a function of curing temperatures ……..... 58
Table 3.7: Young's Modulus of Non-irradiated ECOT as a function of curing temperatures ……..... 60
Table 3.8: Young's Modulus, tensile strength and elongation at break for ECOT as a function of absorbed dose ……..……62
Table 3.9: Young's Modulus of Non-irradiated ECOL samples as a function of curing temperatures ……..... 66
Table 3.10: Young's Modulus, tensile strength and elongation at break for ECOL as a function of absorbed dose ……...67
Table 3.11: Young's Modulus of Non-irradiated EANB samples as a function of curing temperatures ……..……71

Table 3.12: Young's Modulus, tensile strength and elongation at break for EANB as a function of absorbed dose …….. 73
Table 3.13: ATR-FTIR absorption bands of DGEBA resin……..81
Table 3.14: T_g comparison of neat-epoxy at different irradiation doses and non-irradiated epoxy-boron samples……89
Table 3.15: Effect of Filler Ratio on Mechanical Properties of Epoxy-Boron Composites……..99
Table A.1: Chemical Compositions of Epoxy Components……...… 121
Table B.1: Contents of Etibor-68 (Anhydrous Borax)…… 123
Table B.2: Contents of Calcined Tincal…….. 123
Table B.3: Contents of Concentrated Tincal……... 124
Table B.4: Contents of Ground Colemanite…… 124

LIST OF FIGURES

FIGURES

Figure 1.1: The epoxide group structure……..…… 1
Figure 1.2: Curing Process of Thermosetting Polymers……..… 2
Figure 1.3: Structures of Bisphenol A, Epichlorohydrin, Diglycidyl ether of bisphenol-A (DGEBA) and the reaction mechanism. ……..…… 4
Figure 1.4: Reaction of DGEBA and poly functional amine. ……..…… 5
Figure 1.5: Network structure of epoxy resin.……..…… 6
Figure 2.1: Epoxy Reinforcement Procedure.……..…… 19
Figure 2.2: Lloyd Instruments LR 5K Universal Testing Machine……..…… 23
Figure 2.3: Dog-bone shaped dimensions of ASTM D638 Type IV…… 24
Figure 2.4: Thermo Nicolet iS10 ATR-FTIR Spectrometer…… 25
Figure 2.5: Perkin Elmer Pyris Diamond DMA…….…….. 26
Figure 2.6: LECO TGA701 Thermogravimetric Analyzer…….……. 26
Figure 2.7: Zeiss Supra 55 model FE-SEM…….…… 27
Figure 3.1: Color differences of the EPO samples as a function of curing temperature ……..……. 31
Figure 3.2: Color differences of the ECAT samples as a function of boron mineral loading (at 120 ºC) ……..…….…….....31
Figure 3.3: Color differences of the ECAT samples as a function of boron mineral loading (at 200 ºC) ……..……..……... 32
Figure 3.4: Color differences of the ECOL samples as a function of boron mineral loading (at 120 ºC) ……..……..…… 32
Figure 3.5: Color differences of the ECOL samples as a function of boron mineral loading (at 200 ºC) ……..……..…….32
Figure 3.6: Color differences of the ECOT samples as a function of boron mineral loading (at 120 ºC) ……..……..…….33

Figure 3.7: Color differences of the ECOT samples
as a function of boron mineral loading (at 200 ºC)……..…..……...33
Figure 3.8: Color differences of the EANB samples
as a function of boron mineral loading (at 120 ºC) ……..…….…… 33
Figure 3.9: Color differences of the EANB samples
as a function of boron mineral loading (at 200 ºC) ……..…….…… 34
Figure 3.10: Color differences of the EPO samples
as a function of absorbed dose ……39
Figure 3.11: Color differences of the ECAT samples
as a function of absorbed dose ……40
Figure 3.12: Color differences of the ECOL samples
as a function of absorbed dose ……... 41
Figure 3.13: Color differences of the ECOT samples
as a function of absorbed dose ……....42
Figure 3.14: Color differences of the EANB samples
as a function of absorbed dose ……43
Figure 3.15: Young's Modulus, tensile strength and elongation at break
for EPO as a function of absorbed doses by LDR in air…… 48
Figure 3.16: Young's Modulus, tensile strength and elongation at break
for EPO as a function of absorbed doses by HDR in air……....49
Figure 3.17: Young's Modulus, tensile strength and elongation at break
for EPO as a function of absorbed doses by VHDR under vacuum……..…… 50
Figure 3.18: Young's Modulus of Non-irradiated EPO samples as a function of
curing temperature ……..…….. 52
Figure 3.19: Young's Modulus, tensile strength and elongation at break
for ECAT as a function of absorbed doses by LDR in air……..…….. 55
Figure 3.20: Young's Modulus, tensile strength and elongation at break
for ECAT as a function of absorbed doses by HDR in air……..…….. 56
Figure 3.21: Young's Modulus, tensile strength and elongation at break
for ECAT as a function of absorbed doses by VHDR under vacuum……..……..57
Figure 3.22 Young's Modulus of Non-irradiated ECAT samples as a function of
curing temperature ……..…….. 58

Figure 3.23: Young's Modulus of Non-irradiated ECOT samples as a function of curing temperature ……..……...59
Figure 3.24: Young's Modulus, tensile strength and elongation at break for ECOT as a function of absorbed doses by LDR in air……..……63
Figure 3.25: Young's Modulus, tensile strength and elongation at break for ECOT as a function of absorbed doses by HDR in air……64
Figure 3.26: Young's Modulus, tensile strength and elongation at break for ECOT as a function of absorbed doses by VHDR under vacuum……..……..65
Figure 3.27: Young's Modulus of Non-irradiated ECOL samples as a function of curing temperature ……..…….. 66
Figure 3. 28: Young's Modulus, tensile strength and elongation at break for ECOL as a function of absorbed doses by LDR in air……..……... 68
Figure 3.29: Young's Modulus, tensile strength and elongation at break for ECOL as a function of absorbed doses by HDR in air……..……69
Figure 3.30: Young's Modulus, tensile strength and elongation at break for ECOL as a function of absorbed doses by VHDR under vacuum……..……..70
Figure 3.31: Young's Modulus of Non-irradiated EANB samples as a function of curing temperature ……..……...72
Figure 3.32: Young's Modulus, tensile strength and elongation at break for EANB as a function of absorbed doses by LDR in air……..……...74
Figure 3.33: Young's Modulus, tensile strength and elongation at break for EANB as a function of absorbed doses by HDR in air……..……...75
Figure 3.34: Young's Modulus, tensile strength and elongation at break for EANB as a function of absorbed doses by VHDR under vacuum……...76
Figure 3.35: ATR-FTIR spectrum of Boron Minerals……..80
Figure 3.36: ATR-FTIR spectrum of EPO with different irradiations…….... 82
Figure 3.37: FTIR spectrum of ECAT-2,5 samples……..84
Figure 3.38: FTIR spectrum of ECOT-2,5 samples……. 85
Figure 3.39: FTIR spectrum of EANB-2,5 samples……. 86
Figure 3.40: FTIR spectrum of ECOL-2,5 samples……. 87
Figure 3.41: DMA results comparison of neat-epoxy as a function of absorbed doses and non-irradiated epoxy-boron samples…….. 89

Figure 3.42: TGA curves of neat-epoxy as a function of absorbed doses, neat calcined tincal, neat concentrated tincal, ECAT-2.5-non-irradiated and ECOT-2.5-non-irradiated samples……... 91
Figure 3.43: TGA curves of neat-epoxy as a function of absorbed doses, neat calcined tincal, neat concentrated tincal, EANB-2.5-non-irradiated and ECOL-2.5-non-irradiated samples…… 92
Figure 3.44: FE-SEM images of non-irradiated neat-epoxy sample…….... 94
Figure 3.45: FE-SEM images neat-epoxy sample irradiated with 50 kGy by LDR……..... 94
Figure 3.46: FE-SEM images of non-irradiated ECOT-1 sample……..…. 95
Figure 3.47: FE-SEM images of ECOT-1 sample irradiated with 50 kGy by LDR ……..….. 95
Figure 3.48: FE-SEM images of non-irradiated ECOT-5 sample……...… 96
Figure 3.49: FE-SEM images of ECOT-5 sample irradiated with 50 kGy by LDR ……..…...96
Figure 3.50: FE-SEM images of non-irradiated EANB-1 sample……97
Figure 3.51: FE-SEM images of EANB-1 sample irradiated with 50 kGy by LDR ……..….. 97
Figure 3.52: FE-SEM images of non-irradiated EANB-5 sample……98
Figure 3.53: FE-SEM images of EANB-5 sample irradiated with 50 kGy by LDR ……98
Figure 3.54: Effect of Filler Ratio on Mechanical Properties of Epoxy-Boron Composites……..99

LIST OF SYMBOLS AND ABBREVATIONS

BPA: Bisphenol A

ECH: Epichlorohydrin

DGEBA: Diglycidyl ether of bisphenol-A

EPO: Neat Epoxy

COT: Concentrated Tincal

CAT: Calcined Tincal

COL: Colemanite

ANB: Anhydrous Borax

ECOT: Epoxy-Concentrated Tincal Composite

ECAT: Epoxy-Calcined Tincal Composite

ECOL: Epoxy-Colemanite Composite

EANB: Epoxy-Anhydrous Borax Composite

Gy - kGy: Gray - Kilogray

LDR: Low dose rate irradiation

HDR: High dose rate irradiation

VHDR: High dose rate irradiation in vacuum

MPa: Megapascal

T: Temperature at which measurements carried out

°C: Degree Celsius

DMA: Dynamic Mechanical Analysis

T_g: Glass transition temperature, °C

TGA: Thermogravimetric Analysis

ATR-FTIR: Attenuated Total Reflection Fourier Transform Infrared Spectroscopy

SEM: Scanning Electron Microscopy

CHAPTER 1

INTRODUCTION

1.1. Epoxy

Epoxide is a three atom cyclic ring. A compound containing the epoxide functional group can be called as epoxy, epoxide, oxirane and ethylene oxide. Epoxy resins contain epoxide group (Figure 1.1) [1].

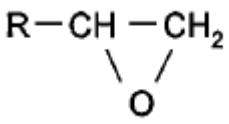

Figure 1.1: The epoxide group structure [1].

Epoxy resin is one of the functional chemical of the polymers. Epoxy resins were first synthesized by Pierre Castan in Switzerland, meantime by S.O. Greenlee in USA late in the 1930s [2].

Epoxy resins are thermosetting polymers such as phenolic and polyester resins. Epoxy resins are formed in a network structure. By contrast with thermoplastics, as an outcome of chemical reactions, firstly epoxy resins increase in viscosity and finally have a crosslink structure and become set. This final form cannot change by flow or dissolve anymore.

Thermosetting polymers include curing reactions. Figure 1.2 shows two-dimensional representation of thermosetting polymers curing process [3]. This process begins with uncured monomers and oligomers. Linear chain becomes growing with branching of chains occurs. During these reaction proceeds molecular weight increases that makes the viscosity increased. Also total number of molecules decreased. The process continues with the gel formation with incompletely crosslink network structure. Finally there are several chains occurred to be linked together where fully curing ended.

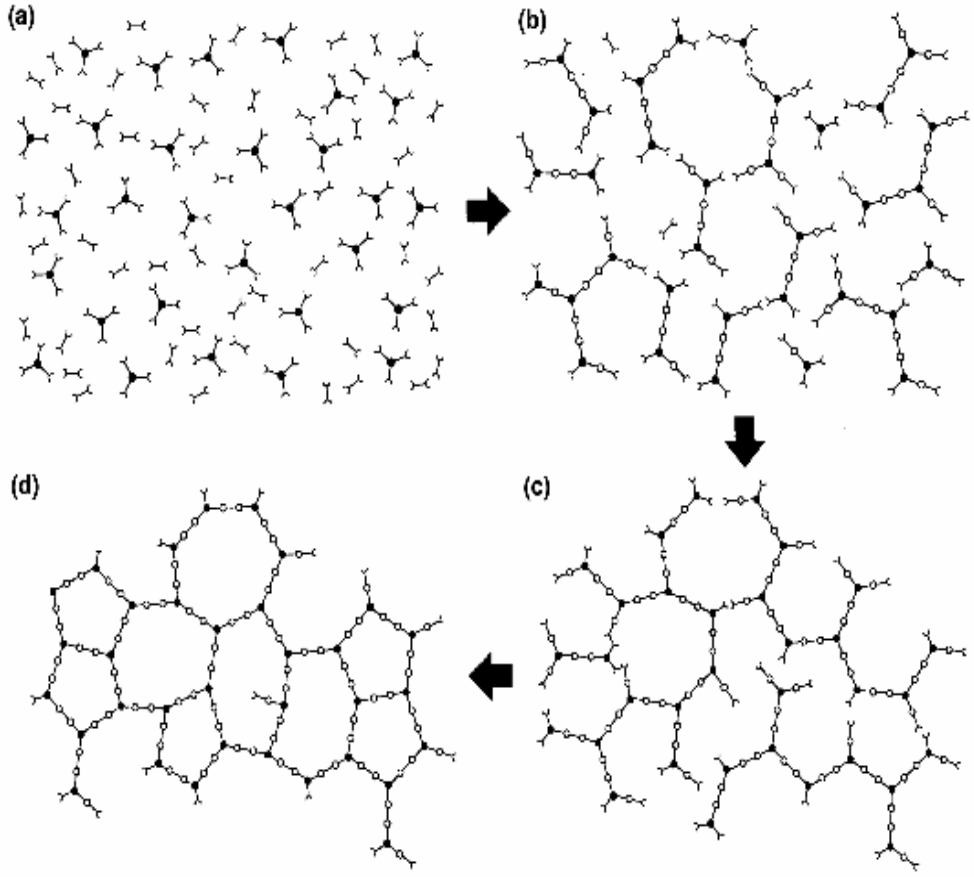

Figure 1.2: Curing Process of Thermosetting Polymers [3].

Thermosetting polymers become tough, hard, 3-dimensional network structured materials. It can be said that the movement of one molecule in any direction is opposed by the crosslinking arrangement.

On the other side, thermoplastic polymers such as polyethylene (PE) and polyvinyl chloride (PVC) may be thought of as compounds composed of long linear chains lying together in all three dimensions without interconnection. Thus, molecular motion in any direction is not restricted.

The basic difference between the crosslinking structures as thermosets and non-crosslinking structures as thermoplastics is the behavior against heat. Thermosets retain their final structure in solid state where thermoplastics can be re-melted with heat back into the initial structure.

BPA (called bisphenol A; bis (4-hydroxy phenylene)-2,2 propane) and ECH (called epichlorohydrin; 1-chloroprene 2 oxide) are the most used chemicals react under sodium hydroxide ambient give the most known epoxy monomer [4]. These monomers called as diglycidyl ether of bisphenol-A (DGEBA). The structures of Bisphenol A, Epichlorohydrin, DGEBA and the reaction mechanism are shown in Figure 1.3.

BPA is the product of the reaction of phenol and acetone in a strongly acidic media [5]. BPA is mostly used for polycarbonate plastics and epoxy resins production.

Epichlorohydrin (ECH) is an organochlorine compound and an epoxide. It is a colorless, mobile liquid having irritating chloroform-like odor. It is a highly reactive compound and used widely in the production of plastics, epoxy resins and elastomers.

Epoxy polymers are the products of the reaction of epoxy monomers with co - monomers such as hardeners as curing agents. This reaction can be a step or a chain

polymerization or both step or chain polymerizations combination. There are several types of curing agents used as hardeners but amines are the mostly used.

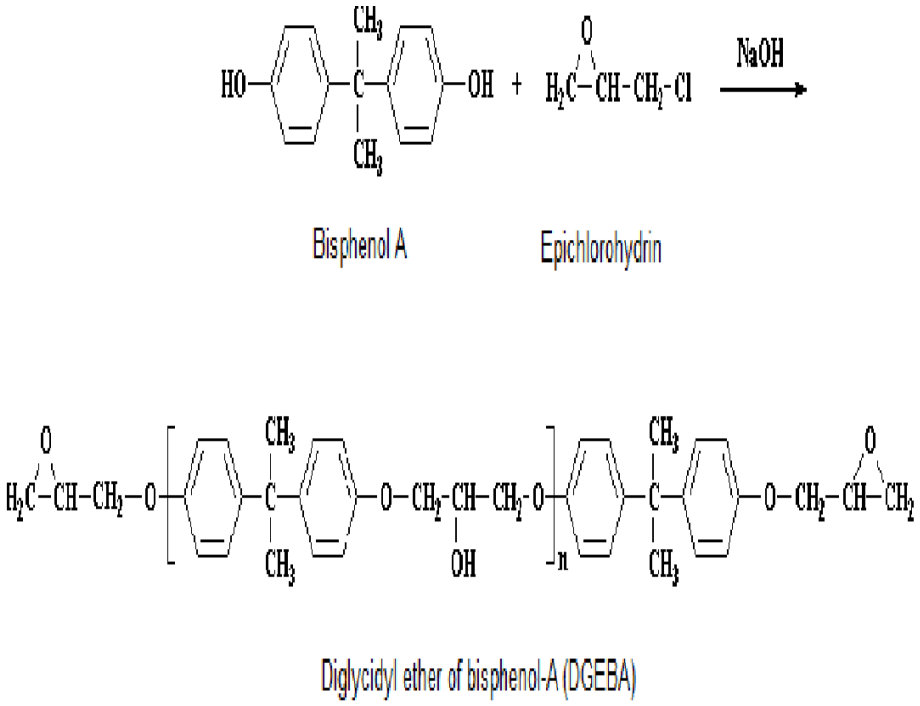

Figure 1.3: Structures of Bisphenol A, Epichlorohydrin, Diglycidyl ether of bisphenol-A (DGEBA) and the reaction mechanism [4].

The n in the final product, DGEBA, represents the number of times the repeating unit in the structure (Figure 1.3). DGEBA is a viscous liquid where n is equal to 0 or 1 but DGEBA is a brittle solid if n > 1.

Figure 1.4 illustrates the crosslinking or curing mechanism of epoxy monomer (DGEBA) and hardener (poly functional amine). The final product of the reaction is solid.

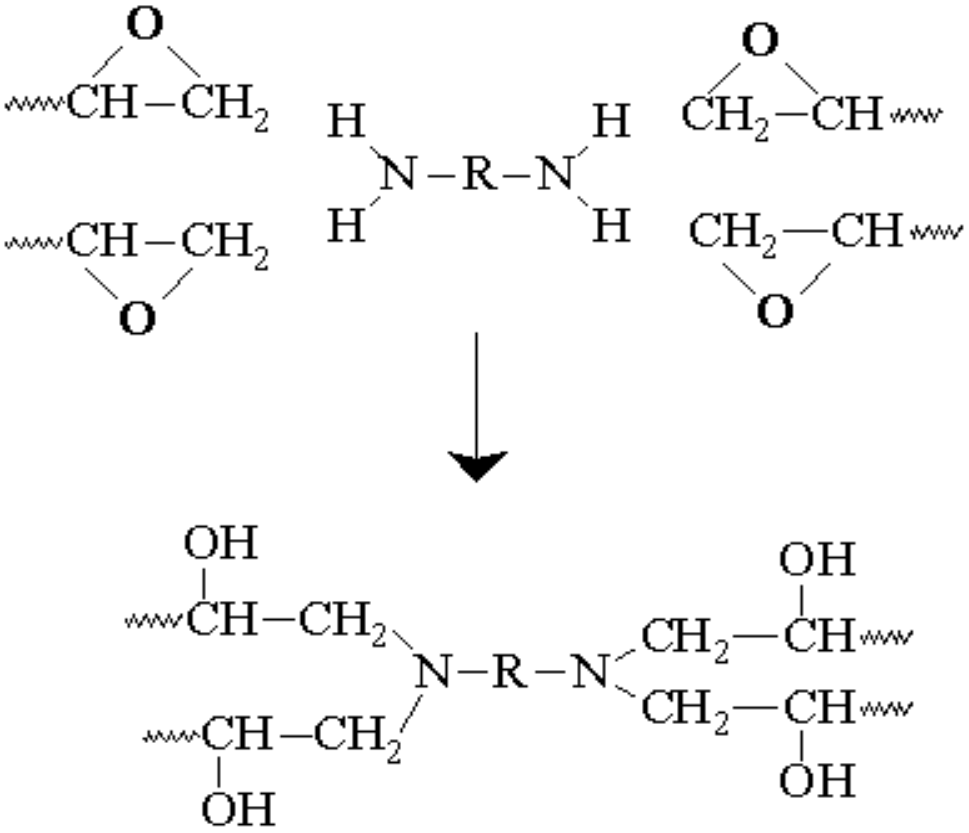

Figure 1.4: Reaction of DGEBA and poly functional amine.

The epoxy prepolymers are tied by adding diamine. The number of epoxy groups which can react with amines depends on the number of hydrogen atoms on the amine group. One of the amine groups on the other end of the diamine is also able to react with two epoxy groups.

Figure 1.4 shows that four epoxy prepolymers connected to one diamine molecule at the end of the reaction. The other amine groups are attached to ends of the diepoxy prepolymers and finally the big cross-linked network structure occurred by the connection of epoxy and amine molecules. Figure 1.5 illustrated the Network structure of epoxy resin.

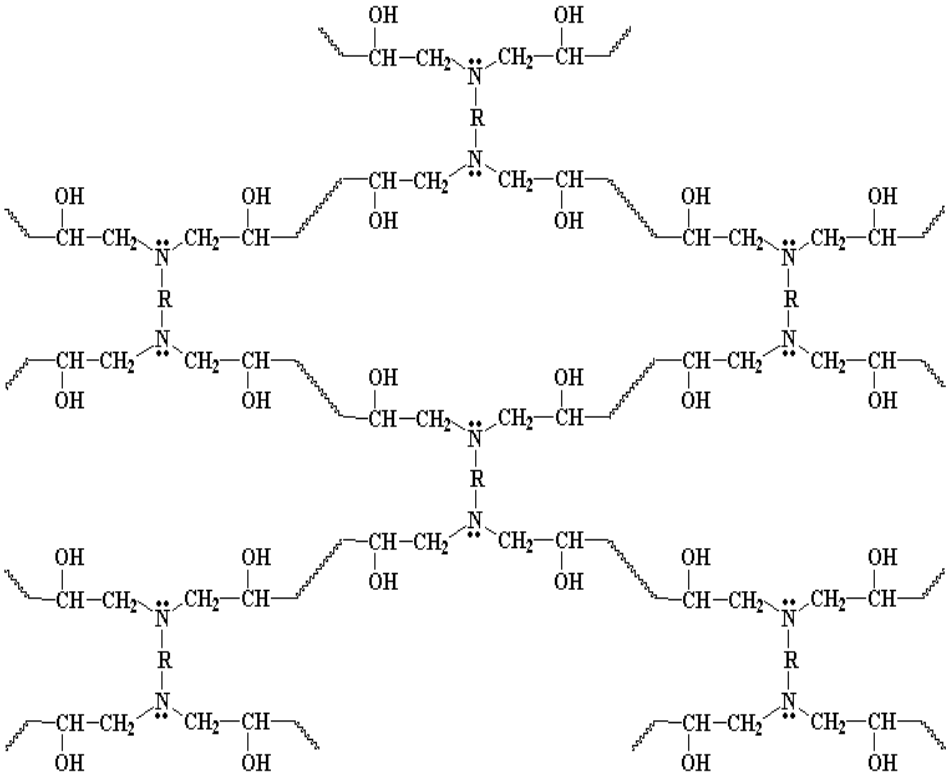

Figure 1.5: Network structure of epoxy resin.

1.2. Reinforcement of Polymers

Most polymeric materials are not a single polymer, but they contain chemicals added to them to modify some physical, biological and/or chemical behavior [6]. These modifications generate new materials with new properties. Particulate fillers or fiber reinforcement are generally incorporated with thermosetting polymers to reduce cost, to modify physical, chemical and mechanical properties. Because of good attributes of thermosetting polymers such as good dimensional stability, thermal stability, chemical resistance, they are used in several applications such as appliance, construction, electrical distribution, energy etc.

The American Society for Testing and Materials standard ASTM D-883, defines fillers as materials added to plastics to reinforce the properties such as strength, permanence or others to lower costs. The fillers added into the reinforced plastics give some strength properties better than the initial plastic structure.

The composite materials or called composites shortly are produced by the reaction of two or more organic or inorganic components which have different physical or chemical properties significantly. The final product have distinctively different properties, too. One component named as a "matrix", which holds everything together, while the other component named as reinforcing material, embedded into the matrix.

Until recently, epoxides, bismaleimides or polyimides are the most common matrix components as "thermosetting" materials where glass fiber, boron & its fiber or carbon fiber are the reinforcing materials. Clay is one of the geological material used as reinforcing material [8,9]. The reinforcing applications are for different purposes such as to improve mechanical properties of polymers [10-12, 16, 17, 19-22], to give thermal resistance and flame retardancy [13-15, 18].

Sporting goods industry is one of the common areas that epoxy-boron composites have been used. Especially because of its good mechanical and thermal properties, boron-fiber in metal matrix composites is used (MMC) more than carbon fiber [7].

1.2.1 Literature Survey About Epoxy Reinforcement

There are so many studies about epoxy resins and reinforcement of epoxy resins with different types of additives to investigate the effects of the reinforcement on mechanical and thermal properties of epoxy resins.

In the study of Pinnavaia the properties of a kind of porous synthetic clay, saponite (SAP) was used to improve the rubbery and glassy structured epoxy polymers [8]. In the study, the diglycidyl ethers of bisphenol A (DGEBA), and

polyoxypropylene diamines were used to produce glassy and rubbery structured epoxy matrices. X-ray diffraction (XRD), transmission electron microscopy (TEM), NMR spectra, tensile mechanical properties, Dynamic mechanical analysis (DMA) were used for the characterization studies. It was mentioned that strength and toughness was provided by disordered clay tactoids. The usage of clay gave cost efficiency by eliminating the usage of an organic modifier.

Iroh et. al. studied the reinforcement of corrosion resistant clay/epoxy ester composite coatings and thin films by adding cloisite 15A clay [9]. The reinforcement study showed a remarkable increase in the glass transition temperature, Tg by adding cloisite.

Fu and friends studied the reinforcement of ether of bisphenol-F epoxy resins by using multi-walled carbon nanotubes (MWCNTs) to modify the cryogenic mechanical properties [10]. The results suggested that appropriate contents of CNTs improved the cryogenic mechanical properties such as tensile strength, Young's modulus, and impact strength. The results showed that the reinforced epoxy resin has good potential to be used in applications of cryogenic engineering areas.

In the study of Yousif and friends, reinforced flexural properties of epoxy were investigated by using unidirectional long kenaf fibre (LKF) [11]. The results showed that treated LKF increased the flexural strength of the epoxy by about 36%, while, untreated fibres increased about 20%.

Exner et. al. studied the bohemite nanoparticles with various surface modifications to produce functional cross-linking agents for epoxy resin material [12]. The epoxy resin composite material was tested with various modified bohemite fillers and characterized for chemical bonding, bending behavior and thermal properties. Various surface modification studies showed a significant influence on the viscosity. The results showed an adverse effect of network interruption because of the the nano particles and stiffness effect of ceramic fillers.

Hu and friends studied the thermal degradation and flame retardancy of epoxy resins affected by borates [13]. The borate used was tris (2-hydroxypropyl) borate

(THPB) and curing agent used was octaaminophenyl POSS (OapPOSS). The final epoxy resin composite reinforced with THPB and OapPOSS showed good flame retardancy property.

Al-Turaif studied the reinforcement of nano TiO_2 particles on mechanical properties of cured epoxy resin [22]. In this study, two different nano-sized TiO_2 (17nm and 50 nm) with various fractions (1%, 3%, 5% and 10% w/w) were used to investigate mechanical properties of toughened epoxy resin. Results showed that loading of small fraction of TiO_2 particles enhanced mechanical properties of epoxy composite. Also it was found that the size parameter of the TiO_2 nano-particles influenced the flexural stress by mean of tensile properties.

1.3. Irradiation of Polymers

Since 1960s, radiation chemistry has been studied remarkably in polymer research. The ionization and radical formation of the polymers occurred under high energy radiation produced by electron beams and x- or beta rays [23].

Various types of reactions occurred such as crosslinking, chain scission (degradation), disproportionation decrease in molecular weight, hydrogen abstraction and formation of new bonds in polymer structure, depending on the chemical formation of the polymer matrix, additives, temperature and irradiation conditions (high or low dose rate, presence of oxygen) [24-25]. Also the formation of peroxides is possible in the presence of oxygen. These trapped peroxides, ions or radicals induce post-irradiation reactions.

Various types of irradiation sources are used depending on the desired applications. High energy radiation is used for polymerization initiation but low energy radiation is used limitedly on the surface treatment because of the less energy delivered.

The major advantages of irradiation are: (i) the desired reactions may occur at lower temperatures, (ii) catalyst contamination can be obstructed during polymerization of monomers, (iii) crosslinking can be performed during fabrication, (iv) coatings can be performed over monomeric form without solvents [26].

The major fields of irradiation studies of polymers are insulation [27-32,35,40,42], radiation shielding [33,34,37,44,46], polymeric material modification [36,38-41,43,45]. By gamma or electron irradiation, the properties of polymers such as heat resistance and strength are increased where stress cracking, permeability are decreased. On the other hand with low energy irradiations using ultraviolet light, surface improvements, such as weather resistance, hardening, dyeability, or destaticizing are improved.

γ- and β-ray emitters are the common radioactive sources used commercially. Cobalt-60, strontium-90, and cesium-137 are the most preferred sources due to their useful characteristics, reasonably long half-life, availability, and cost [10].

Ionizing radiation (gamma rays and high-energy electrons) is practical way to convert monomers and oligomers from liquid form into solid form. Meantime, there occur major changes in properties of the solid polymers [47].

Polymers are organic molecules which contain susceptible bonds such as C-C, C-H, C-O to radiation [48]. These susceptible bonds are excited by ionizing radiation. Excited bonds result in bond cleavage and radicals formation. Then, formed radicals cause reactions in polymer matrix. The polymer chain is effected as constructive (crosslinking) and destructive (degradation) by virtue of the ionizing radiation at the end of these reactions [49]. Six different reactions are caused by ionizing radiation on polymers [48, 49]. These are (a) recombination reactions, (b) cross-linking, (c) chain scission, (d) formation of volatile products, (e) formation of peroxy radicals in presence of oxygen and (f) unsaturation production or deterioration.

Crosslinking and chain scission are classified as primary reactions and occur in the structure of the polymers at the same time during radiation [48, 50]. One of these reactions rule overs numerically in the structure and this domination determines whether or not the polymer is crosslinkable or degradable under ionizing radiation [48, 50].

In crosslinkable polymers, scission reactions and crosslinking reactions occur in the main chain. Scission reactions take place in the C-H bonds where hydrogens in C-H bonds are ruptured by the effect of radiation and newly formed radicals are connected to each other at their radicalic sites [51]. But in degradable polymers, scission reactions take place both in the C-H bonds and in the main chain (i.e. C-C bond cleavage). Therefore, in degradable polymers, molecular weight decreasing and depletion in the chemical and the mechanical properties are observed [51].

1.3.1 Literature Survey About Irradiation of Epoxy

Humer et. al. studied the effect of irradiation on the mechanical properties of insulators used for fusion magnets [27]. In the study, types of magnet insulation systems consist of boron-free glass fiber reinforcement materials in both commercial and new epoxy resins. The mechanical properties of the insulators were investigated at 77 K in tension as well as in inter laminar shear before and after irradiation both under static and dynamic conditions.

Prokopec and friends studied the qualification of the resin for the International Thermonuclear Experimental Reactor (ITER) TF coil insulation [28]. The results showed that the mechanical properties of materials were significantly affected by neutron irradiation.

Song et. al. studied the properties of radiation stable, low viscosity impregnating resin for cryogenic insulation system by using triglycidyl-p-aminophenol (TGPAP) epoxy resin and bis [(2-glycidyloxy-3-n-butoxy)-1-propylether] (IPBE) [31]. The results showed that IPBE improved the processing

characteristic. The irradiation of the composites, reinforced by boron-free glass fiber, by ^{60}Co γ-ray up to the dose of 1×10^6 Gy showed that irradiation did not influence the mechanical properties significantly where the composites showed resistance to radiation up to a dose of 1 MGy.

In the study of Djouani, they worked the degradation of epoxy coatings under gamma irradiation. The samples were prepared by curing of Diglycidyl ether of bisphenol A (DGEBA) and Jeffamine (POPA) or polyamidoamine (PAA). The gamma irradiation was done at 25 °C in air with different dose rates of 50, 200 or 2000 Gy h^{-1} for up to 100 kGy absorbed dose [34]. It was observed that there were various oxidation products, among which amides were predominate in DGEBA-PAA network. The dominant reaction was chain scissions in comparison with crosslinking, whereas for the DGEBA-POPA network, crosslinking was observed slightly as the dominant reaction, at least for the lowest dose rate.

Wei et. al. studied irradiation effects on a glycidylamine epoxy resin system used for insulation in fusion reactor [35]. The resin system used in the study showed good performance of radiation resistance against irradiation dose of 25.9 MGy. It was revealed that the hardener contents influenced the crosslinking degree of resins which was an important effect in irradiation resistance.

Craciun et. al. studied the gamma radiation effects on the stability of epoxy resins [39]. The resins were modified with titania nanoparticles. The thermal stability of epoxy composites were not affected up to 1000 kGy. According to the results the thermal resistance of epoxy resin modified with titania nanoparticles was significant, due to the action of filler concerning the adsorption of degradation intermediates.

Hoffman et. al. investigated the radiation effects on epoxy/carbon-fiber composite [43]. The results of composite bars showed any change in modulus, strain to failure, or fracture strength after exposures. But, the results of neat epoxy matrix showed significant changes in hardness, thermal properties, and spectroscopy with increasing gamma irradiation.

Korkut et. al. studied the investigation of neutron shielding properties of various types of boron minerals. The minerals choice was depending on number of boron atoms for colemanite, ulexite and tincal ores. The results were gained by both experiments and FLUKA Monte Carlo simulations [44]. The results showed that loading with minerals containing increasing number of boron atoms enhanced the neutron shielding property of samples.

1.4. Boron and Boron Minerals

Boron (represented as B) is a semiconductor element. Its atomic number is 5 and atomic mass is 10.81. Boron is composed of the its isotopes as; ^{8}B, ^{10}B, ^{11}B, ^{12}B, ^{13}B in which the most stable ones are ^{10}B and ^{11}B. The natural abundances of these isotopes are 19.1-20.3% and 79.7 - 80.9% respectively.

More than 70% of known deposits of boron are in Turkey and half of world production is provided also from Turkey and these deposits are with high isotope ^{10}B content.

The morphology and grain size are decisive in the chemical properties of boron. The micron sized amorphous form of boron can react easily and sometimes intensely, but crystalline form of boron is reluctant to react.

All boron minerals contain triangular (BO_3) and/or tetragonal (BO_4) structural units [52]. These B-O groups tend to form ring structures where boron minerals can polymerize to result in networks or chains. Colemanite is a good example where its structure contains long B-O chains with a ring of one triangular and two tetragonal units.

Tincal is in the form of $Na_2B_4O_7.10H_2O$ or $Na_2[B_4O_5(OH)_4].8H_2O$ contains two triangular and two tetragonal units. The structure of boron minerals with H_2O can be affected by temperature.

Boron minerals are used in various fields in the industry as crude minerals but generally, the applications after refining and end-products are used more than crude ones. The principal markets are: Glass, ceramics, flame retardants, agriculture and nuclear.

The highest consumption of boron occurs in the glass industry. Boron increases the viscosity of the glass and improves the strength and surface hardness.

Boron is used in glazing and frits in ceramics industry as a function of providing the thermal balance between the material and glass.

In addition, boron suppresses combustion by sealing the surface of the burning material which blocks the contact with oxygen. This ability makes it used as flame retardant material in various materials (PVC, timber, and textiles).

Moreover, boron plays role in the diffusion of glucose in the cells and photosynthesis metabolism. Boron can be applied to the soil as a neutralizer of the pH value.

The ^{10}B isotope is known as great thermal neutron absorber where it can be employed in nuclear power plants for controlling / terminating fission reactions and its supplies. It is known as every boron atom absorbs one neutron [53]. Especially, colemanite and ulexite is used for the storage of nuclear wastes [54].

1.5. Aim of The Study

With the development of nuclear energy, the necessity for various types of radiation shielding materials is ascending. These materials are used to reduce the effects of certain types of radiation. The choice of these shielding materials depends on several factors such as strength, thermal properties, resistance to damage, attenuation effectiveness and cost efficiency.

Boron is preferred for blocking or reducing the intensity of neutron radiation because of its low atomic number that makes it to have more probability of forming cross-sections to interact with neutrons. The effective performance due to neutron absorbing makes boron applicable in nuclear industry [55].

There are various types of materials which are being used for the attenuation of gamma radiation such as epoxy resin, polyethylene, colemanite, glasses, lead and concentrate which have been used for neutron and gamma shield [56].

Taking into account the respective advantage of epoxy and boron, it was aimed to produce composite shielding materials against both gamma and neutron radiation. The composites were made by epoxy resin filled with different types of boron minerals, which contain B_2O_3 in different percentages. The investigation of those materials was done in terms of mechanical properties, thermal properties and on radiation stability.

CHAPTER 2

EXPERIMENTAL

2.1. Materials

2.1.1. Epoxy Resin

Boron-epoxy samples were prepared by utilizing epoxy resin based on Bisphenol A (Adriapox Special, Adria, Italy). Indurente A37 (Adria, Italy) was used as hardener. Chemical compositions are given in Appendixes. Epoxy composition is 63% resin – 37% hardener in w/w as recommended by the manufacturer.

2.1.2. Boron Minerals

Table 2.1 shows the boron minerals used in this study. Their chemical formulas and their B_2O_3 content are also given in Appendix.1 [57]. All boron minerals were provided form ETİ Maden. Informations about the boron minerals are given in Appendixes.

Table 2.1: Boron Minerals Used in This Study

Boron Mineral	**Chemical Formula**	**B_2O_3 Content (%)**
Calcined Tincal	$Na_2O.2B_2O_3.2H_2O$	52.0
Concentrated Tincal	$Na_2O.2B_2O_3.10H_2O$	29.0
Ground Colemanite	$2CaO.3B_2O_3.5H_2O$	40.0
Etibor-68 (Anhydrous Borax)	$Na_2O.2B_2O_3$	68.0

2.1.3. Epoxy-Boron Polymers

Preparation of reinforced epoxy resins performed as illustrated in Figure 2.1. The used boron minerals were with particle size of - 230 mesh (63 μm). The four types of boron minerals shown in Table 2.1 in different mass fractions were added into commercial epoxy resin. Epoxy resin composition is 63% resin – 37% hardener as curing agent in w/w.

The interval of mixing the epoxy resin, reinforcement material and then the curing agent is due to the epoxy resin type. The mixing ratio also depends on the epoxy resin type. During the mixing period some bubbles may occur. To avoid the bubbles, mixing should be done carefully. Also a vacuum chamber or an ultrasonic bath can be used to remove bubbles from the mixture. Finally, the product is cured at room temperature or in an oven at desired temperature again depending on the type of epoxy resin.

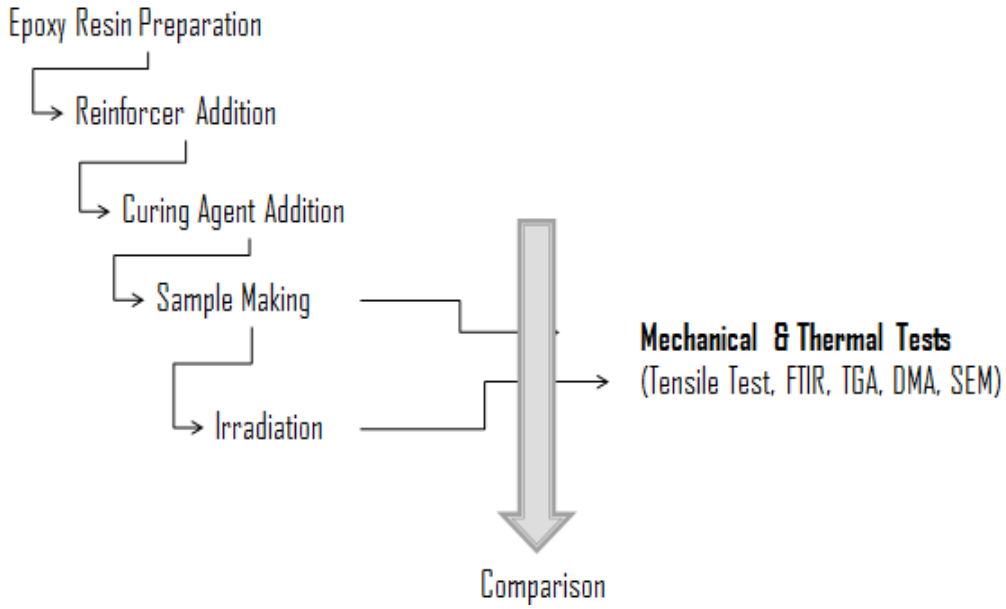

Figure 2.1: Epoxy Reinforcement Procedure

Mass fractions of boron minerals and abbreviations of composites are given in the Table 2.2.

Table 2.2: Epoxy – Boron Polymer Compositions

Boron Mineral	**Total amount of Epoxy-Boron Polymer (g)**	**Amount of Boron Mineral in Epoxy-Boron Polymer (g)**	**Abbreviation**
Pure Epoxy	100	-	EPO
Calcined Tincal	100	1 / 2.5 / 5	ECAT 1-2.5-5
Concentrated Tincal	100	1 / 2.5 / 5	ECOT 1-2.5-5
Ground Colemanite	100	1 / 2.5 / 5	ECOL 1-2.5-5
Etibor-68 (Anhydrous Borax)	100	1 / 2.5 / 5	EANB 1-2.5-5

After addition of boron minerals into epoxy resin, they were stirred mechanically for 20 min and the gas produced during the mixture is removed in a vacuum chamber until no bubbles occurred than curing agent was added and stirred for another 5 min and again degassed in a vacuum chamber until no bubbles observed. Mixtures were poured into silicon rubber molds. Then, they were cured in an oven at 60 °C for 2 hrs.

2.2. Irradiation

Irradiation process of epoxy-boron samples were done in three different way by gamma sources ; low dose rate (LDR), high dose rate (HDR) and high dose rate under vacuum (VHDR).

2.2.1. Low Dose Rate Irradiation (LDR)

Low dose rate irradiation studies were done with Co-60 source performed in Gammacell 220. Dose rate of gamma source was 30 Gy/h (August, 2012) when samples were placed. The total doses of 54 kGy, 138 kGy and 245 kGy were applied to the test specimens.

2.2.2. High Dose Rate Irradiation (HDR)

High dose rate irradiation studies were done with Co-60 source in JS 9600 model at GAMMA PAK Irradiation Facility, Çerkezköy. Dose rate of gamma source was 2.5 kGy/h. The total doses of 500 kGy, 1000 kGy and 2500 kGy were applied to the test specimens.

2.2.3. High Dose Rate Irradiation under vacuum (VHDR)

High dose irradiations under vacuum were performed in JS 9600 model including Co-60 source. Total source capacity is 300.000 Ci (in 2012). Dose rate of gamma source was 2.5 kGy/h. Irradiations under vacuum were carried out for only high dose rate irradiation up to 2500 kGy .

For the vacuum process, the samples were placed into pyrex tubes under the pressure of 10^{-3} torr before irradiation.

Absorbed doses and rates for irradiation process summarized in Table 2.3.

Table 2.3: Dose rates and absorbed dose (kGy) values for irradiated samples

	Absorbed Dose by Low Dose Rate Irradiation in air (kGy)			**Absorbed Dose by High Dose Rate Irradiation in air (kGy)**			**Absorbed Dose by High Dose Rate Irradiation under vacuum (kGy)**		
All samples	54	138	245	500	1000	2500	500	1000	2500

2.3. Characterization of Samples

2.3.1. Curing Temperature Comparison

Epoxy resins generally exhibit poor chemical and mechanical properties before curing. After forming a three-dimensional cross-linked thermoset structures of epoxy, the polymer have good properties. The curing is exothermic for epoxy resins.

Some epoxy resin / hardener systems are cured at room temperature, some require heat, with temperatures up to 200°C. Mechanical and chemical properties reduced with insufficient heat during cure because of incomplete polymerization in network.

Three curing temperatures were studied; 60 ^{o}C, 120 ^{o}C (1 hr post-curing at 150 ^{o}C) , 200 ^{o}C for non-irradiated samples.

2.3.2. Water Absorption Test

Water absorption test was done according to "Method of Test for Water Absorption of Epoxy Resin System" of US Louisiana Transportation Research Center (LTRC) - DODT TR 704-85 standard and ASTM D570 standard.

Water absorption test is the determination the amount of water absorbed under specific conditions. Water absorption is affected by different factors such as type of polymers, additives used, temperature and period of immersion.

The method is intended to determine the amount of water absorption of cured epoxy resin systems. Basically, the weighted epoxy specimens were dipped into water for 24 hours. After 24 hrs, the specimens were weighted again and then the

difference before and after the absorption gave the amount of water absorption of epoxy. The mathematical equation is;

$$W = \frac{WW-CW}{CW} \times 100$$

where;

WW : wet weight, g

CW : conditioned weight, g

W : swelling, %

2.3.3. Tensile Tests

Tensile tests were performed on the Lloyd LR 5K (Figure 2.2) in accordance with to BS EN ISO 527-1 and BS2782 Part 3 Method 322 standards with a crosshead displacement rate of 1 mm/min taken. Tensile tests gave the Young's modulus, tensile strength and elongation at break results.

Figure 2.2: Lloyd Instruments LR 5K Universal Testing Machine

The specimens for tensile tests are with dimensions of 115 x 19 x 33 mm according to the ASTM D638 standard as shown in Figure 2.3 below.

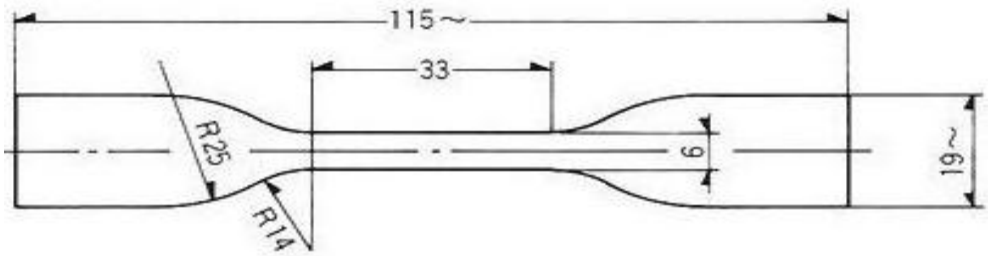

Figure 2.3: Dog-bone shaped dimensions of ASTM D638 Type IV

2.3.4. Attenuated Total Reflection Fourier Transform Infrared (ATR-FTIR)

Infrared Spectroscopy (IR) is one of the reliable fingerprinting methods to characterize many substances with identifying and quantifying. FT-IR spectroscopy is a powerful and versatile technique for monitoring transient chemical change during the cure process, and structural change during the deformation process [58]. It helps to obtain detailed information about molecular orientation and relaxation behavior of the materials by monitoring during the curing process or deformation process. The technique of Attenuated Total Reflectance (ATR) is the most widely used FTIR sampling tool because of non-sampling or easy sample preparation, which makes the analysis quickly.

ATR-FTIR results of the epoxy samples aid in estimating the possible reactions which occurred in epoxy structure via radiation. ATR-FTIR spectra of epoxy samples were noted at 25 °C on a Thermo Nicolet iS10 FT-IR Spectrometer. Samples were scanned from 4000 cm^{-1} to 600 cm^{-1} with a resolution of 8 cm^{-1} (Figure 2.4).

All FT-IR spectra of samples were normalized. Normalization of spectral intensities is the way of elimination the path length variation and also reduction the differences between each single measurement of the samples. In normalization, the spectra are divided by the selected peak (generally the most intense band) intensity or area [59].

Figure 2.4: Thermo Nicolet iS10 ATR-FTIR Spectrometer

2.3.5. Dynamic Mechanical Analysis (DMA)

DMA is the technique used to measure damping which is the measure of the energy dissipation of the material and stiffness by using the properties of the materials as a function of time, temperature, atmosphere, stress and frequency. DMA tests were done with Perkin Elmer Pyris Diamond DMA to study viscoelastic behavior of composites. Samples having dimensions of 3 x 13 x 55 mm were heated from -150 °C to 250 °C with constant heating rate of 5 °C/min and they were tested at a frequency of 1 Hz. (Figure 2.5).

Figure 2.5: Perkin Elmer Pyris Diamond DMA

2.3.6. Thermogravimetric Analysis (TGA)

TGA is one of the basic analysis methods to determine weight loss of the material function of increasing temperature in a controlled environment. TGA was performed with LECO TGA701 Thermogravimetric Analyzer and 0.5 g samples were heated from room temperature to 900 °C in an inert (N_2) atmosphere with constant heating rate of 3 °C/min (Figure 2.6).

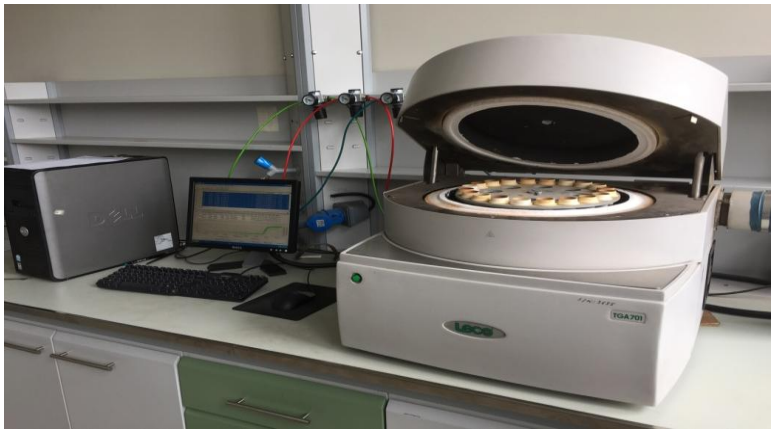

Figure 2.6: LECO TGA701 Thermogravimetric Analyzer

2.3.7. Field Emission Scanning Electron Microscopy (FE-SEM)

FE-SEM is a type of microscope that scans a focused beam of high-energy electrons over a surface to produce various signals at the surface of solid specimens which produces images of the sample. The electrons in the beam interact with atoms in the solid specimens, producing a variety of signals to be detected and that reveal information about the sample's surface topography and composition. FE-SEM analysis were done with Zeiss Supra 55 (Figure 2.7).

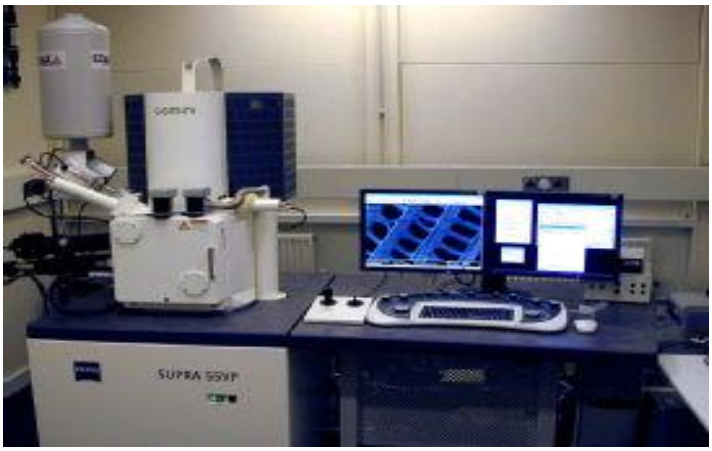

Figure 2.7: Zeiss Supra 55 model FE-SEM

CHAPTER 3

RESULTS AND DISCUSSION

3.1. Non-Irradiated Samples

The nature of epoxy adhesives can explain the influence of temperature on the curing process. The properties of epoxy adhesive are dependent on its thermal and environmental background [60]. The glass transition temperature (T_g) is one of the important features of thermosets [61]. T_g of a polymer is a phase change of amorphous solids. A non-crystalline material is transformed to a soft, elastic-plastic and rubbery state from a relatively hard, elastic and glassy state from when heated through its T_g [62]. T_g is influenced by different parameters such as crosslink density, composition of the resin molecule, the polar nature of the functional groups of resin molecules, the catalyst or curing agent, curing time and curing temperature [63].

The curing temperature determines many of the properties of epoxy adhesives. The cure time and temperature may affect the T_g of any given epoxy system. At temperatures close to T_g, the values of the mechanical properties such as tensile strength and modulus can be reduced.

The curing temperature had a significant influence on the mechanical properties of epoxy adhesives. It was observed that increasing temperature effected the curing reaction of all of epoxy-boron samples.

3.1.1. Curing Temperature Comparison

The tensile tests were done for non-irradiated epoxy samples. Three curing temperatures were studied 60 ºC, 120 ºC (1 hr post-curing at 150 ºC) , 200 ºC for those non-irradiated samples. Young's modulus of the epoxy samples are given below Table 3.1.

Table 3.1: Young's modulus of the epoxy samples cured at different temperatures.

	Young's modulus (MPa)		
Curing Temp. / Sample Type	**60 ºC**	**120 ºC**	**200 ºC**
EPO	200	1001	1279
ECAT-1	310	1319	986
ECAT-2.5	387	991	1307
ECAT-5	416	715	595
ECOL-1	256	1353	1042
ECOL-2.5	354	1441	1256
ECOL-5	264	976	1009
ECOT-1	141	1639	524
ECOT-2.5	200	997	722
ECOT-5	405	686	466
EANB-1	247	1183	1275
EANB-2.5	226	1177	1477
EANB-5	225	1130	1588

The mechanical results of the epoxy-boron samples changed as a function of curing temperature. These changes were attributed to reinforcement by various boron minerals. Neat epoxy had the highest Young's modulus after 200 ºC curing. Young's

modulus of Epoxy-Anhydrous Borax (EANB) samples increases with increasing curing temperatures. However, highest Young's modulus were obtained upon curing at 120 ^{o}C (post-curing at 150 ^{o}C) for the other boron containing samples (i.e., ECAT, ECOL and ECOT)

The color of the samples changes due to the degradation during the curing process at high temperatures. Figures 3.1 – 3.9 shows the color changes of the epoxy samples during the curing.

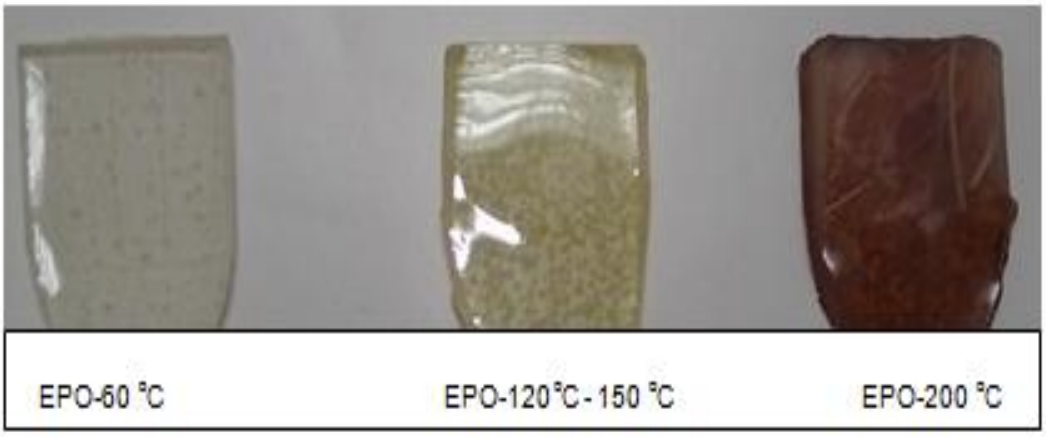

Figure 3.1: Color differences of the EPO samples as a function of curing temperature

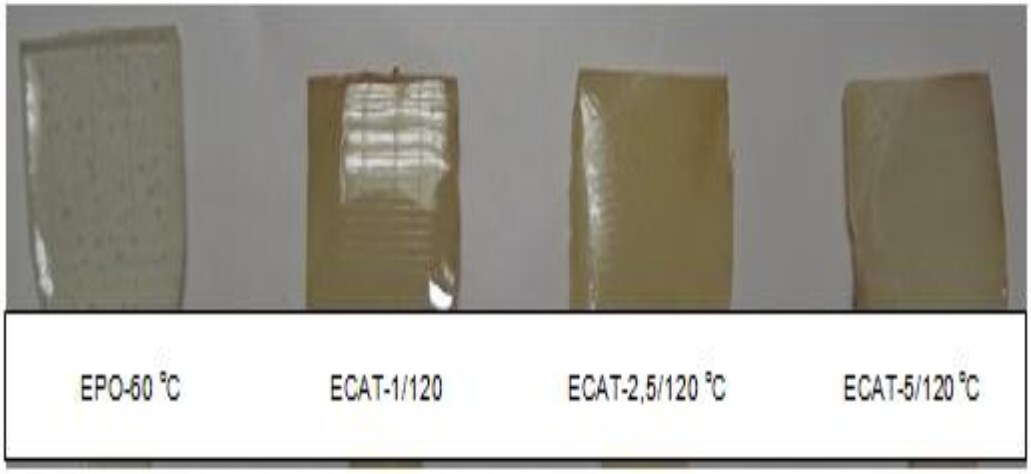

Figure 3.2: Color differences of the ECAT samples as a function of boron mineral loading (at 120 ^{o}C)

Figure 3.3: Color differences of the ECAT samples as a function of boron mineral loading (at 200 ºC)

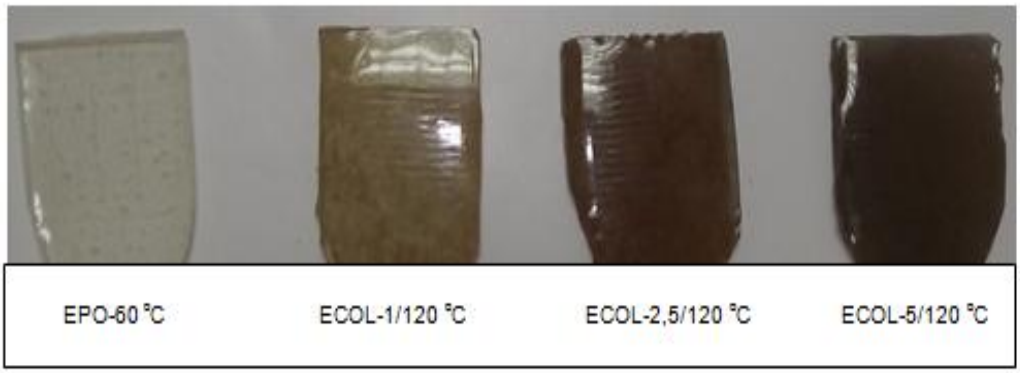

Figure 3.4: Color differences of the ECOL samples as a function of boron mineral loading (at 120 ºC)

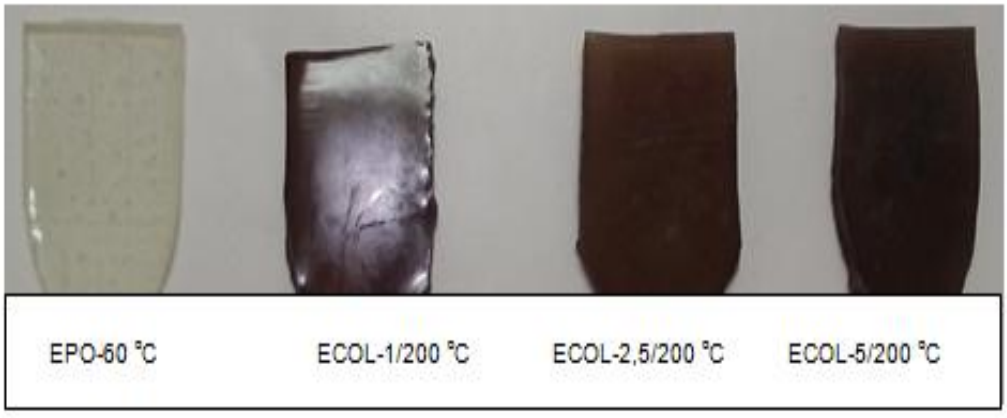

Figure 3.5: Color differences of the ECOL samples as a function of boron mineral loading (at 200 ºC)

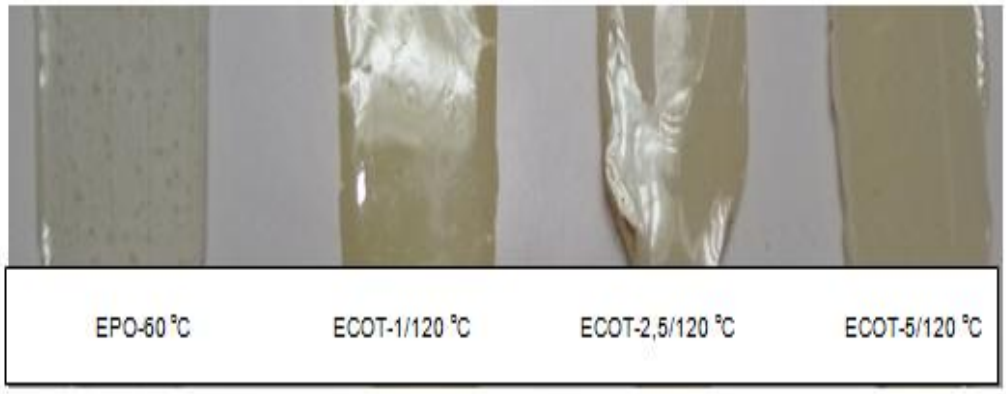

Figure 3.6: Color differences of the ECOT samples as a function of boron mineral loading (at 120 ^{o}C)

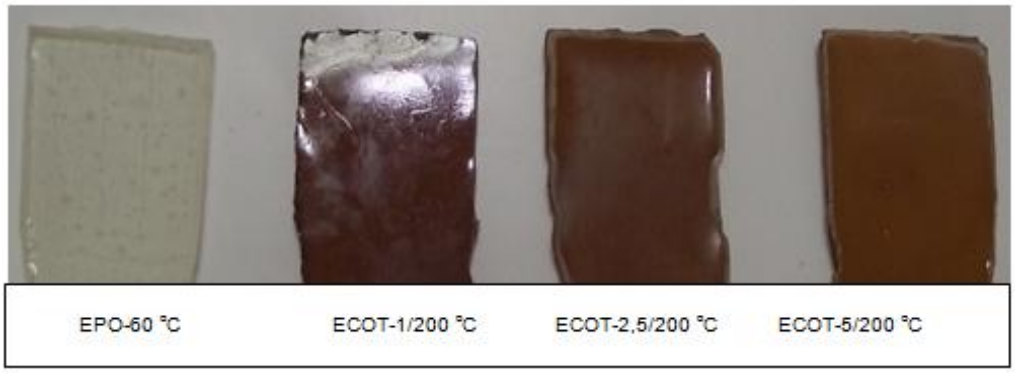

Figure 3.7: Color differences of the ECOT samples as a function of boron mineral loading (at 200 ^{o}C)

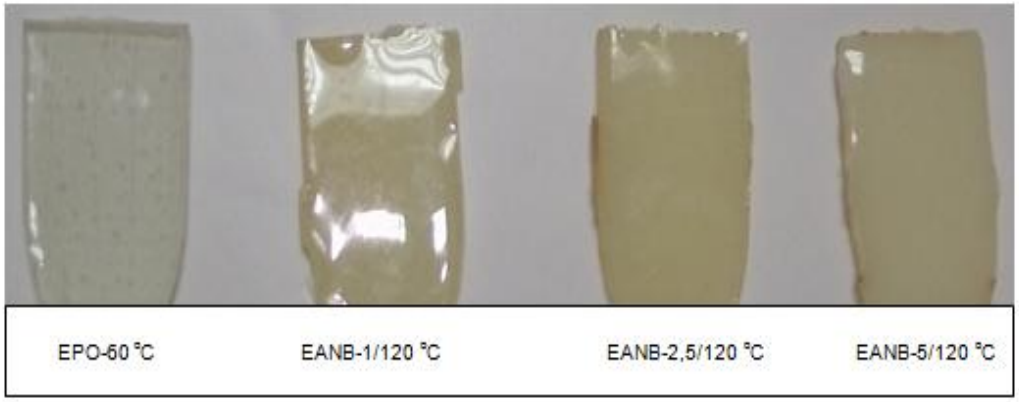

Figure 3.8: Color differences of the EANB samples as a function of boron mineral loading (at 120 ^{o}C)

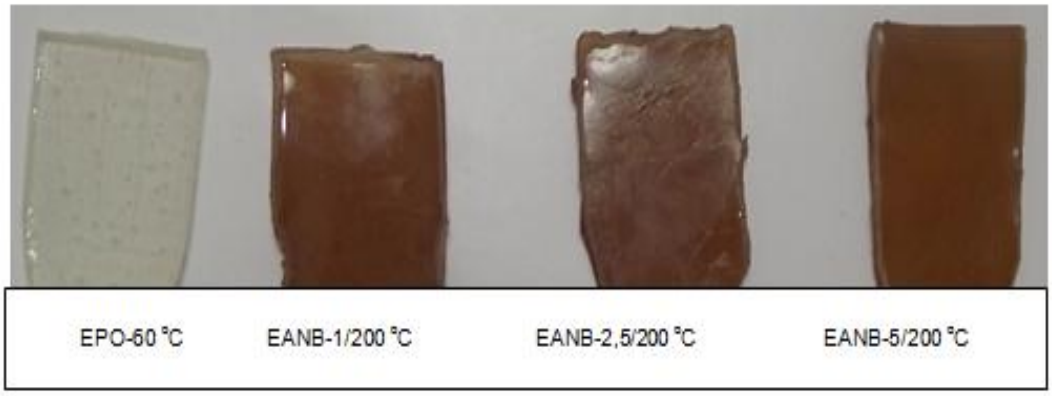

Figure 3.9: Color differences of the EANB samples as a function of boron mineral loading (at 200 ^{o}C)

As seen from the pictures of epoxy-boron samples in Figures 3.1 – 3.9, all samples became darker with increasing curing temperature. Yellowing/Discoloration is one of the problems associated with high temperature, improper temperature and/or uneven temperature distribution for epoxy resins. This discoloration is due to the formation of thermo-oxidative cross-links under exposure to high temperatures. Carbon monoxide (CO) and carbon dioxide (CO_2) are the chemicals to react with components of the newly applied epoxy and cause discoloration.

The discoloration may appear worse due to higher concentrations of CO_2. Another cause of discoloration not associated with the reaction of CO_2 may be the disproportional mixing of the epoxy components. "Amine Blush" or "Surface Enrichment" may occur during interrupted or slow curing. The amine hardener separates from the epoxy matrix and floats to the surface of the composite sample then it oxidizes and become yellowish or brownish in color [64, 65].

The chemical reactions occurred during the thermal degradation induce physical and chemical property changes relative to the initial properties. Due to the exothermic behavior of curing process of epoxy resins, it may produce enough heat to cause thermal degradation if it is not controlled. The thermal degradation may cause various changes in the polymer property such as reduced ductility and embrittlement, chalking, color changes and cracking.

3.1.2. Water Absorption Test

There are different materials with different abilities better suited for certain types of radiation. The differences are determined by the interaction of the components of the materials and the chemical properties of the shielding material. Lead, iron, concrete, and water are most common shielding materials for gamma radiation regarded to their effectiveness against absorbed gamma dose. As a comparison of those materials resistance to the same gamma radiation exposure level at the outside, it needs 1 unit length lead, 2 units length iron, 4 units length concrete and 6 units length water.

Water, itself is one of the shielding material against gamma radiation but also it behaves as a degradation agent for polymeric materials. Water absorption capacity of epoxy is an important parameter for radiation studies.

The water absorption test was done for non-irradiated epoxy samples. The results are shown in Table 3.2. The ASTM D570 standard is the most commonly used test standard for water absorption of polymers. The standard is used for two main purposes. Firstly, it gives a rate for water absorption over time and secondly, it expresses a sense as to what the specific effects of humidity or long-term exposure to water would be on the polymer under examination.

Water absorption capacity of neat epoxy at 25°C was 0.74 % in this study where it was found about 0.70 % at 25°C and 1.80 % at 95°C by Hüner [66] and as 2.09 % in the study of water absorption test at 95°C by Dutta [67]. In this study, the water absorption behavior of treated boron reinforced epoxy composites were below 2% lower than that of untreated epoxy. The water absorption capacity was found to be maximum for ECAT-5; 2.08. In general, water absorption decreases with the boron contents for un-advanced epoxy thermosets and more secondary hydroxyl groups in advanced epoxy resin cause higher water absorption [68-70].

Table 3.2: Water absorption capacity of the non-irradiated epoxy samples with different boron-minerals at 25 °C (Samples were cured at 60 °C)

Epoxy-Boron Type	CW (Conditioned Weight) g	WW (Wet Weight) g	W (increase in weight)%
Neat Epoxy	0.5000	0.5037	0.74
Epoxy-Concentrated Tincal (% 1)		0.5061	1.23
Epoxy-Concentrated Tincal (% 2,5)		0.5073	1.46
Epoxy-Concentrated Tincal (% 5)		0.5044	0.88
Epoxy-Anhydrous Borax (% 1)		0.5035	0.70
Epoxy-Anhydrous Borax (% 2.5)		0.5091	1.82
Epoxy-Anhydrous Borax (% 5)		0.5046	0.93
Epoxy-Calcined Tincal (% 1)		0.5080	1.60
Epoxy-Calcined Tincal (% 2.5)		0.5055	1.10
Epoxy-Calcined Tincal (% 5)		0.5104	2.08
Epoxy-Colemonite (% 1)		0.5044	0.88
Epoxy-Colemonite (% 2.5)		0.5041	0.82
Epoxy-Colemonite (% 5)		0.5058	1.17

One of the main challenge of epoxy resin is its high water uptake. The results showed that the epoxy reinforced with boron fillers absorbed about the same and/or smaller amount of water as the neat epoxy for a given humidity. It seems that each boron minerals had affinity towards themselves.

In the studies of Li et al., [70-71] it is shown that the water absorption including the surrounding environmental condition with gases affected the properties of the epoxy matrix composites. Epoxy resin absorbs water molecules from the surrounding environment till to the equilibrium condition with respect to various parameters such as the ambient, penetration time and the penetration of the water molecules at the surface of the composite material through the diffusion. Also, it is possible that, the water molecules can be absorbed small-sized cracks on to the surfaces of the material or along the matrix-additive interface. Water uptake can also be reduced by the connection of hydrophobic functional groups to the surface of the particles. The chemical surface treatments replace hydroxyl groups on the surface and also related to the surface of the particle, water is blocked physically [72]. The presence of water can also have more adverse effects on the behavior of composites later in processing [73].

The water uptake mechanism and the effects of such parameters as the matrix-additive interface, free space and polar radicals were also studied [74-77]. Water worsens the thermomechanical properties such as T_g, Young's modulus, tensile strength, toughness and adhesion. Also it induces the chemical degradation of the network structure and generates stresses due to the swelling [78-82]. The presence of water on hygroscopic particles can restricted the separation of them due to the agglomeration [83-84].

3.2. Irradiated Samples

The initial structure of polymers is destroyed upon irradiation by free radical formation, crosslinking, irreversible bond cleavages etc. which occurred in the fragmentation of molecules. This fragmentation causes the formation of saturated

and unsaturated groups [85-87]. The oxidation caused from the irradiation formed radicals which induce the reactions as crosslinking mentioned before [88]. The products resulted of the degradation come from the oxidation of the DGEBA part or oxidation of the amine cross-link units. The dominant mechanism of formation is the chain scission reactiona of polymeric chains, essentially.

It is showed that the degradation mechanisms of the diglycidyl ether of bisphenol-A mainly involves the reactivity of the aromatic ether function and the cleavage of the CH_3–C bond of the isopropylidene group. The main oxidative reaction of the epoxy resin is the abstraction of the hydrogen atom on the secondary carbon atom of ether bond. This causes the formation of phenyl formats. The abstraction of the hydrogen of primary carbon of the isopropylidene group produces mainly acetophenone end-groups [89]. Benzene, styrene, benzaldehyde, benzophenone and benzoic acid were the other identified products [90]. The defection inside the polymers is responsible for change in the optical and structural properties of the polymers [91].

The non-irradiated epoxy-boron polymers were nearly colorless or colored by the boron minerals; however, they showed significant color sensitivity towards gamma irradiation. The color of the epoxy-boron polymers turned to yellowed/discolored in color while increasing the irradiation dose.

The study of color changes is necessary for polymer irradiation helps to determine physical changes in polymers [92]. After irradiation the sample became yellowed / discolored in color where the extent of color change is dependent on absorbed dose. This was ascribed to a double bond in the benzene ring of the epoxy resin molecule being oxidized related to the formation of a quinone methide structure [93]. Also, the chromophoric ethers of bisphenol-A groups may absorb the gamma irradiation which causes the degradation. The strong discoloration may occur due to the formation of thermo-products containing conjugated structures resulting, for example, from dehydration reactions involving the hydroxyl groups of the DGEBA units [94].

The change of color of the epoxy-boron samples due to the dose rate conditions was denoted the oxidation reaction or degradation of the material. The figures from Figures 3.10 – 3.14 are related to differences of epoxy-boron samples due to the irradiation.

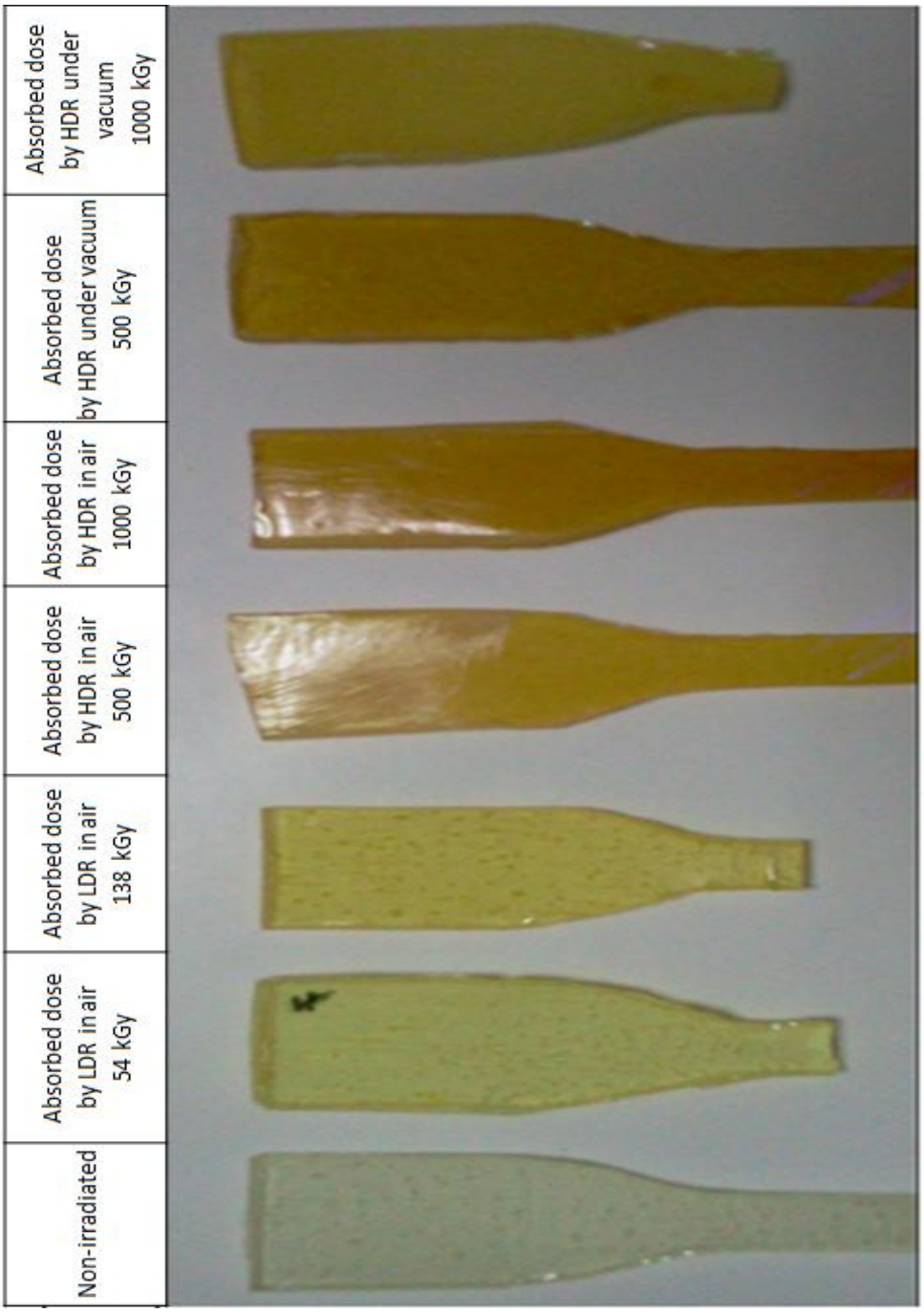

Figure 3.10: Color differences of the EPO samples as a function of absorbed dose (Samples were cured at 60 °C)

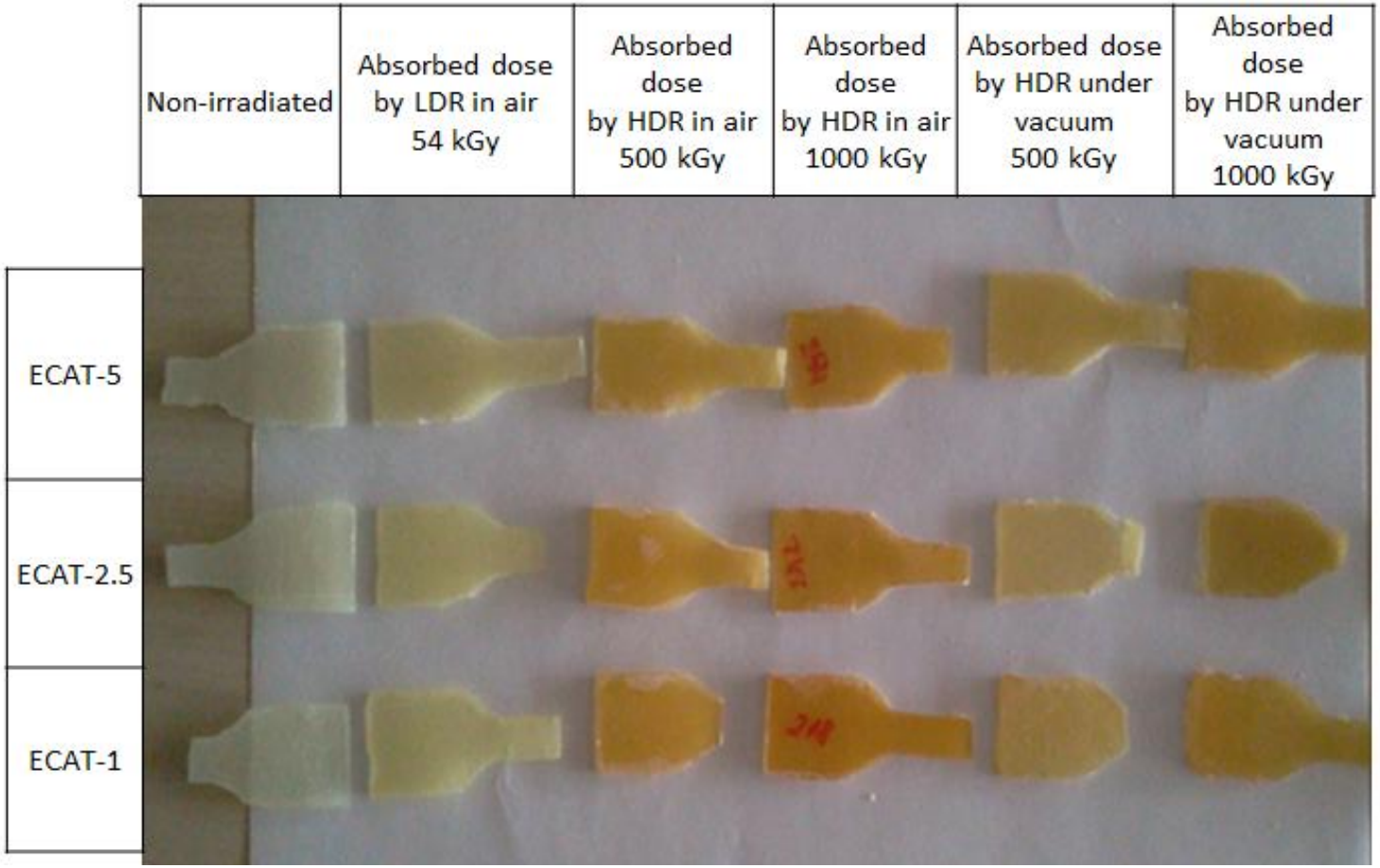

Figure 3.11: Color differences of the ECAT samples as a function of absorbed dose

(Samples were cured at 60 °C)

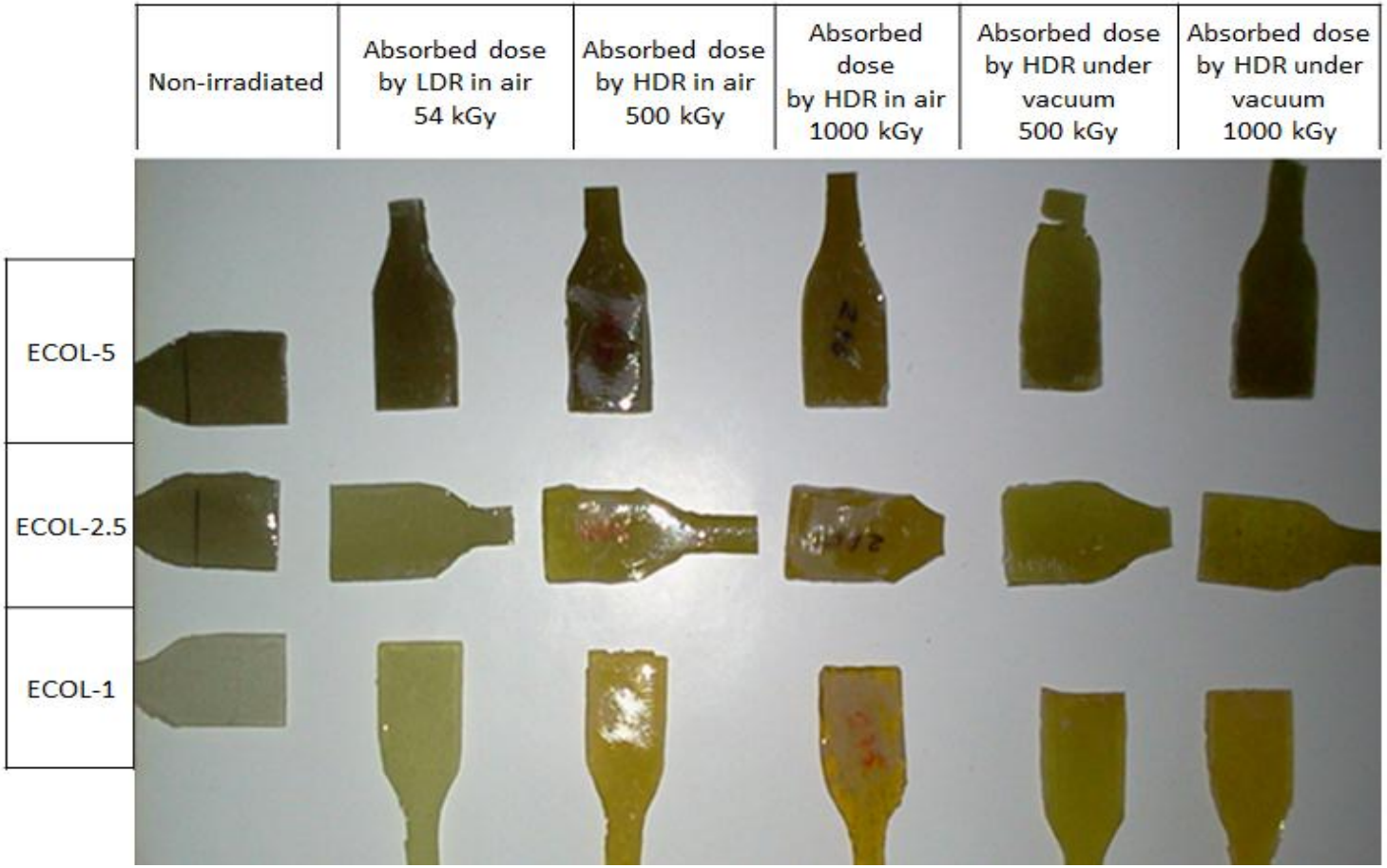

Figure 3.12: Color differences of the ECOL samples as a function of absorbed dose (Samples were cured at 60 °C)

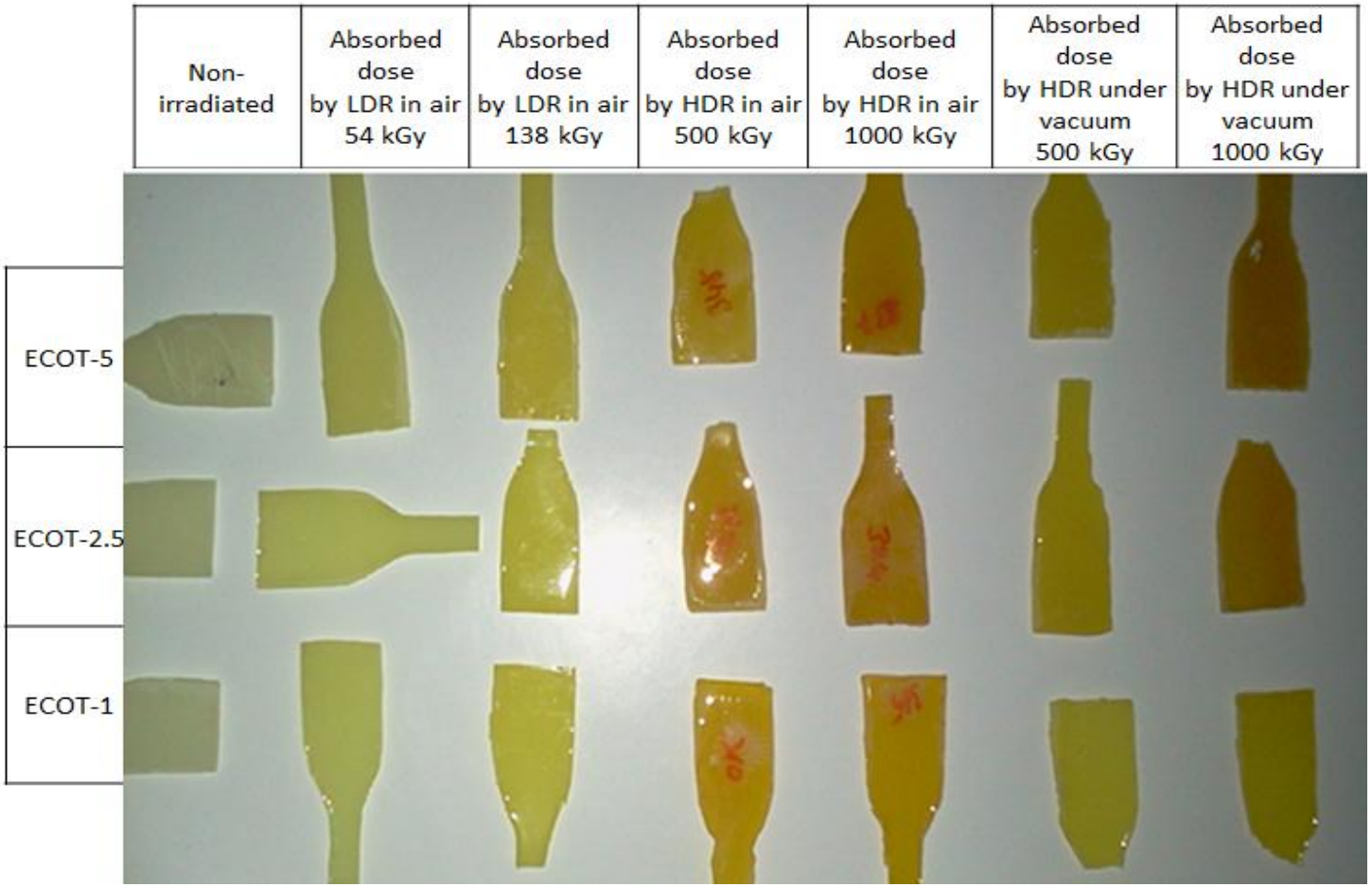

Figure 3.13: Color differences of the ECOT samples as a function of absorbed dose (Samples were cured at 60 °C)

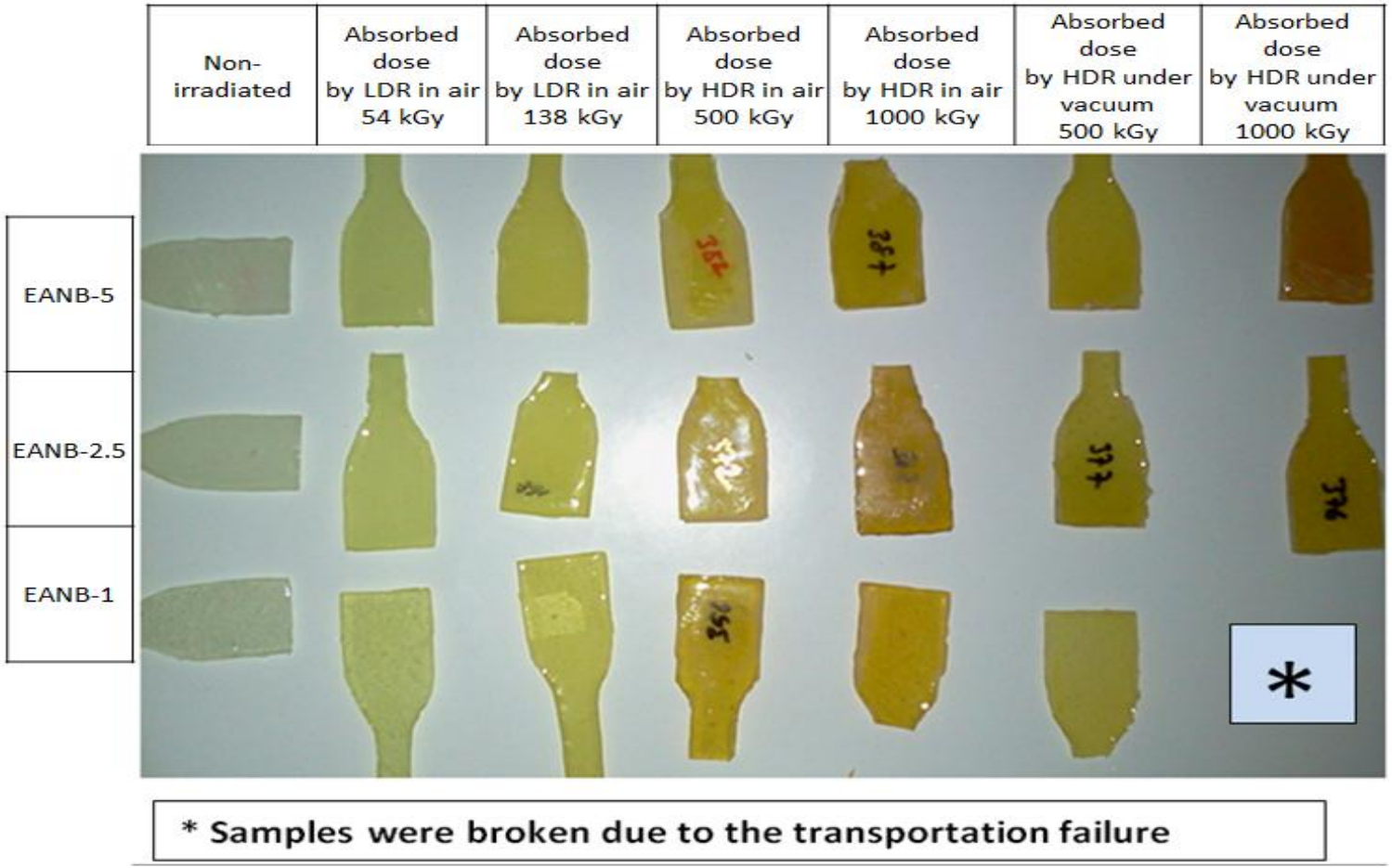

Figure 3.14: Color differences of the EANB samples as a function of absorbed dose

(Samples were cured at 60 °C)

3.2.1 Mechanical Tests

Tensile tests were done for both non-irradiated and irradiated samples. Tensile Strength is represented as the ultimate strength of a material subjected to a tensile loading which means the maximum load that a material can support to the point where it breaks [95].

This tensile test is one of the most common types of mechanical test which is simple and relatively cheap. By pulling on the samples, it will be determined how the material will react against the applied forces in tension. While the material is being pulled, it will be found how its strength along with and how much it will elongate. The measured properties are Young's modulus, tensile strength and elongation at break etc.

The results of Young's modulus, tensile strength and elongation at break for each epoxy-boron samples are given below:

3.2.1.1 Mechanical Tests for Neat Epoxy (EPO)

Epoxy thermosets are limited to lower temperature applications [96]. The employing temperature is generally between the ambient temperature and 120 °C. Some modifications allow the upper operating temperature up to 200 °C [97]. Other types of adhesives are able to employed at higher temperatures but they are lack the advantages of epoxy adhesives such as high adhesive strength, easy processing, and good wetting properties [98]. Insufficient heat during the curing process will result in a network with incomplete polymerization which reduces mechanical and chemical properties.

Most of the theoretical crosslinking reactions are resulted during the curing process [99]. Generally, epoxy systems cured to at least 90% conversion will exhibit mechanical and physical properties as they will have after fully reacted conditions. It

is clear that the faster a thermoset is cured, the more stress is imparted to it. Therefore, sometimes it is not preferred to cure quickly at the highest temperatures. Also it may be necessary to control the temperature ascending to the desired cure condition, or start with a lower temperature pre-cure to obtain lower stress bond lines for some special applications.

In order to characterize the influence of temperature on the curing process three different temperatures were used: 60 °C, 120 °C and 200 °C where rheological information may be related directly to the mechanical properties of the adhesive such as stiffness, tensile strength and Young's modulus [100]. The effect of temperature on the curing process can be explained by the nature of epoxy, where the properties of a material as thermoset are dependent on the test environment but also on its thermal and environmental history.

Many properties of epoxy can be determined by the cure temperature (T_{cure}). The glass transition temperature (T_g) can be a measure of the degree of cure of an epoxy resin system. T_{cure} can have an effect upon T_g of epoxy. At temperatures close to T_g, the mechanical properties such as tensile strength and Young's modulus are reduced [99-101]. The change of the T_{cure} and T_g happened as;

- when curing occurred below the glass transition temperature of the fully cured network structure ($T_{g\infty}$) and the T_g is higher than the cure temperature, the strength and stiffness of the epoxy increase as T_{cure} increases [102-103].
- when curing occurred above $T_{g\infty}$ and the T_g is higher than T_{cure}, the strength and stiffness decrease as T_{cure} increases [104]. Above $T_{g\infty}$, the network structure is being kept in the rubbery state after gelation which leads a thermal degradation or oxidative cross-linking. The degradation of network structure occurs and the properties are altered [105-106].
- when below the T_{cure} at which the $T_{g\infty}$ is achieved, the strength and stiffness of the epoxy increase as the T_{cure} increases.
- when above the T_{cure} at which the $T_{g\infty}$ is achieved, there is an opposite behavior, i.e. the strength and stiffness decrease as T_{cure} increases.

The effect of post curing may have on the polymer is shifting the Tg to a higher temperature [107].

The Young's modulus, tensile strength and elongation at break results for EPO samples for various irradiation doses are shown in Table 3.3 and Figures 3.15-3.17 below.

Table 3.3: Young's Modulus, tensile strength and elongation at break for EPO as a function of absorbed doses

(Irradiation samples were cured at 60 °C)

Young's Modulus (MPa)										
Sample Type	Non-irradiated	Absorbed dose by LDR in air 54 kGy	Absorbed dose by LDR in air 138 kGy	Absorbed dose by LDR in air 245 kGy	Absorbed dose by HDR in air 500 kGy	Absorbed dose by HDR in air 1000 kGy	Absorbed dose by HDR in air 2500 kGy	Absorbed dose by HDR under vacuum 500 kGy	Absorbed dose by HDR under vacuum 1000 kGy	Absorbed dose by HDR under vacuum 2500 kGy
EPO	**200**	**435**	**160**	**740**	**727**	**1209**	**870**	**554**	**572**	**not available**
Tensile Strength (MPa)										
Sample Type	Non-irradiated	Absorbed dose by LDR in air 54 kGy	Absorbed dose by LDR in air 138 kGy	Absorbed dose by LDR in air 245 kGy	Absorbed dose by HDR in air 500 kGy	Absorbed dose by HDR in air 1000 kGy	Absorbed dose by HDR in air 2500 kGy	Absorbed dose by HDR under vacuum 500 kGy	Absorbed dose by HDR under vacuum 1000 kGy	Absorbed dose by HDR under vacuum 2500 kGy
EPO	**13**	**14**	**6**	**7**	**29**	**35**	**10**	**20**	**17**	**not available**
Elongation at Break (%)										
Sample Type	Non-irradiated	Absorbed dose by LDR in air 54 kGy	Absorbed dose by LDR in air 138 kGy	Absorbed dose by LDR in air 245 kGy	Absorbed dose by HDR in air 500 kGy	Absorbed dose by HDR in air 1000 kGy	Absorbed dose by HDR in air 2500 kGy	Absorbed dose by HDR under vacuum 500 kGy	Absorbed dose by HDR under vacuum 1000 kGy	Absorbed dose by HDR under vacuum 2500 kGy
EPO	**20**	**8**	**16**	**2**	**7**	**5**	**2**	**6**	**4**	**not available**

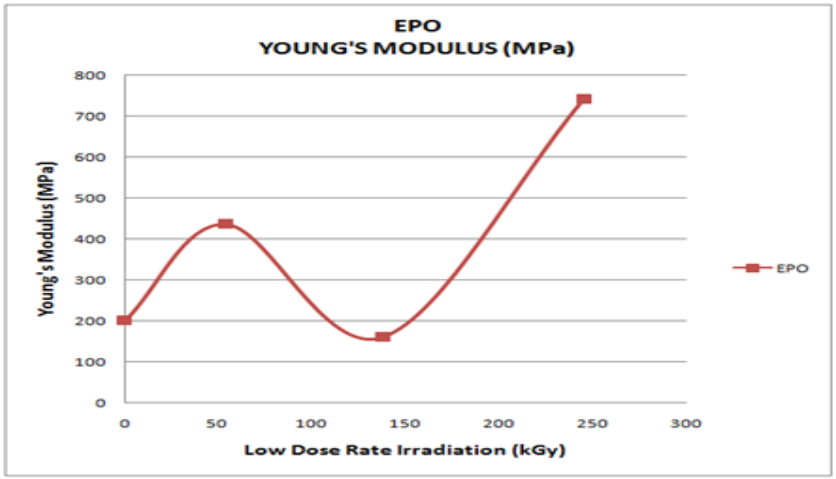

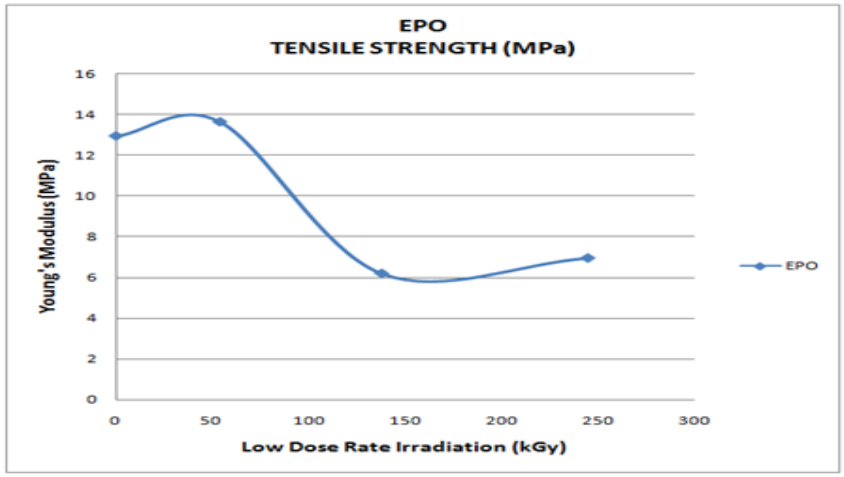

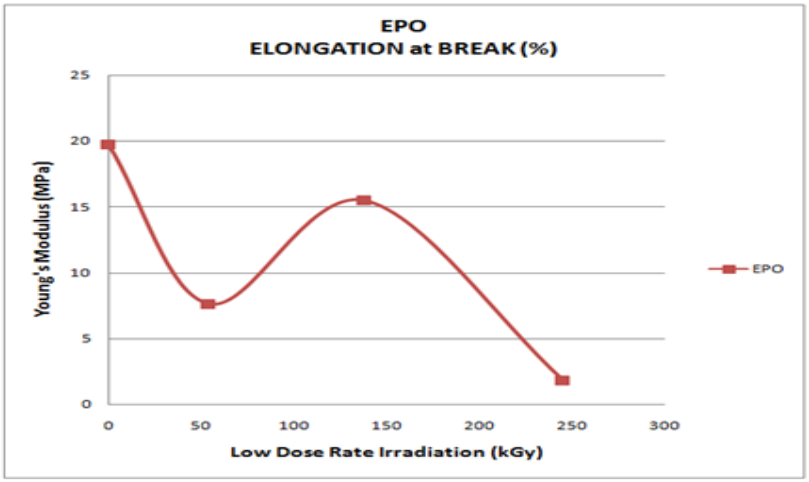

Figure 3.15: Young's modulus, tensile strength and elongation at break for EPO as a function of absorbed doses by LDR in air

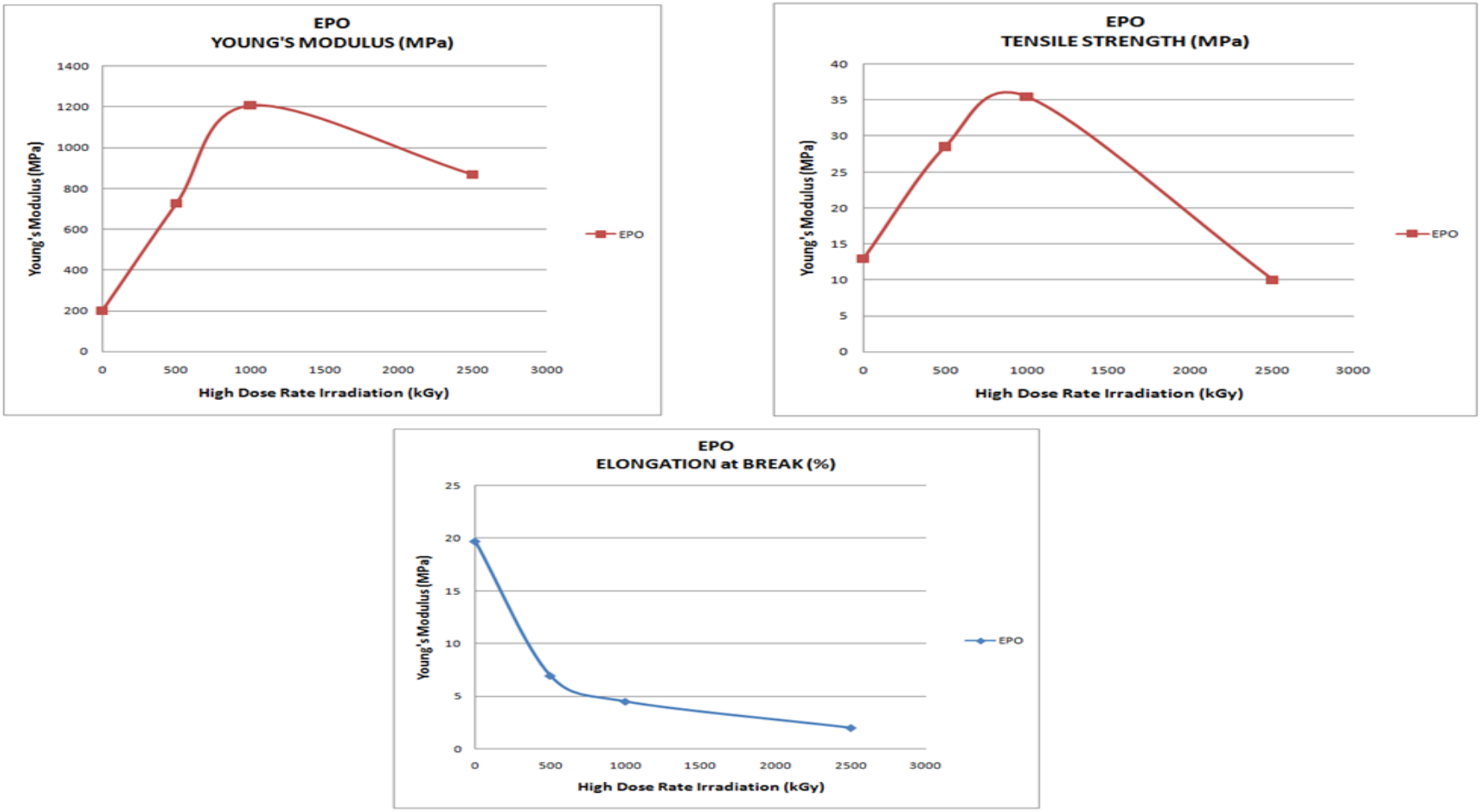

Figure 3.16: Young's modulus, tensile strength and elongation at break for EPO as a function of absorbed doses by HDR in air

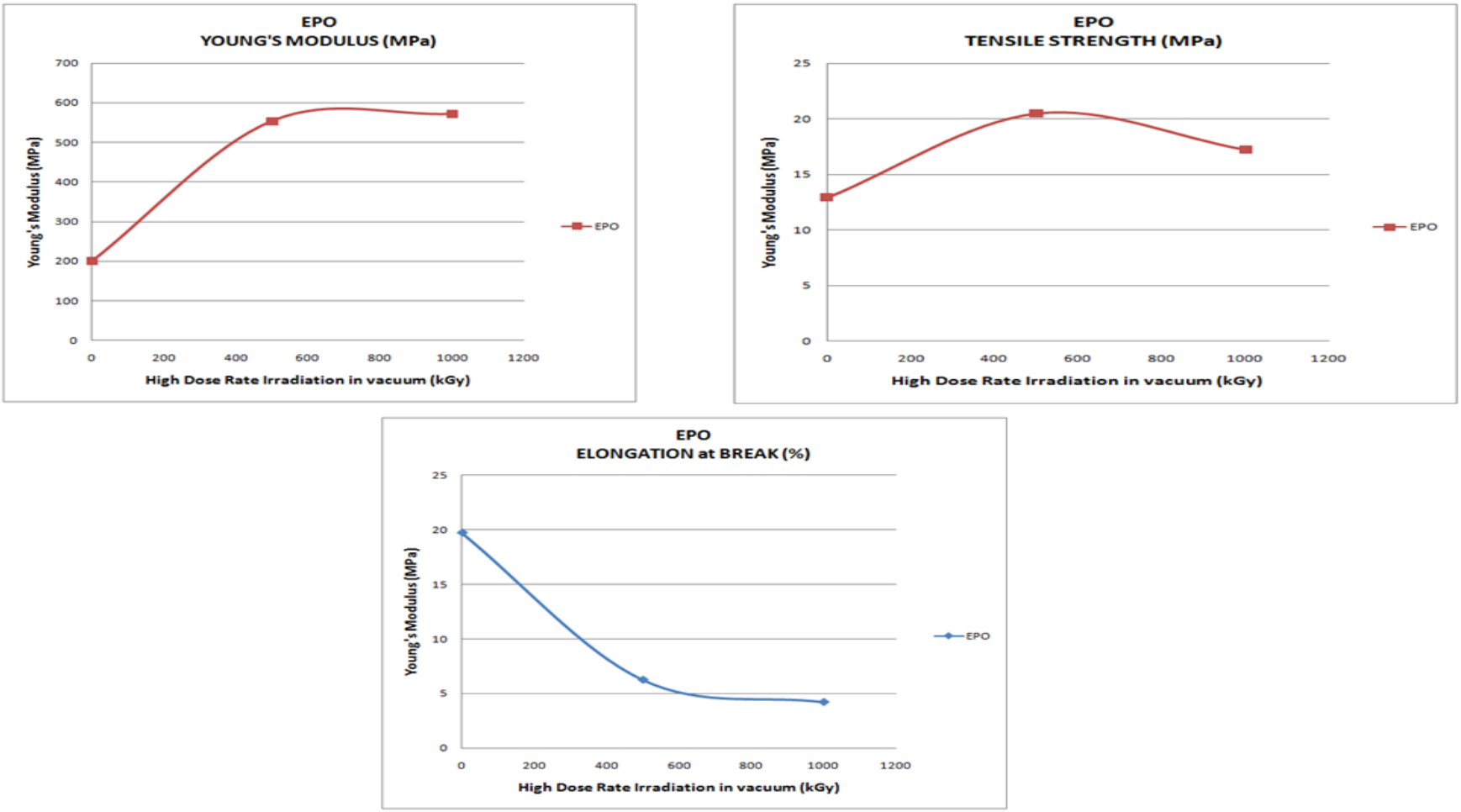

Figure 3.17: Young's modulus, tensile strength and elongation at break for EPO as a function of absorbed doses by VHDR under vacuum

As seen from Table 3.4 and Figure 3.18, neat epoxy showed an increase in Young's Modulus from 200 MPa (60 °C) to 1279 MPa (200 °C). The results in Figure 3.18 showed that the curing temperature had a significant influence on the mechanical property of the investigated epoxy. Some previous studies showed that the mechanical properties as Young's modulus of polymeric adhesives are strongly related to the increase of cure temperature (T_{cure}) (108-112).

The increase in Young's modulus may be on the ground of the increase in chain branching and molecular bond strength which affect the polymeric structure. The phenomenon for this result is "the higher the cross-linked density and the higher the modulus" [113].

Thermal degrative stability has been related to the degree of cure [114]. The results were related to higher cure temperature result in higher degree of crosslinking causing an increase in the energy to degrade the products. It is possible that epoxy-amine systems with higher functionality would have exhibited significant differences in mechanical properties due to their higher degree of crosslinking.

Table 3.4 Young's Modulus of Non-irradiated samples as a function of curing temperature

Young's Modulus (MPa)			
Sample Type	60 °C	120 °C	200 °C
EPO	200	1001	1279

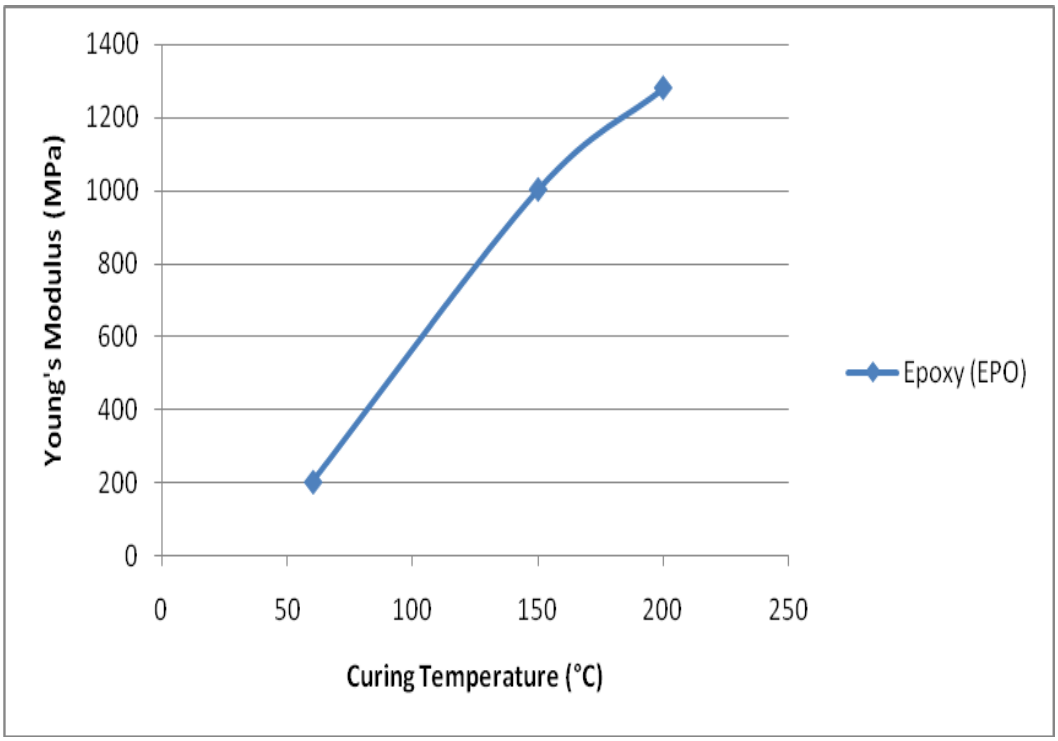

Figure 3.18 Young's Modulus of Non-irradiated EPO samples as a function of curing temperature

It is seen that Young's modulus of neat epoxy samples (cured at 60 °C) first decreased then increased when increasing the total applied dose of 245 kGy by low dose rate (Figure 3.15).

When a polymer is irradiated by gamma rays, X-rays, or accelerated electrons, various effects can be expected from the ionizations [115]. The ratio of curing, crosslinking, and chain scission may show variability from polymer to polymer and from part to part related to the chemical structure and morphology of the polymer, from the total radiation dose absorbed, and from the rate at which the dose was deposited.

The irradiated EPO samples of resin showed three stages: in the first stage the Young's Modulus increased up to 435 MPa from 0 to 54 kGy; then the value decreased to 160 MPa for 138 kGy (second stage); and finally it increased again up to 740 MPa for 245 kGy (Table 3.3 and Figure 3.15). Thus an ‘‘increment-

decrement-increment'' phenomenon is present which is called as periodical behavior [116]. An explanation of the periodical behavior might be related to the fact noted as irradiation causes chain scission, but it also produces relaxation and cage breaking.

Young's Modulus of neat epoxy for high dose rate irradiation was increased. If the dose rate is high, oxygen does not diffuse into polymers fast enough to cause these detrimental radical reactions. High dose rates of ionizing radiation have less impact on the properties of polymers compared to low dose rates.

At high dose rate, the time of radiation is shorter than low dose rate where more oxygen may not permeate into the material from its external surfaces which allow to the material to have constructive reactions. Crosslinking generates large polymer network which leads to noticeable increases in mechanical properties such as Young's modulus and tensile strength, and other key physical properties of the polymer. The increase up to 1000 kGy in Young's modulus can be seen from Table 3.3 and Figure 3.16 for neat epoxy samples. After 1000 kGy the value decreased to 870 MPa for 2500 kGy.

High dose rate irradiation in vacuum results did not show notable changes. This can be due to the high polymer resistance against irradiation in vacuum conditions. Essentially all thermosets can withstand high radiation without significant damage. Table 3.3 and Figure 3.17 showed that EPO samples have similar Young's modulus at high dose irradiation in vacuum where a little increase occurs in 1000 kGy. This little increment may be caused of a bit more crosslinking due to irradiation time period.

3.2.1.2 Mechanical Tests for Epoxy-Calcined Tincal (ECAT)

The Young's modulus, tensile strength and elongation at break values for ECAT samples for different doses are shown in Table 3.5 and Figure 3.19-3.21 below.

Table 3.5 Young's Modulus, tensile strength and elongation at break for ECAT as a function of absorbed doses

(Irradiation samples were cured at 60 °C)

Sample Type	Non-irradiated	Absorbed dose by LDR in air 54 kGy	Absorbed dose by LDR in air 138 kGy	Absorbed dose by LDR in air 245 kGy	Absorbed dose by HDR in air 500 kGy	Absorbed dose by HDR in air 1000 kGy	Absorbed dose by HDR in air 2500 kGy	Absorbed dose by HDR under vacuum 500 kGy	Absorbed dose by HDR under vacuum 1000 kGy	Absorbed dose by HDR under vacuum 2500 kGy
EPO	200	435	160	740	727	1209	870	554	572	not available
ECAT-1	310	412	604	370	799	909	1340	321	603	not available
ECAT-2,5	387	557	675	746	662	769	830	668	279	620
ECAT-5	416	247	396	560	495	631	840	455	428	495
Tensile Strength (MPa)										
Sample Type	Non-irradiated	Absorbed dose by LDR in air 54 kGy	Absorbed dose by LDR in air 138 kGy	Absorbed dose by LDR in air 245 kGy	Absorbed dose by HDR in air 500 kGy	Absorbed dose by HDR in air 1000 kGy	Absorbed dose by HDR in air 2500 kGy	Absorbed dose by HDR under vacuum 500 kGy	Absorbed dose by HDR under vacuum 1000 kGy	Absorbed dose by HDR under vacuum 2500 kGy
EPO	13	14	6	7	29	35	10	20	17	not available
ECAT-1	15	10	13	9	23	18	34	15	22	not available
ECAT-2,5	16	11	13	19	19	11	18	14	19	13
ECAT-5	13	14	26	8	12	12	16	10	17	10
Elongation at Break (%)										
Sample Type	Non-irradiated	Absorbed dose by LDR in air 54 kGy	Absorbed dose by LDR in air 138 kGy	Absorbed dose by LDR in air 245 kGy	Absorbed dose by HDR in air 500 kGy	Absorbed dose by HDR in air 1000 kGy	Absorbed dose by HDR in air 2500 kGy	Absorbed dose by HDR under vacuum 500 kGy	Absorbed dose by HDR under vacuum 1000 kGy	Absorbed dose by HDR under vacuum 2500 kGy
EPO	20	8	16	2	7	5	2	6	4	not available
ECAT-1	9	11	4	4	4	3	4	9	5	not available
ECAT-2,5	8	8	3	4	5	3	4	5	10	4
ECAT-5	11	10	4	3	7	3	4	8	8	3

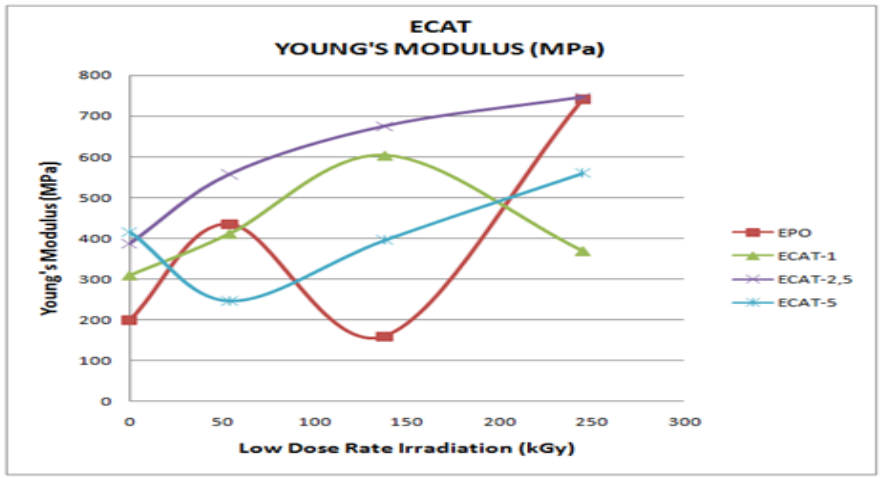

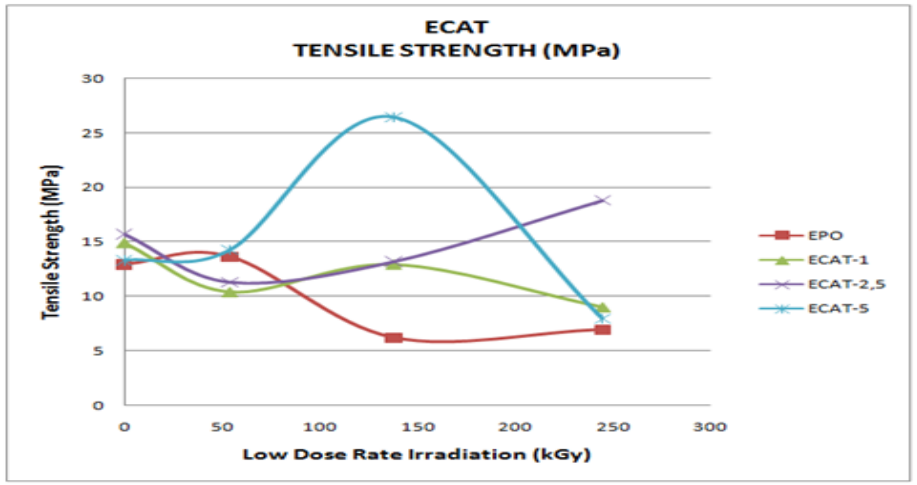

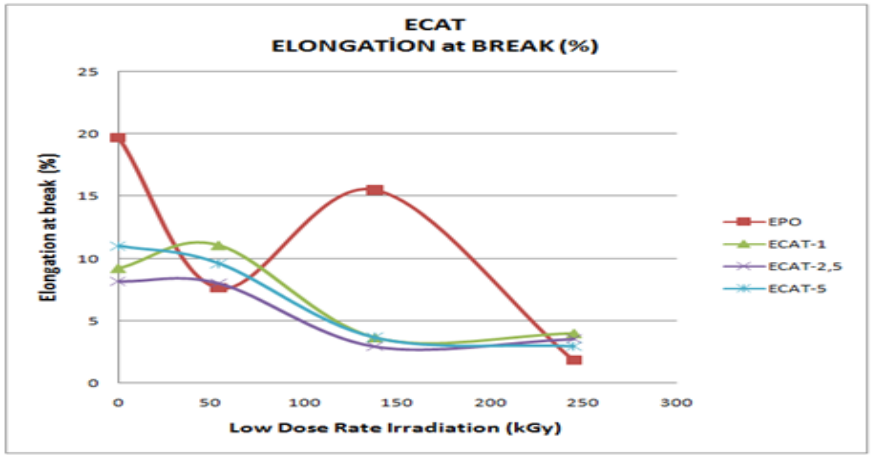

Figure 3.19: Young's modulus, tensile strength and elongation at break for ECAT as a function of absorbed doses by LDR in air

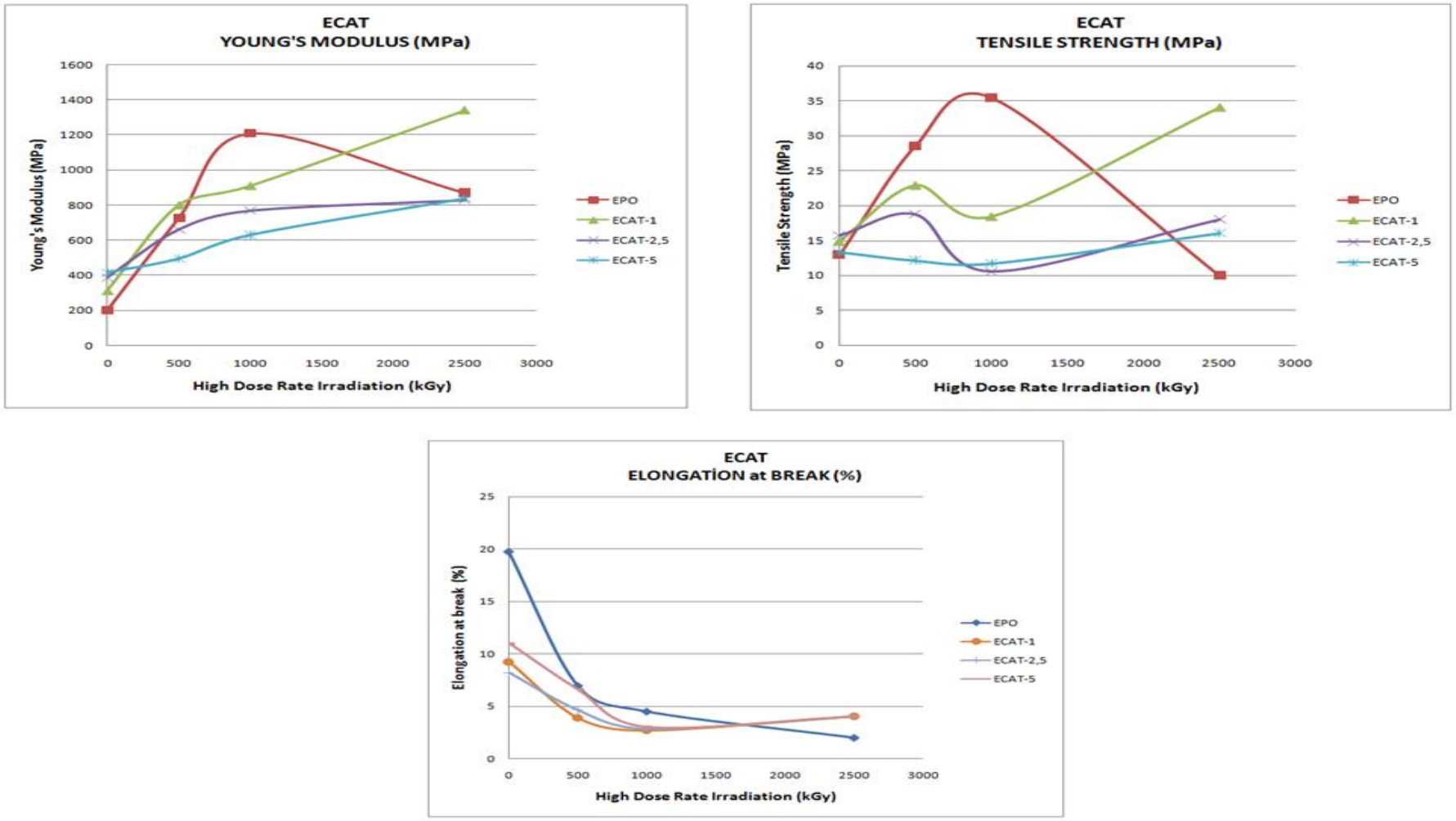

Figure 3.20: Young's modulus, tensile strength and elongation at break for ECAT as a function of absorbed doses by HDR in air

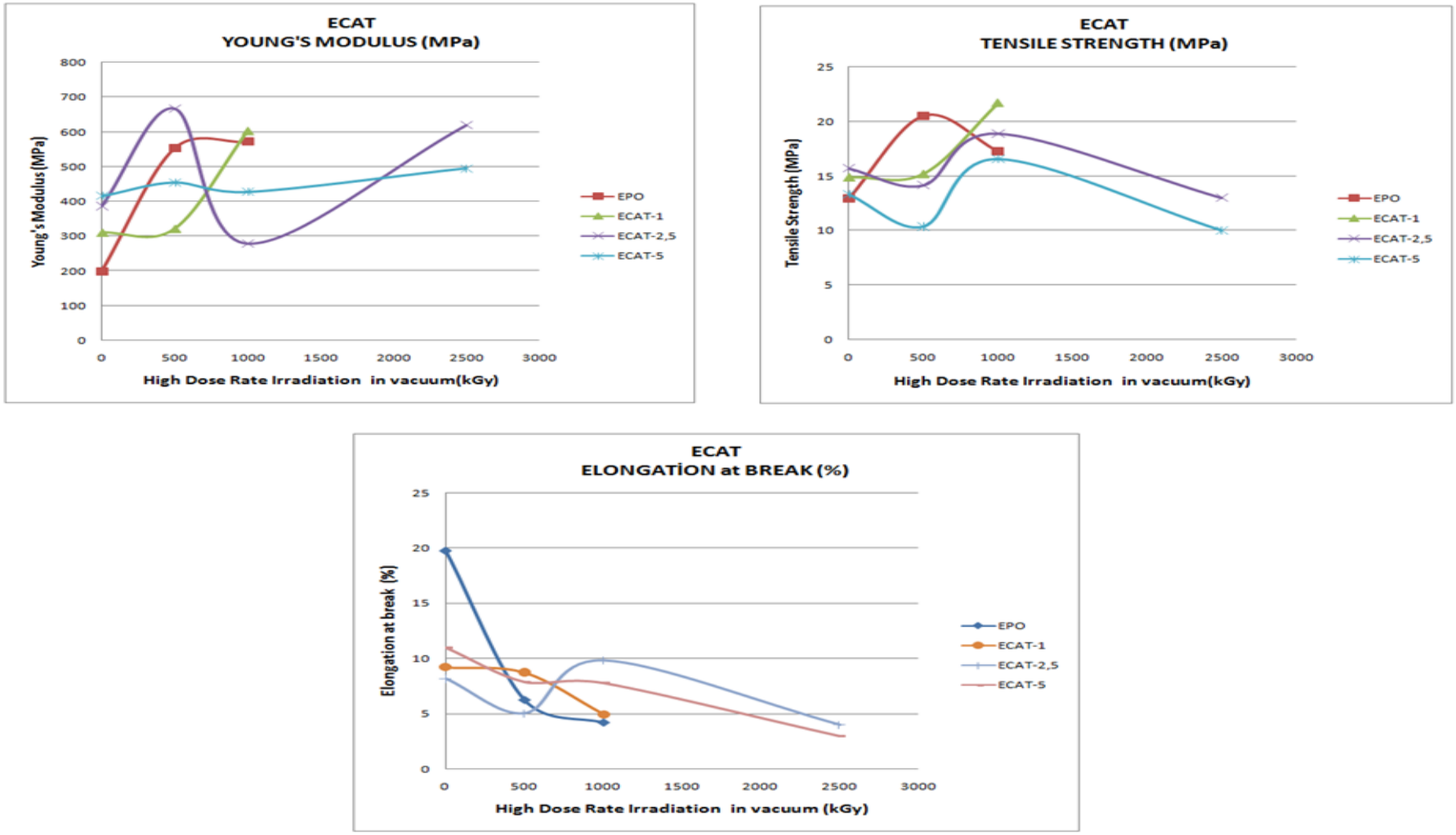

Figure 3.21: Young's modulus, tensile strength and elongation at break for ECAT as a function of absorbed doses by VHDR under vacuum

Table 3.6: Young's Modulus of Non-irradiated ECAT samples as a function of curing temperature

Young's Modulus (MPa)			
Sample Type	60 °C	120 °C	200 °C
ECAT-1	310	1319	986
ECAT-2.5	387	991	1307
ECAT-5	416	715	595

Table 3.6 and Figure 3.22 show that increasing in curing temperature gives an increase in Young's Modulus for ECAT-2.5 samples but for ECAT-1 and ECAT-5 samples it showed decrease at 200 °C. The maximum Young's Modulus is around 1300 MPa for both ECAT-1 and ECAT-2.5 samples.

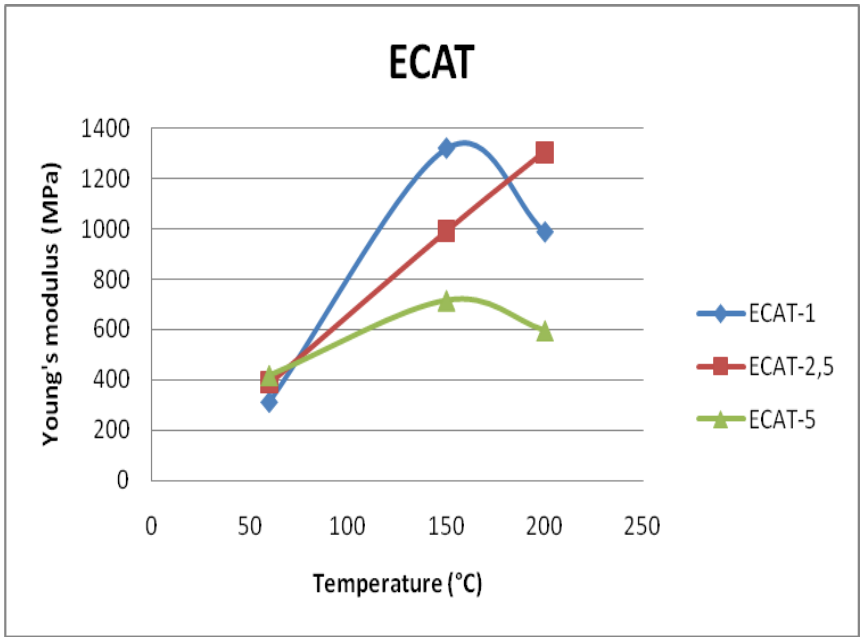

Figure 3.22: Young's Modulus of Non-irradiated ECAT samples as a function of curing temperature

Young's modulus of ECAT samples were increased due to the increase of the boron-mineral concentration (cured at 60 °C). From Table 3.5 and Figure 3.19, it seems that low dose irradiation caused crosslinking to ECAT-1 and ECAT-2.5 samples but on the other hand, because of the higher concentration of boron mineral for ECAT-5 samples, crosslinking could not be occurred which caused chain-scission that decreased Young's modulus. Oxidation seemed to be occurred in ECAT-5 samples that changed the structure.

Young's modulus of ECAT samples irradiated at high dose rate increased with increasing absorbed dose. The destructive conditions for epoxy such as free radical formation were not able to occur at high dose rate irradiation because oxygen could not diffuse into polymers fast enough. The short time of irradiation without or with low amount of oxidation caused crosslinking in the structure which increased the Young's modulus (Table 3.5 and Figure 3.20).

On the other hand, by increasing the boron-mineral concentration, Young's modulus was decreased at high dose rate irradiation because the filler loading boost the stiffness more than the strength.

High dose rate irradiation in vacuum results for ECAT samples showed such like a periodical behavior (Table 3.5 and Figure 3.21). The reason for high dose rate irradiation in vacuum results can be due to the capacity of polymer resistance against radiation which may be because of cross-linking during irradiation.

3.2.1.3 Mechanical Tests for Epoxy-Concentrated Tincal (ECOT)

The change in the curing temperature for those ECOT samples had difference of Young's modulus which showed such like a periodical behavior. The highest values were at 120 °C curing temperature than decreased at 200 °C. The reason can be due to the capacity of polymer resistance against radiation where the crosslinking was continuing that the bonds seemed to be weakened because of the degradation started at 200 °C (Table 3.7 and Figure 3.23).

Table 3.7: Young's Modulus of Non-irradiated ECOT samples as a function of curing temperature

Young's Modulus (MPa)			
Sample Type	60 °C	120 °C	200 °C
ECOT-1	141	1639	524
ECOT-2.5	200	997	722
ECOT-5	405	686	466

The Young's modulus, tensile strength and elongation at break values for ECOT samples for different doses are shown in Table 3.8 and Figure 3.24-3.26 below.

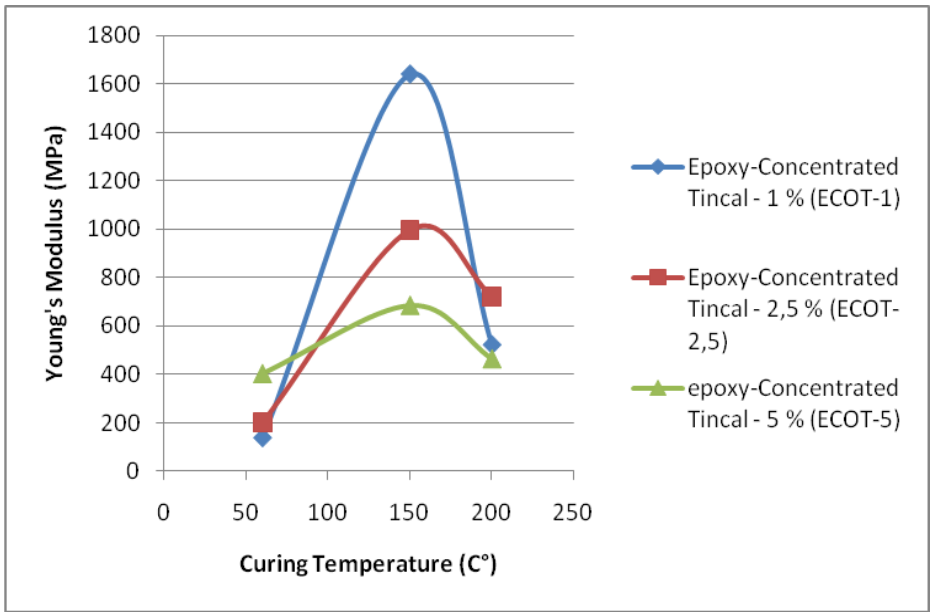

Figure 3.23: Young's Modulus of Non-irradiated ECOT samples as a function of curing temperature

Low dose rate irradiation for ECOT samples show that Young's modulus were firstly decreased than increased. This was because of chain-scission and crosslinking proceeding during the irradiation dose changes.

Young's modulus of ECOT samples at high dose rate irradiation had the lowest values after 500 kGy and the highest values after 1000 kGy. After 2500 kGy it declined again. This may be caused until an optimum dose crosslinking was occurred but then degradation started that caused Young's modulus lowered (Table 3.8 and Figure 3.25).

High dose rate irradiation in vacuum results for ECOT samples were different from the results obtained in air. The increase of boron mineral concentration in the samples may cause bit more cross-linking during irradiation which made the polymer resistance against higher radiation.

Table 3.8: Young's Modulus, tensile strength and elongation at break for ECOT as a function of absorbed doses

(Irradiation samples were cured at 60 °C)

Young's Modulus (MPa)										
Sample Type	Non-irradiated	Absorbed dose by LDR in air 54 kGy	Absorbed dose by LDR in air 138 kGy	Absorbed dose by LDR in air 245 kGy	Absorbed dose by HDR in air 500 kGy	Absorbed dose by HDR in air 1000 kGy	Absorbed dose by HDR in air 2500 kGy	Absorbed dose by HDR under vacuum 500 kGy	Absorbed dose by HDR under vacuum 1000 kGy	Absorbed dose by HDR under vacuum 2500 kGy
EPO	200	435	160	740	727	1209	870	554	572	not available
ECOT-1	141	296	186	662	549	697	670	289	682	295
ECOT-2,5	200	336	137	799	541	962	950	465	428	505
ECOT-5	405	791	316	976	594	1298	1070	261	1028	1200
Tensile Strength (MPa)										
Sample Type	Non-irradiated	Absorbed dose by LDR in air 54 kGy	Absorbed dose by LDR in air 138 kGy	Absorbed dose by LDR in air 245 kGy	Absorbed dose by HDR in air 500 kGy	Absorbed dose by HDR in air 1000 kGy	Absorbed dose by HDR in air 2500 kGy	Absorbed dose by HDR under vacuum 500 kGy	Absorbed dose by HDR under vacuum 1000 kGy	Absorbed dose by HDR under vacuum 2500 kGy
EPO	13	14	6	7	29	35	10	20	17	not available
ECOT-1	13	12	5	13	17	16	19	17	26	4
ECOT-2,5	14	14	6	15	23	18	23	18	24	7
ECOT-5	18	23	10	14	23	21	22	18	33	22
Elongation at Break (%)										
Sample Type	Non-irradiated	Absorbed dose by LDR in air 54 kGy	Absorbed dose by LDR in air 138 kGy	Absorbed dose by LDR in air 245 kGy	Absorbed dose by HDR in air 500 kGy	Absorbed dose by HDR in air 1000 kGy	Absorbed dose by HDR in air 2500 kGy	Absorbed dose by HDR under vacuum 500 kGy	Absorbed dose by HDR under vacuum 1000 kGy	Absorbed dose by HDR under vacuum 2500 kGy
EPO	20	8	16	2	7	5	2	6	4	not available
ECOT-1	25	16	31	2	7	3	5	10	7	2
ECOT-2,5	16	8	37	2	6	2	4	6	9	3
ECOT-5	9	4	5	3	5	3	3	10	5	3

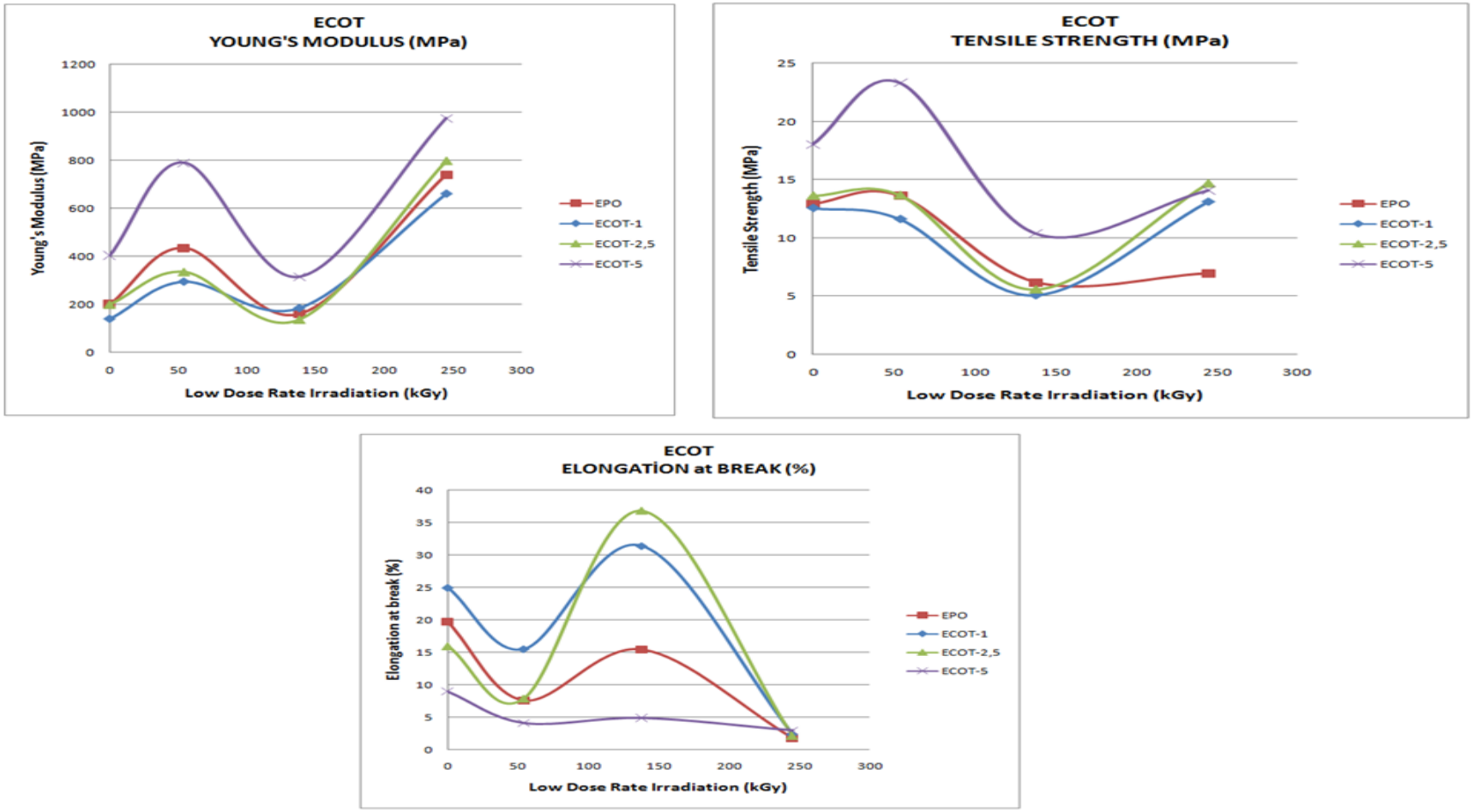

Figure 3.24: Young's modulus, tensile strength and elongation at break for ECOT as a function of absorbed doses by LDR in air

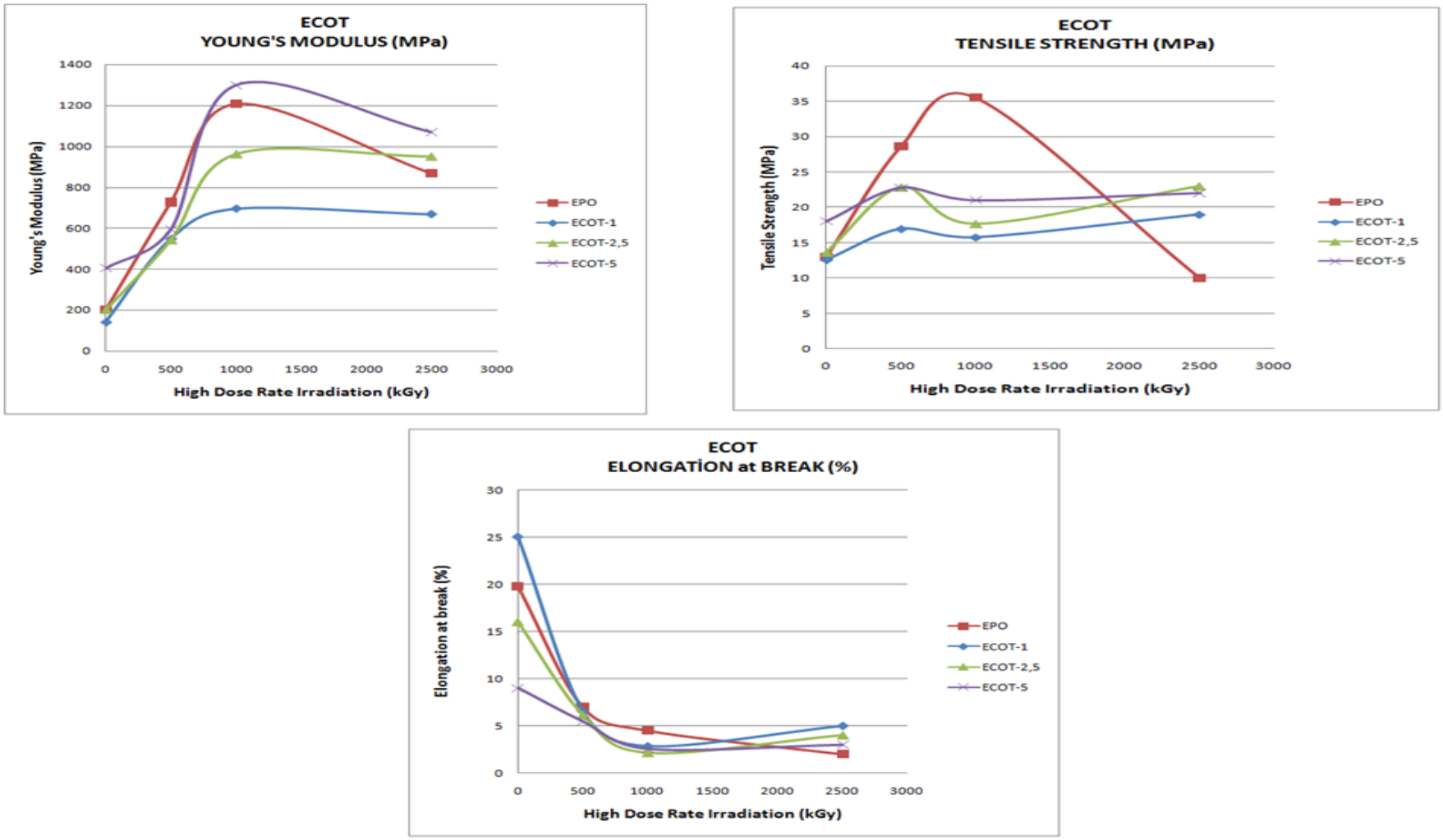

Figure 3.25: Young's modulus, tensile strength and elongation at break for ECOT as a function of absorbed doses by HDR in air

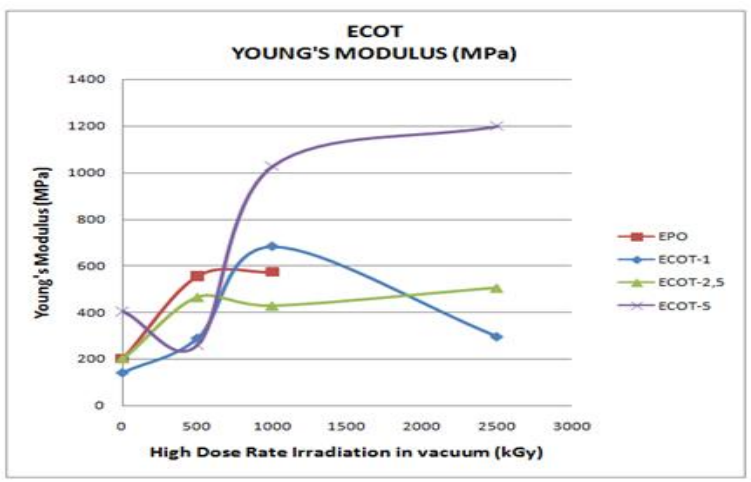

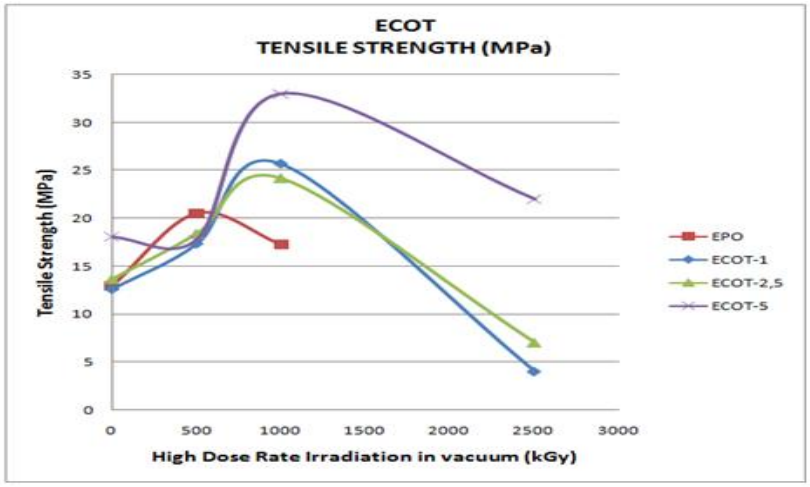

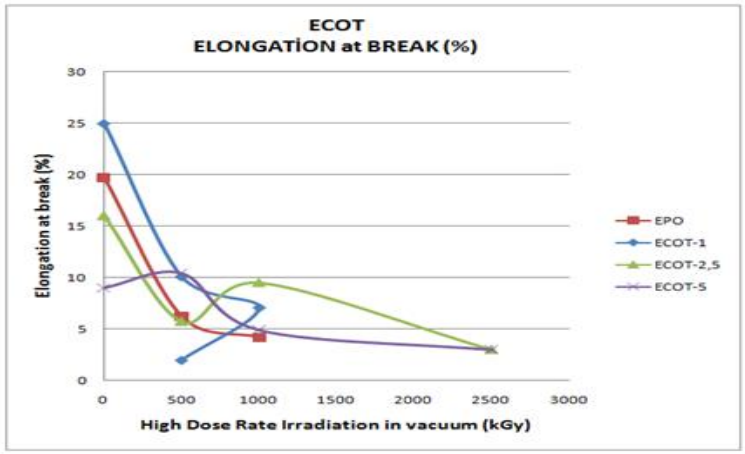

Figure 3.26: Young's modulus, tensile strength and elongation at break for ECOT as a function of absorbed doses by VHDR under vacuum

3.2.1.4 Mechanical Tests for Epoxy-Colemanite (ECOL)

Changing the curing temperature for ECOL samples caused the variations in the Young's modulus remarkably where the values were around 1000 MPa to 1400 MPa (Table 3.9 and Figure 3.27). The highest values were at 120 °C curing temperature than decreased at 200 °C.

Table 3.9: Young's Modulus of Non-irradiated ECOL samples as a function of curing temperature

Young's Modulus (MPa)			
Sample Type	60 °C	120 °C	200 °C
ECOL-1	256	1353	1042
ECOL-2.5	354	1441	1256
ECOL-5	264	976	1009

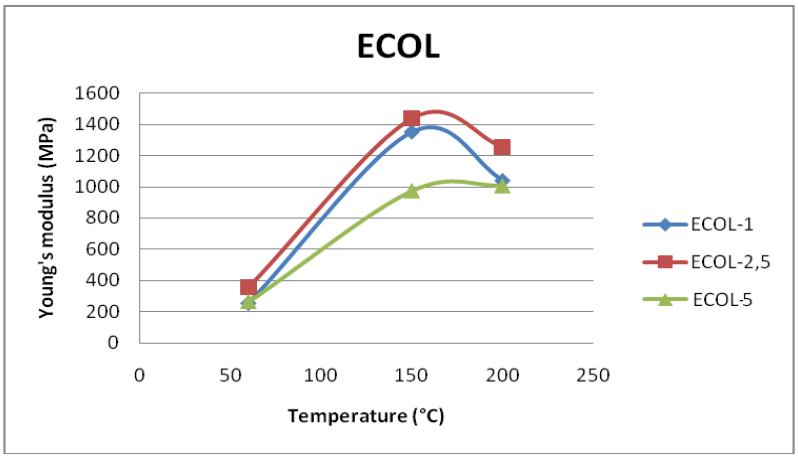

Figure 3.27: Young's Modulus of Non-irradiated ECOL samples as a function of curing temperature

The Young's modulus, tensile strength and elongation at break values for ECOL samples for different doses are shown in Table 3.10 and Figure 3.28-3.30 below.

Table 3.10: Young's Modulus, tensile strength and elongation at break for ECOL as a function of absorbed doses

(Irradiation samples were cured at 60 °C)

Young's Modulus (MPa)										
Sample Type	Non-irradiated	Absorbed dose by LDR in air 54 kGy	Absorbed dose by LDR in air 138 kGy	Absorbed dose by LDR in air 245 kGy	Absorbed dose by HDR in air 500 kGy	Absorbed dose by HDR in air 1000 kGy	Absorbed dose by HDR in air 2500 kGy	Absorbed dose by HDR under vacuum 500 kGy	Absorbed dose by HDR under vacuum 1000 kGy	Absorbed dose by HDR under vacuum 2500 kGy
EPO	200	435	160	740	727	1209	870	554	572	not available
ECOL-1	256	512	580	440	1095	862	870	856	734	850
ECOL-2,5	354	559	577	572	761	612	774	280	510	710
ECOL-5	264	350	726	440	668	638	930	618	717	1200
Tensile Strength (MPa)										
Sample Type	Non-irradiated	Absorbed dose by LDR in air 54 kGy	Absorbed dose by LDR in air 138 kGy	Absorbed dose by LDR in air 245 kGy	Absorbed dose by HDR in air 500 kGy	Absorbed dose by HDR in air 1000 kGy	Absorbed dose by HDR in air 2500 kGy	Absorbed dose by HDR under vacuum 500 kGy	Absorbed dose by HDR under vacuum 1000 kGy	Absorbed dose by HDR under vacuum 2500 kGy
EPO	13	14	6	7	29	35	10	20	17	not available
ECOL-1	15	10	13	8	25	17	33	21	28	15
ECOL-2,5	17	14	10	12	30	12	15	16	25	15
ECOL-5	9	13	14	8	20	16	18	13	18	27
Elongation at Break (%)										
Sample Type	Non-irradiated	Absorbed dose by LDR in air 54 kGy	Absorbed dose by LDR in air 138 kGy	Absorbed dose by LDR in air 245 kGy	Absorbed dose by HDR in air 500 kGy	Absorbed dose by HDR in air 1000 kGy	Absorbed dose by HDR in air 2500 kGy	Absorbed dose by HDR under vacuum 500 kGy	Absorbed dose by HDR under vacuum 1000 kGy	Absorbed dose by HDR under vacuum 2500 kGy
EPO	20	8	16	2	7	5	2	6	4	not available
ECOL-1	36	20	3	3	4	3	6	4	5	3
ECOL-2,5	8	8	3	4	5	3	4	9	8	3
ECOL-5	10	11	3	4	4	3	3	5	5	4

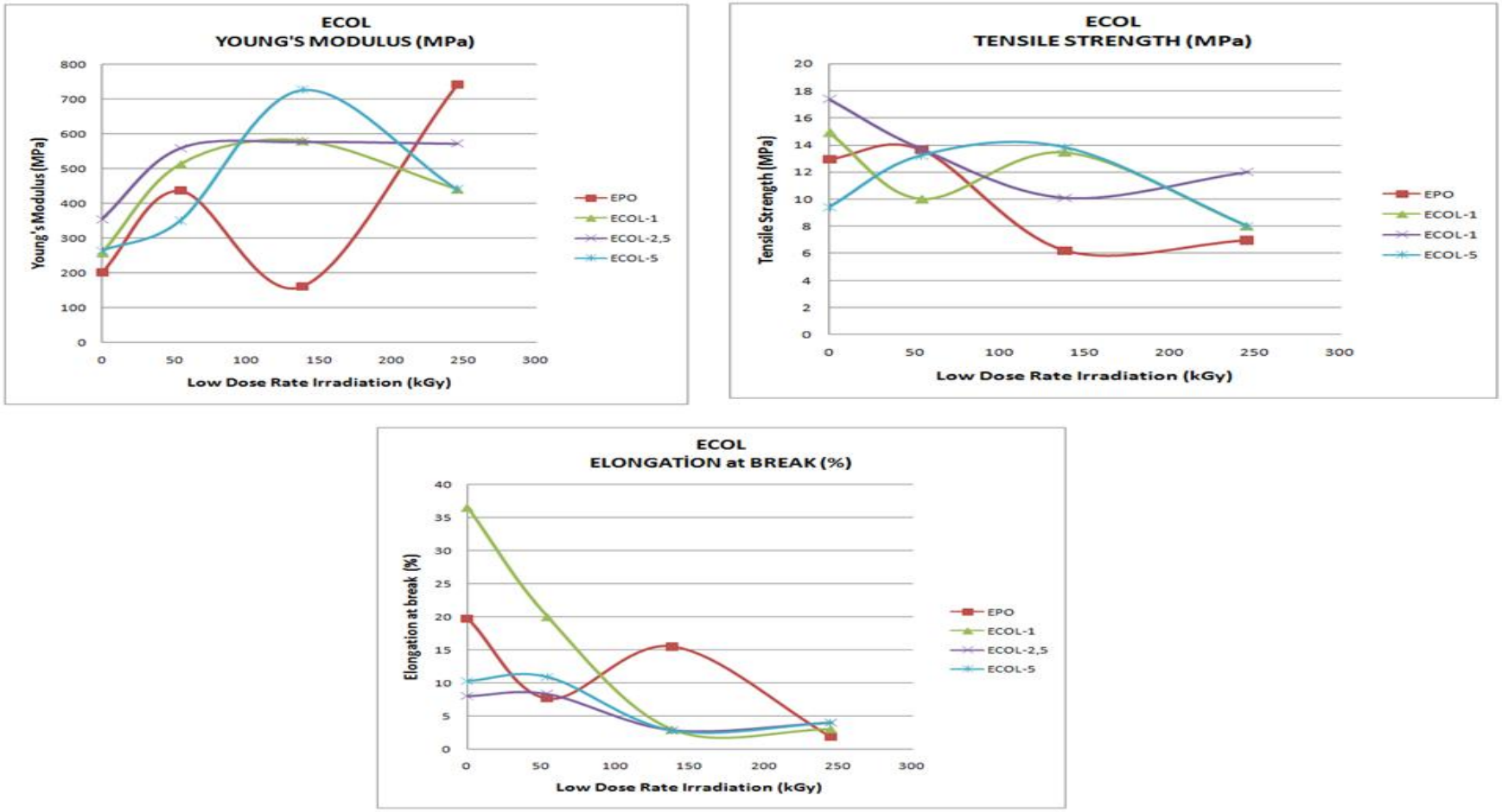

Figure 3.28: Young's modulus, tensile strength and elongation at break for ECOL as a function of absorbed doses by LDR in air

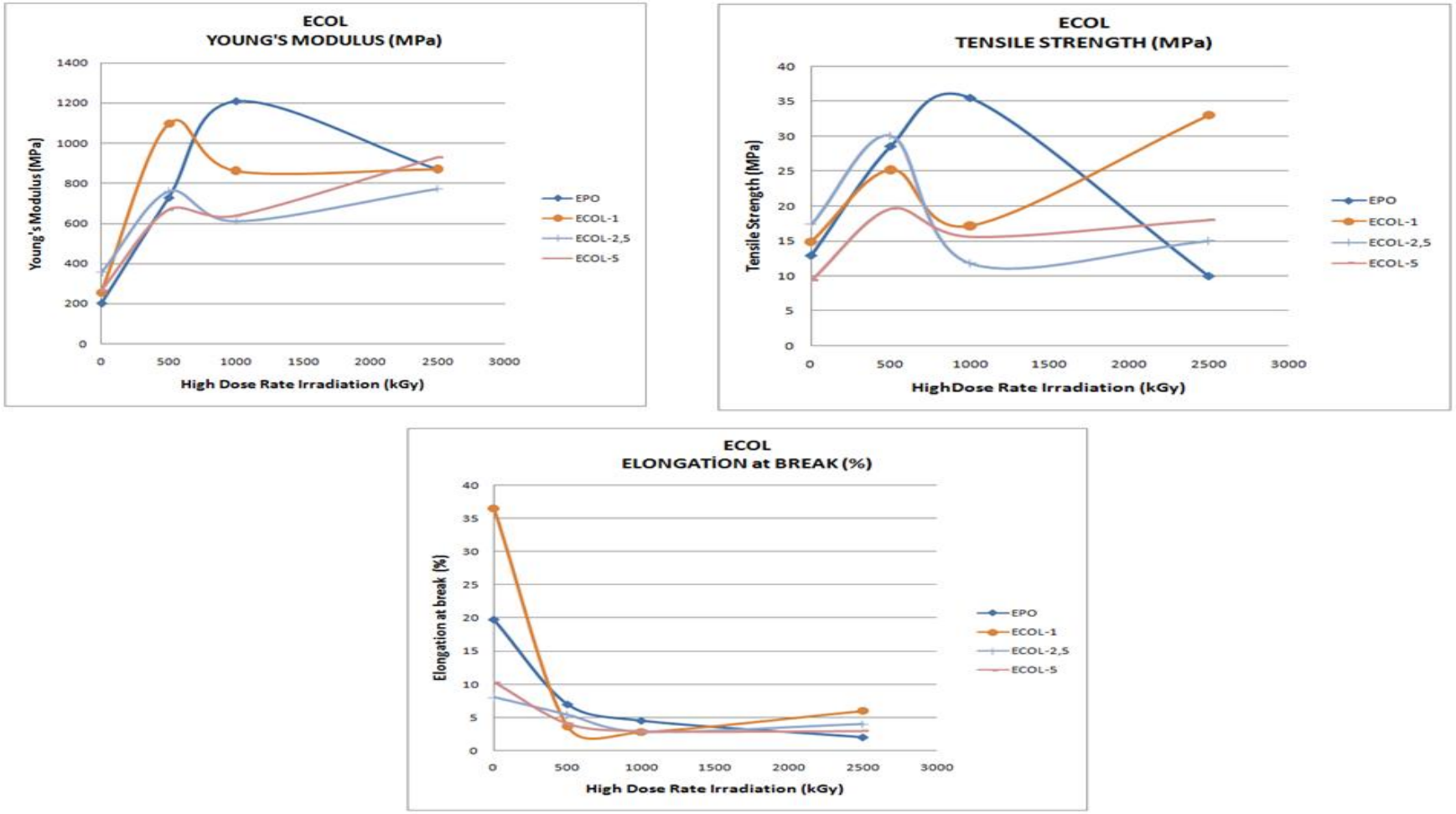

Figure 3.29: Young's modulus, tensile strength and elongation at break for ECOL as a function of absorbed doses by HDR in air

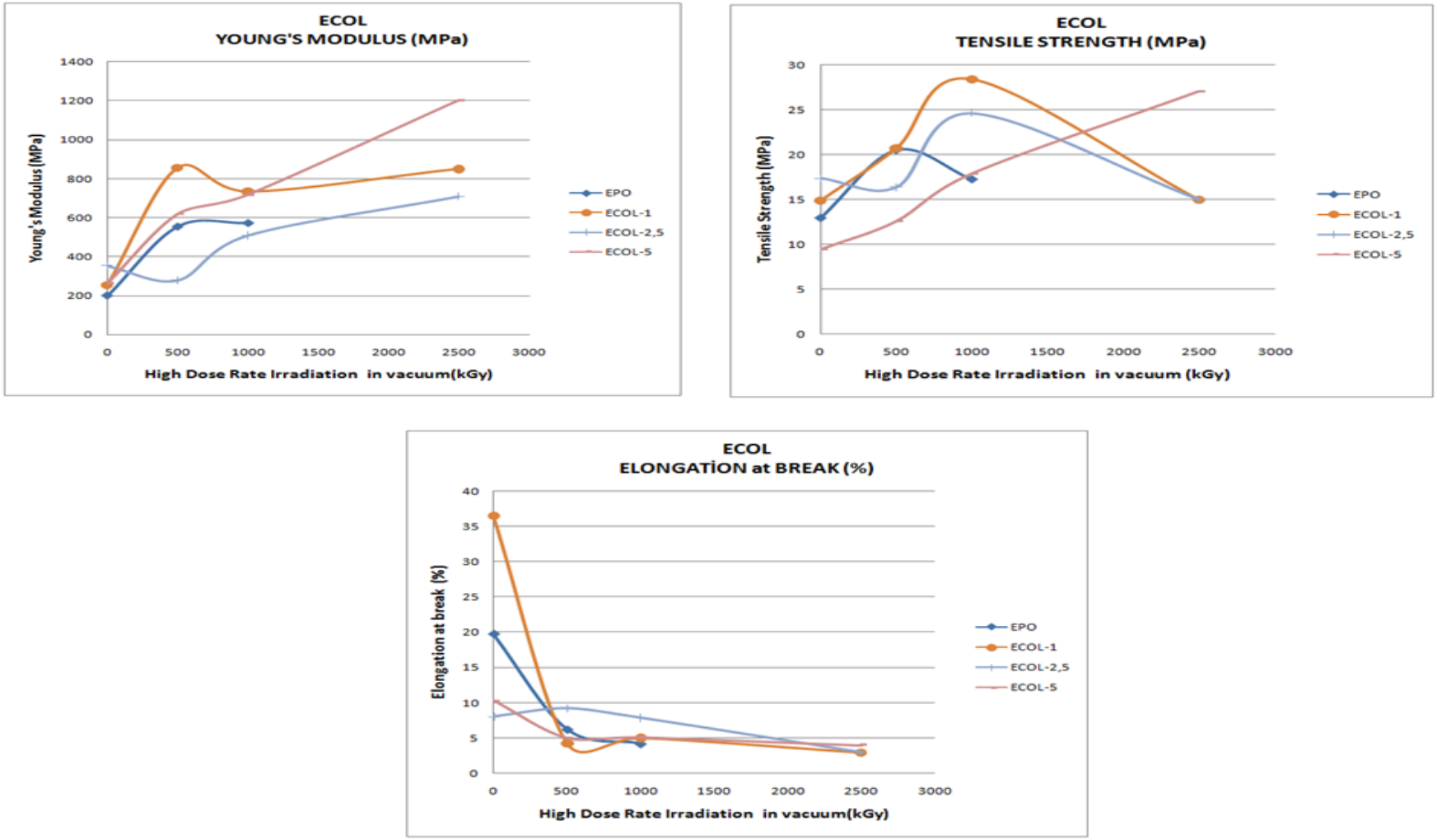

Figure 3.30: Young's modulus, tensile strength and elongation at break for ECOL as a function of absorbed doses by VHDR under vacuum

Low dose rate irradiation for ECOL samples showed that Young's modulus were doubled for ECOL-1 and ECOL-2.5 (Table 3.10 and Figure 3.28). This was because of crosslinking proceeding.

High dose rate irradiation for ECOL samples behavior is same as the curing temperature behavior of ECOL in which an increase occurred at 500 kGy than a decrease at 1000 kGy.

High dose rate irradiation in vacuum results for ECOL samples showed different behaviors (Table 3.10 and Figure 3.30). The tensile strength of ECOL samples at 245 kGy and at 2500 kGy were higher than neat epoxy. This may be caused of colemanite addition which made the polymer resistance against radiation higher.

3.2.1.5 Mechanical Tests for Epoxy-Anhydrous Borax (EANB)

The Young's Modulus of EANB samples increased while the curing temperature increased. The reason can be due to the capacity of polymer resistance against radiation where the crosslinking was continuing till to the highest temperature (Table 3.11 and Figure 3.31).

Table 3.11: Young's Modulus of Non-irradiated EANB samples as a function of curing temperature

Young's Modulus (MPa)			
Sample Type	60 °C	120 °C	200 °C
EANB-1	247	1183	1275
EANB-2.5	226	1177	1477
EANB-5	225	1130	1588

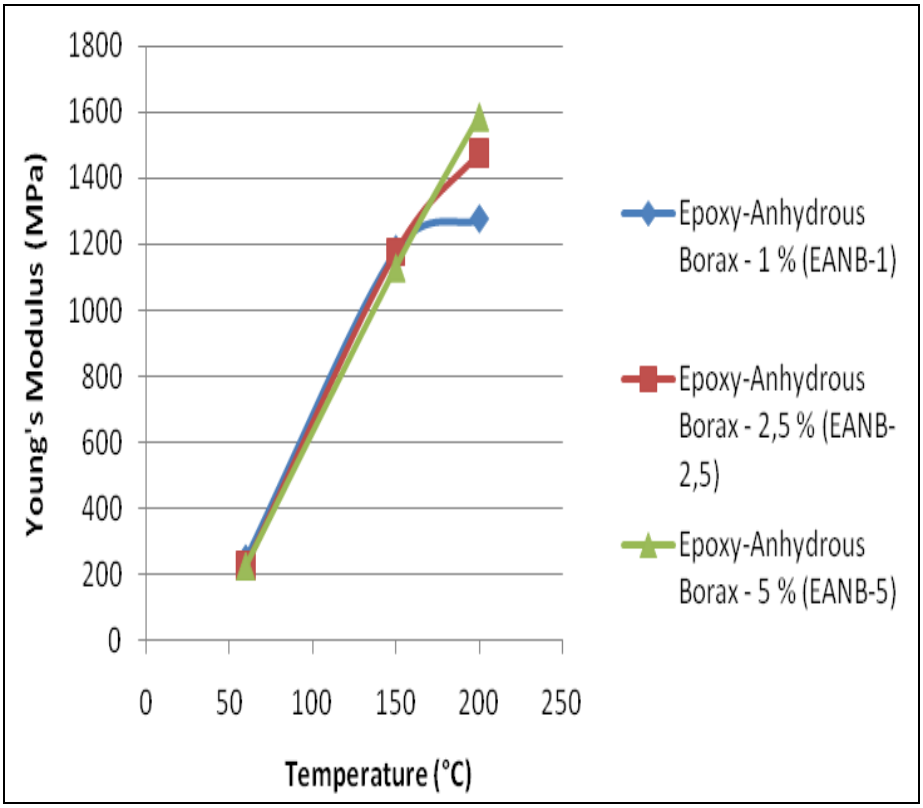

Figure 3.31: Young's Modulus of Non-irradiated EANB samples as a function of curing temperature

The Young's modulus, tensile strength and elongation at break values for EANB samples for different doses are shown in Table 3.12 and Figure 3.32-3.34 below.

Both low and high dose rate irradiations for EANB samples show that Young's modulus was firstly decreased than increased. This was because of chain-scission and crosslinking processes during the irradiation dose changes and showed a periodical behavior.

Table 3.12: Young's Modulus, tensile strength and elongation at break for EANB as a function of absorbed doses

(Irradiation samples were cured at 60 °C)

Young's Modulus (MPa)										
Sample Type	Non-irradiated	Absorbed dose by LDR in air 54 kGy	Absorbed dose by LDR in air 138 kGy	Absorbed dose by LDR in air 245 kGy	Absorbed dose by HDR in air 500 kGy	Absorbed dose by HDR in air 1000 kGy	Absorbed dose by HDR in air 2500 kGy	Absorbed dose by HDR under vacuum 500 kGy	Absorbed dose by HDR under vacuum 1000 kGy	Absorbed dose by HDR under vacuum 2500 kGy
EPO	200	435	160	740	727	1209	870	554	572	not available
EANB-1	247	559	163	782	840	748	not available	883	not available	not available
EANB-2,5	226	403	126	865	858	431	710	589	809	not available
EANB-5	225	378	148	762	763	457	580	415	641	not available
Tensile Strength (MPa)										
Sample Type	Non-irradiated	Absorbed dose by LDR in air 54 kGy	Absorbed dose by LDR in air 138 kGy	Absorbed dose by LDR in air 245 kGy	Absorbed dose by HDR in air 500 kGy	Absorbed dose by HDR in air 1000 kGy	Absorbed dose by HDR in air 2500 kGy	Absorbed dose by HDR under vacuum 500 kGy	Absorbed dose by HDR under vacuum 1000 kGy	Absorbed dose by HDR under vacuum 2500 kGy
EPO	13	14	6	7	29	35	10	20	17	not available
EANB-1	16	18	8	8	26	15	not available	23	not available	not available
EANB-2,5	11	17	5	21	11	9	10	19	28	not available
EANB-5	11	12	9	10	24	9	11	15	24	not available
Elongation at Break (%)										
Sample Type	Non-irradiated	Absorbed dose by LDR in air 54 kGy	Absorbed dose by LDR in air 138 kGy	Absorbed dose by LDR in air 245 kGy	Absorbed dose by HDR in air 500 kGy	Absorbed dose by HDR in air 1000 kGy	Absorbed dose by HDR in air 2500 kGy	Absorbed dose by HDR under vacuum 500 kGy	Absorbed dose by HDR under vacuum 1000 kGy	Absorbed dose by HDR under vacuum 2500 kGy
EPO	20	8	16	2	7	5	2	6	4	not available
EANB-1	12	5	7	2	5	3	not available	5	not available	not available
EANB-2,5	10	8	32	4	3	3	3	5	5	not available
EANB-5	15	6	30	3	5	3	3	6	5	not available

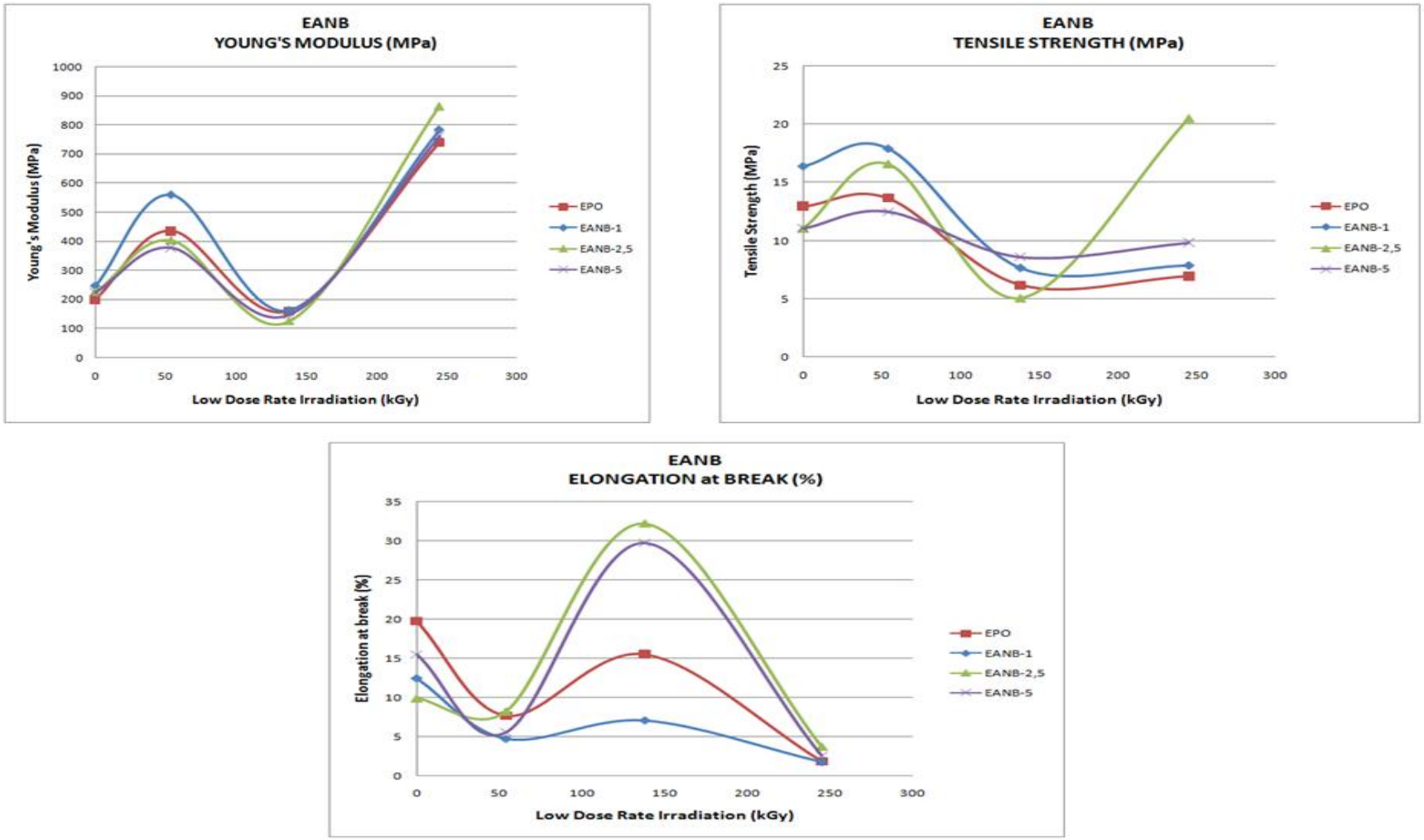

Figure 3.32: Young's modulus, tensile strength and elongation at break for EANB as a function of absorbed doses by LDR in air

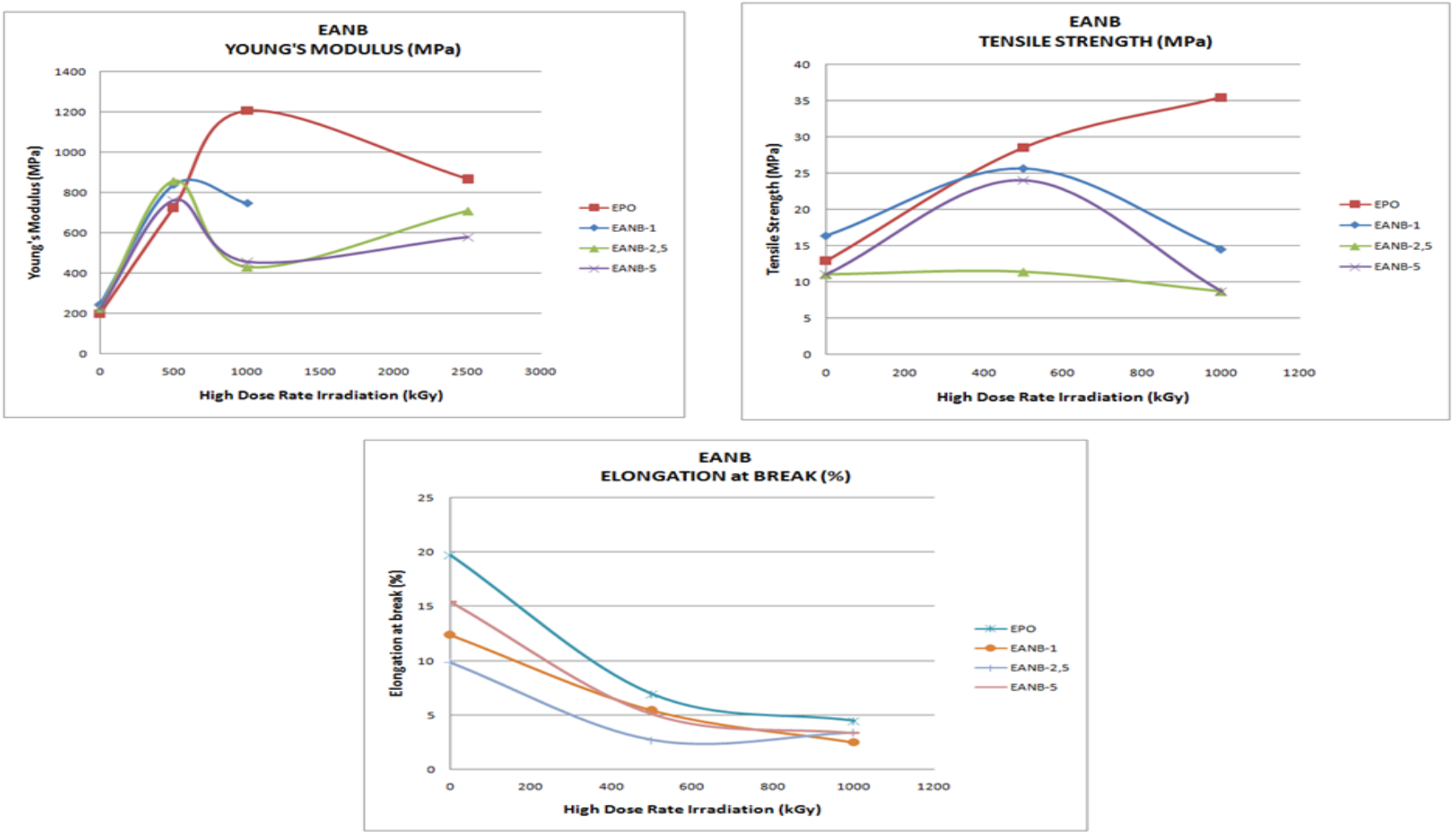

Figure 3.33: Young's modulus, tensile strength and elongation at break for EANB as a function of absorbed doses by HDR in air

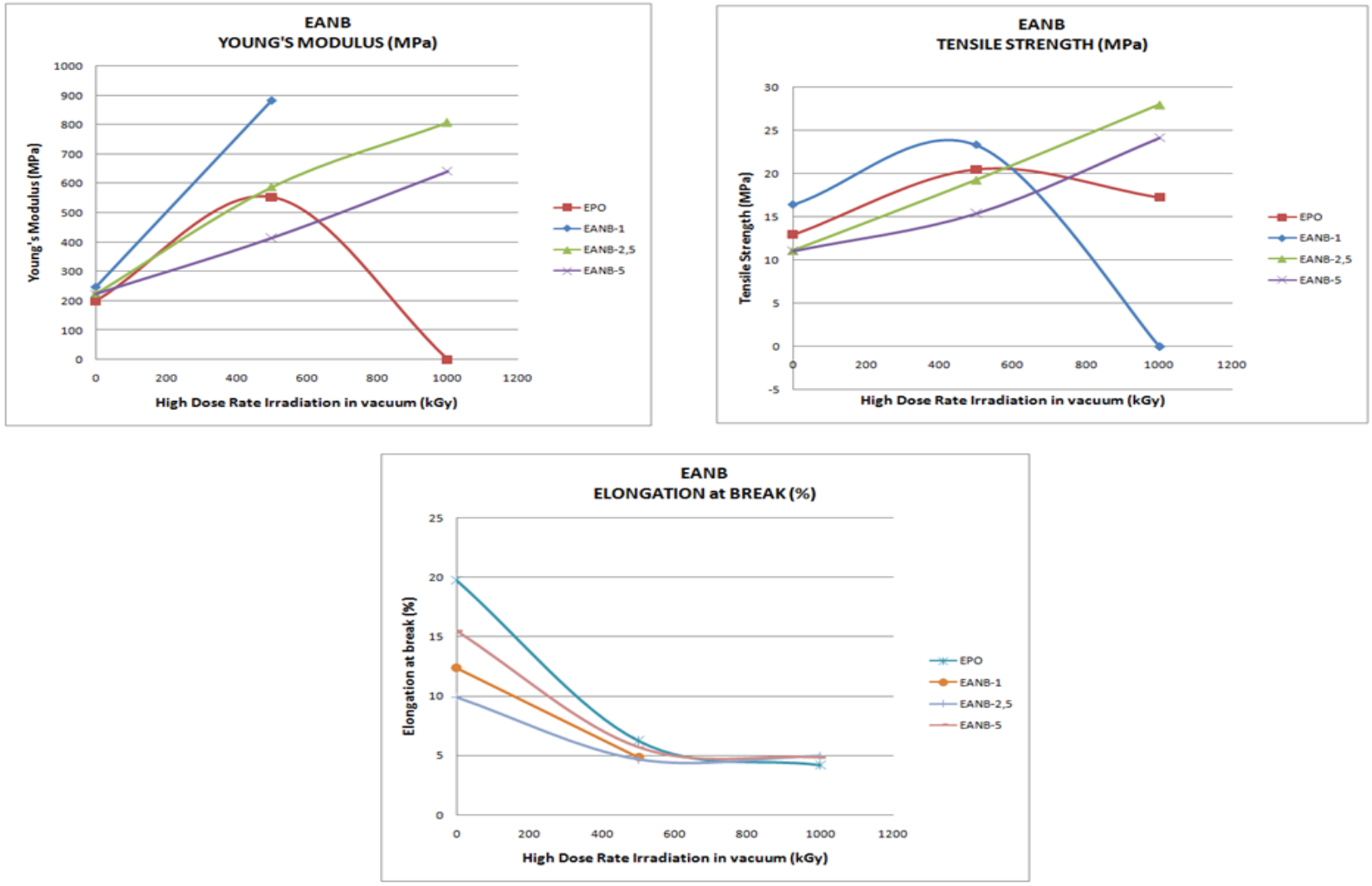

Figure 3.34: Young's modulus, tensile strength and elongation at break for EANB as a function of absorbed doses by VHDR under vacuum

3.2.1.6 Summary of Mechanical Tests

According to mechanical test results, the highest tensile strength (33 MPa at 2500 kGy HDR) and the highest Young's modulus (1095 MPa at 500 kGy LDR) were achieved for ECOL-1 sample in LDR and HDR conditions.

The epoxy-boron samples showed three stages during the irradiations. This ''increment-decrement-increment'' phenomenon is called as periodical behavior [116]. An explanation of the periodical behavior might be related to the fact noted as irradiation causes chain scission, but it also produces relaxation and cage breaking (CB). CB is the breaking of bonds under deformation where linked atoms are compelled to be separated from the original cages.

Similar observations with mechanical tests have been shown in the study of Chang [117]. In that study, as the irradiation dose increased, the free radicals concentration of system increased, which meant that low dose irradiation would induce some weak chemical bonds to be broken and resulted in molecular chain to be ruptured [118]. When irradiation dose reached more higher, chain crosslinking reactions would become the dominant reactions. By further raising irradiation dose, the free radicals concentrations would ascend again since higher energy radiation would cause more and more chains scission. This showed that there is a competition reaction between chain scission and chain crosslinking when the resin is irradiated by γ -rays [119]. However, with the increase of irradiation dose, thermal stability and mechanical properties of composites decreased firstly, then increased slightly, and declined sharply at the end due to competition reaction between chain scission and cross-linking originated from γ-rays radiation.

3.2.2 Attenuated Total Reflection Fourier Transform Infrared Spectroscopy (ATR-FTIR)

FTIR determined the identifications of functional groups and crosslinking occurred in compounds [120]. ATR-FTIR results can be used to estimate chemical structure of samples and reactions occurred in structure via curing and irradiation process.

3.2.2.1 ATR-FTIR Results of Boron Minerals

The affinity for oxygen of the boron is high so that it allows forming strong covalent bonds between boron and oxygen that makes compounds known as borates. Borate minerals with crystalline structure are composed of both trigonal and tetrahedral borate units. These units can connect through B-O-B bonds to form chain polyborates or they may connect with three or four boron atoms of the rings, that is, tri- and tetraborates.

Basic structure of COL is endless B-O chains (Figure 3.35) where it has some differences with COT, CAT and ANB minerals where COL has more trigonal units than tetrahedral units in its crystal structure. The more trigonal units means the more intense of BO_4 and B-OH bands. Many borate minerals contain waters of hydration.

The spectra of colemanite are complex especially in the IR spectrum. This complexity comes from the bands of four different coordination polyhedra namely BO_3^3, $B(OH)_3$, BO_4^5 and $B(OH)_4$. The infrared bands at 1019 and 1044 cm^{-1} are attributed to the trigonal symmetric stretching mode. The intense infrared bands at 887 and 933 cm^{-1} with shoulder bands at 838, 856 and 958 cm^{-1} are attributed to water librational (restricted rocking motions) bands.

The IR spectrum of colemanite shows complexity in the 650–800 cm^{-1} with several infrared bands being observed. IR bands are found at 669, 674, 692, 718 and

731 cm $^{-1}$. These bands may be related to the out-of-plane BOH bending modes. In a manner the same spectral pattern is observed for the IR spectrum in Figure 3.35.

The mineral colemanite is characterized by a very intense sharp band at 3605 cm $^{-1}$ attributed to the stretching vibration of OH units from water. Infrared spectra of colemanite are identified by more than one water stretching band. These bands indicate water as an important structure in the colemanite. The other observed IR bands are at 2846, 3040, 3154, 3230, 3305, 3423 and 3532 cm $^{-1}$. These bands are the other water stretching vibration bands.

The characteristic FT-IR spectra of ANB, CAT and COT samples can be seen from Figure 3.35. Peaks can be represented as;

- 705 cm^{-1} of B-O-B ring bending,
- 880 and 1255 cm^{-1} of bending of B-OH. These peaks could not be appeared at ANB because of absence of the B-OH units.
- 820, 990, 1075 and 1130 cm^{-1} of stretching of tetragonal units (BO_4)
- 940, 1340 and at 1425 cm^{-1} of stretching of trigonal boron groups (BO_3)
- 3345 cm^{-1} bending of O-H [120-127].

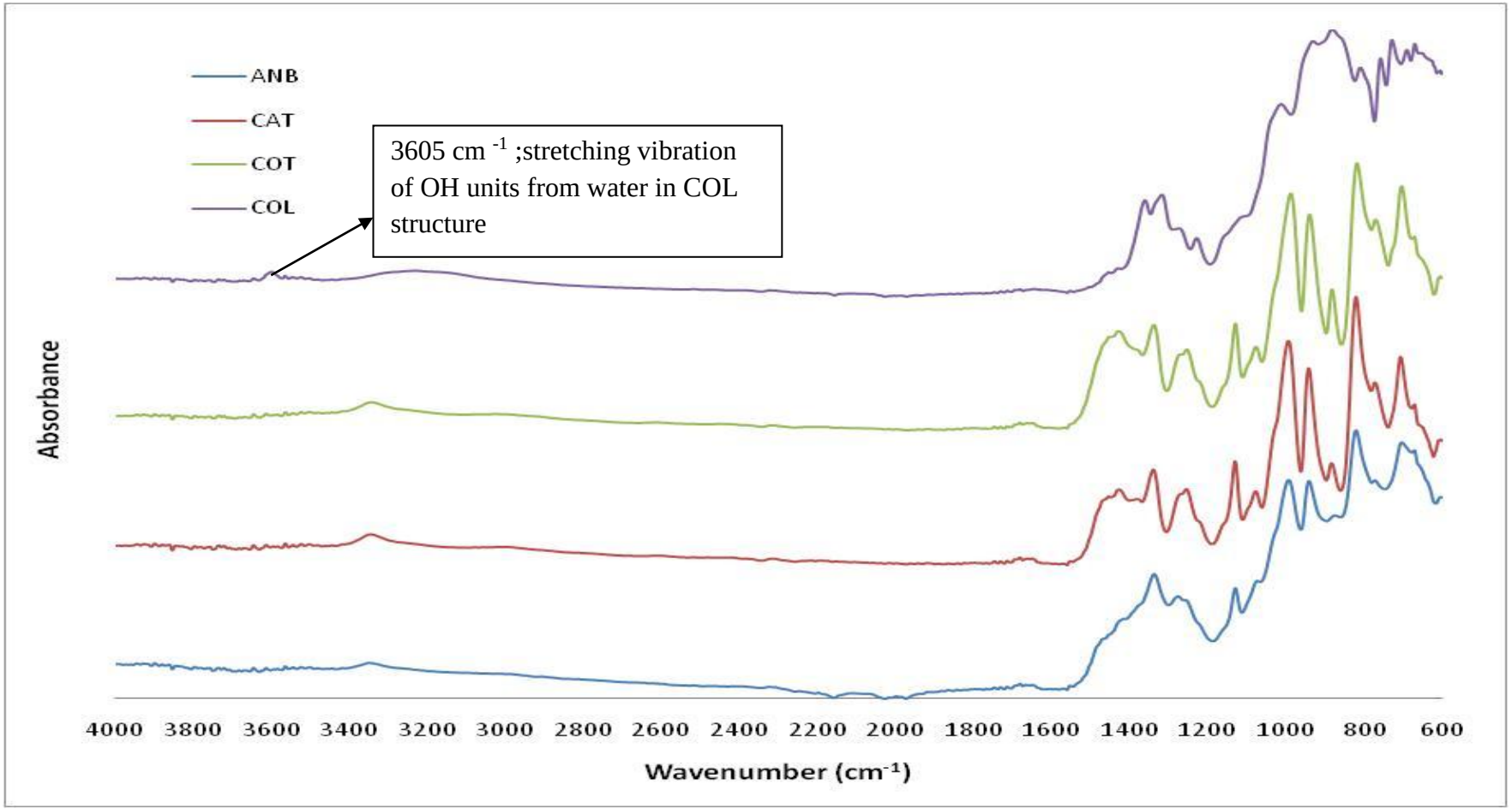

Figure 3.35: ATR-FTIR spectrum of Boron Minerals

3.2.2.2. ATR-FTIR Results of Neat Epoxy Samples

The ATR-FTIR bands of the epoxy appeared at 1290 cm^{-1}, 1245 cm^{-1} and 1120 cm^{-1} showed the symmetric and asymmetric stretching vibrations of C-O band [128-129]. The peaks observed at 3040 cm^{-1}, 1600 cm^{-1}, 1514 cm^{-1} and 822 cm^{-1} are also characteristic of aromatic ring, while the peak at 1190 cm^{-1} indicates the stretching vibration in ether band [129-130].

The peaks observed at 2800–2990 cm^{-1} region are characteristic of methyl structures where it decreases after irradiation. This was related to the crosslinking. and the peaks at 3100 and 3600 cm^{-1} are characteristic of the stretching vibration of OH group.

There was a decrease at 1510 cm^{-1} by increasing absorbed irradiation dose related to the chain scission in the backbone of the epoxy system.

After irradiations, a decrease in intensities of some absorption bands such as C-CH_3 indicates that the C-CH_3 groups were degraded. Peaks around 1040 cm^{-1} and around 1250 cm^{-1} of which represent the stretching vibrations of olefinic (C-C) and carbonyl groups (C-O) decreased as shown in Table 3.13 and Figure 3.36 [129-131].

Table 3.13: ATR-FTIR absorption bands of DGEBA resin [132]

Peak (cm^{-1})	**Functions**
3340	residual OH
2900, 1500, 1450	methylene CH
3040, 1600, 760	Para-substituted aromatic ring
1230	aromatic OC (Ar-O)
1030, 1090, 1180	CO alcohols and ethers
910, 830	epoxy

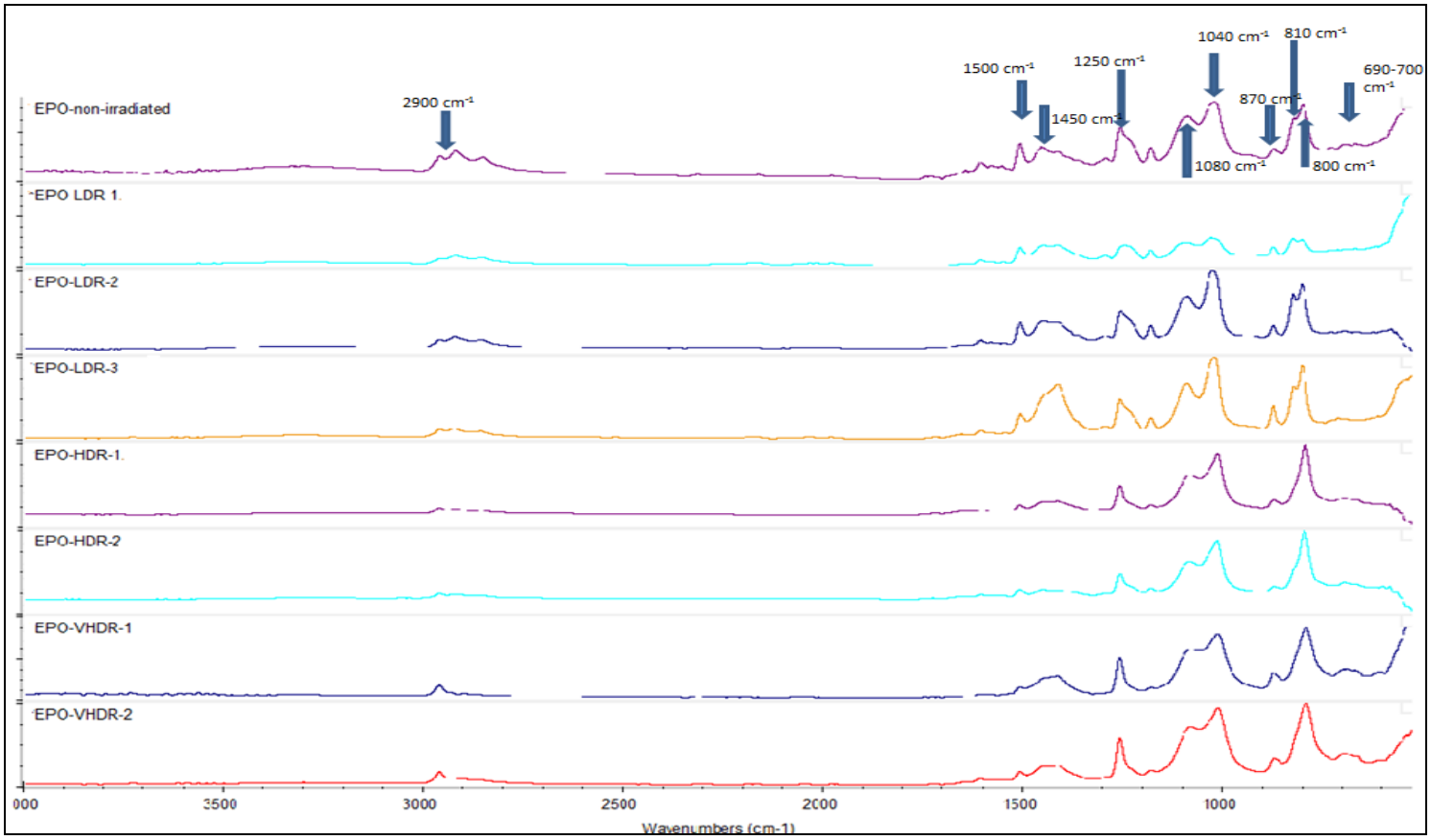

Figure 3.36: ATR-FTIR spectrum of EPO under different irradiations

3.2.2.3. ATR-FTIR Results of Epoxy-Boron Samples

The investigated samples by ATR-FTIR were cured at 60 °C and at concentration of 2.5 % boron minerals (Figures 3.37–3.40). The intensities were investigated after normalization as described Section 2.3.4. The absorption intensity of 1454 cm^{-1} means the scissoring of -CH_3 band increased while total dose of low dose rate increased. In high dose and vacuum irradiation processes, the intensity of 1454 cm^{-1} band was also increased while total dose increased. These changes indicate that the resin cured at a higher irradiation doses has a lower conversion of reactive groups [133]. Higher bonds after reinforcement by boron minerals showed chain scission as a result of degradation where partially blocked and this could be related to positive effect of boron minerals on shielding against radiation.

It was noticed that when the total dose was raised the relative intensities of the band at 813, 1185 and 1252 cm^{-1} increased and those of the band at 806 cm^{-1} decreased. Such changes are supposed to be connected with the rotational isomerism [134]. If the bands of the samples showed higher intensity by increasing irradiation doses, it can be caused from prevention of formation of crosslinks.

Bands of aromatic ring at 875 cm^{-1} and 1370 cm^{-1}, and bands in the region of 2600-3100 cm^{-1} lowering can be attributed to prevention of degradation and oxidizing reactions due to beginning of high dose irradiation by boron minerals.

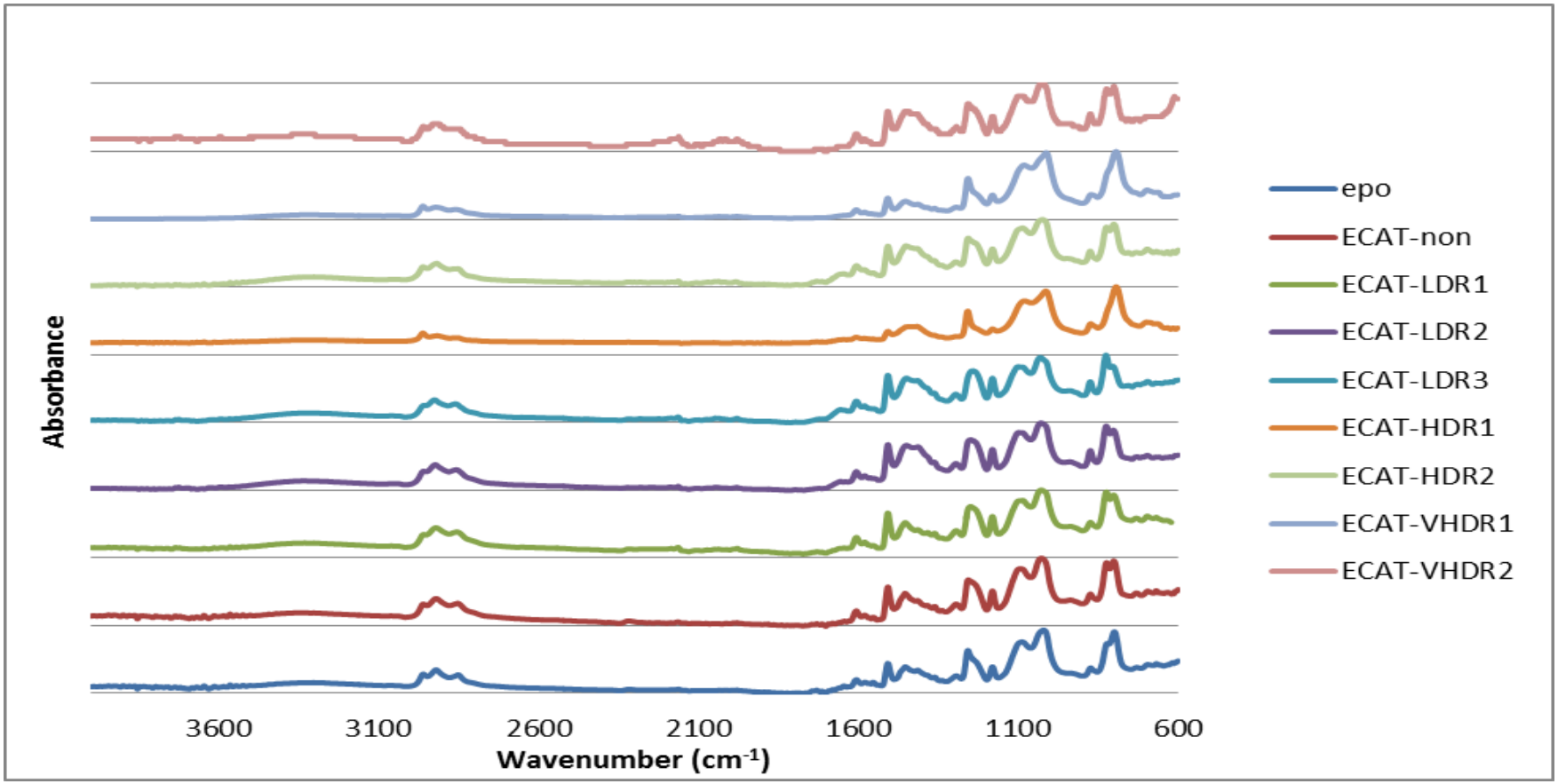

Figure 3.37: FTIR spectrum of ECAT-2,5 samples

(Samples were cured at 60 °C)

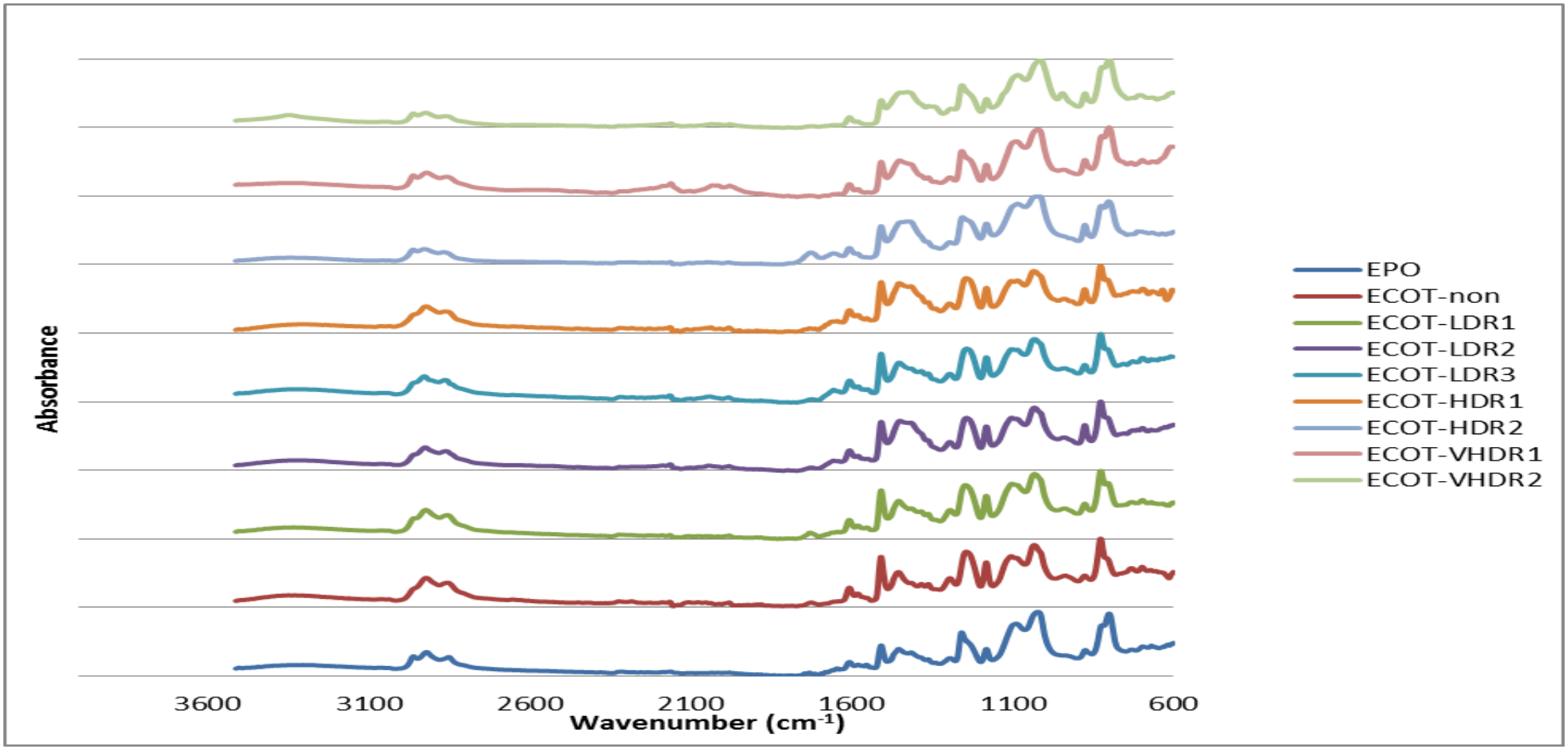

Figure 3.38: FTIR spectrum of ECOT-2,5 samples

(Samples were cured at 60 °C)

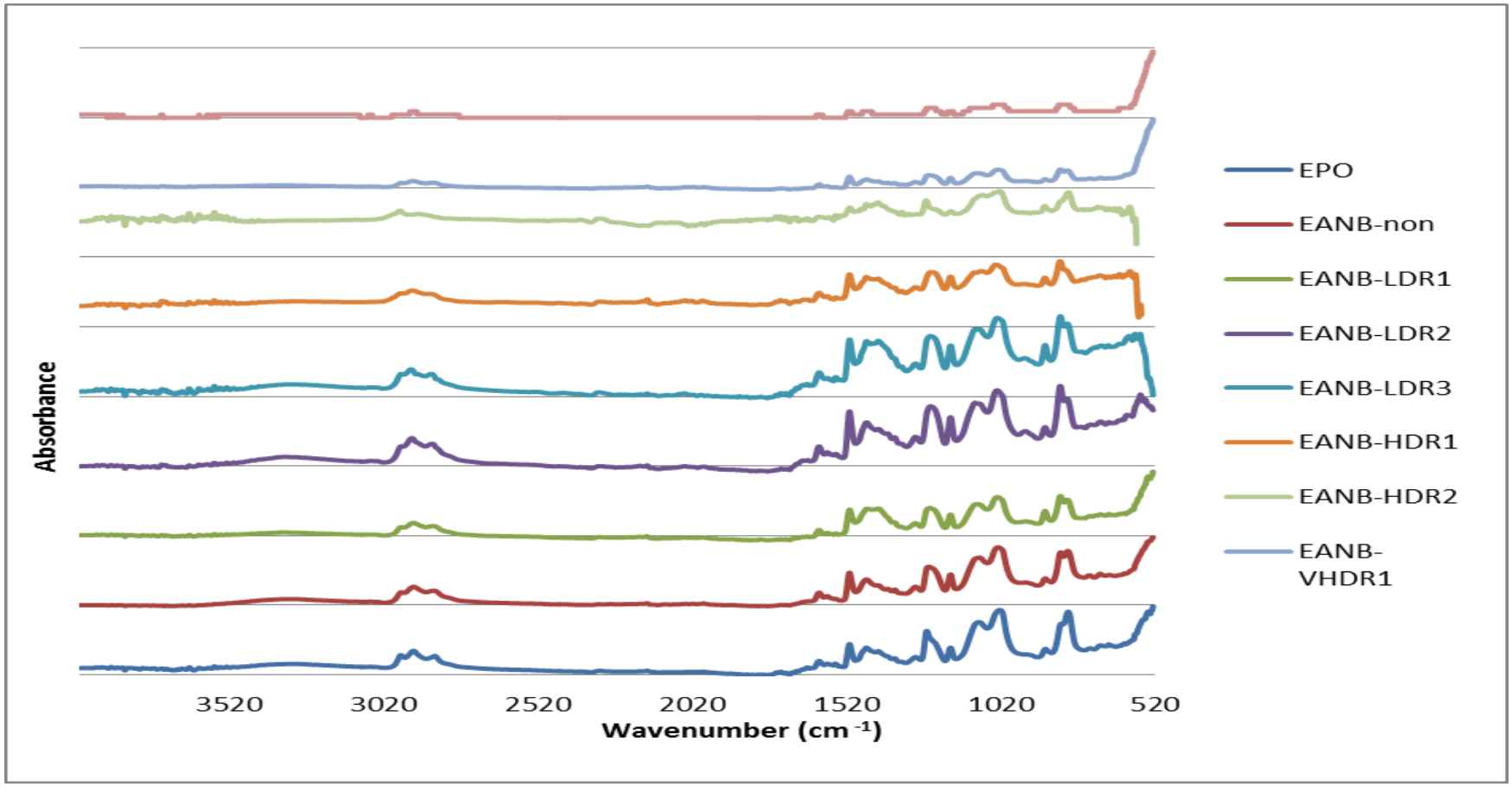

Figure 3.39: FTIR spectrum of EANB-2,5 samples

(Samples were cured at 60 °C)

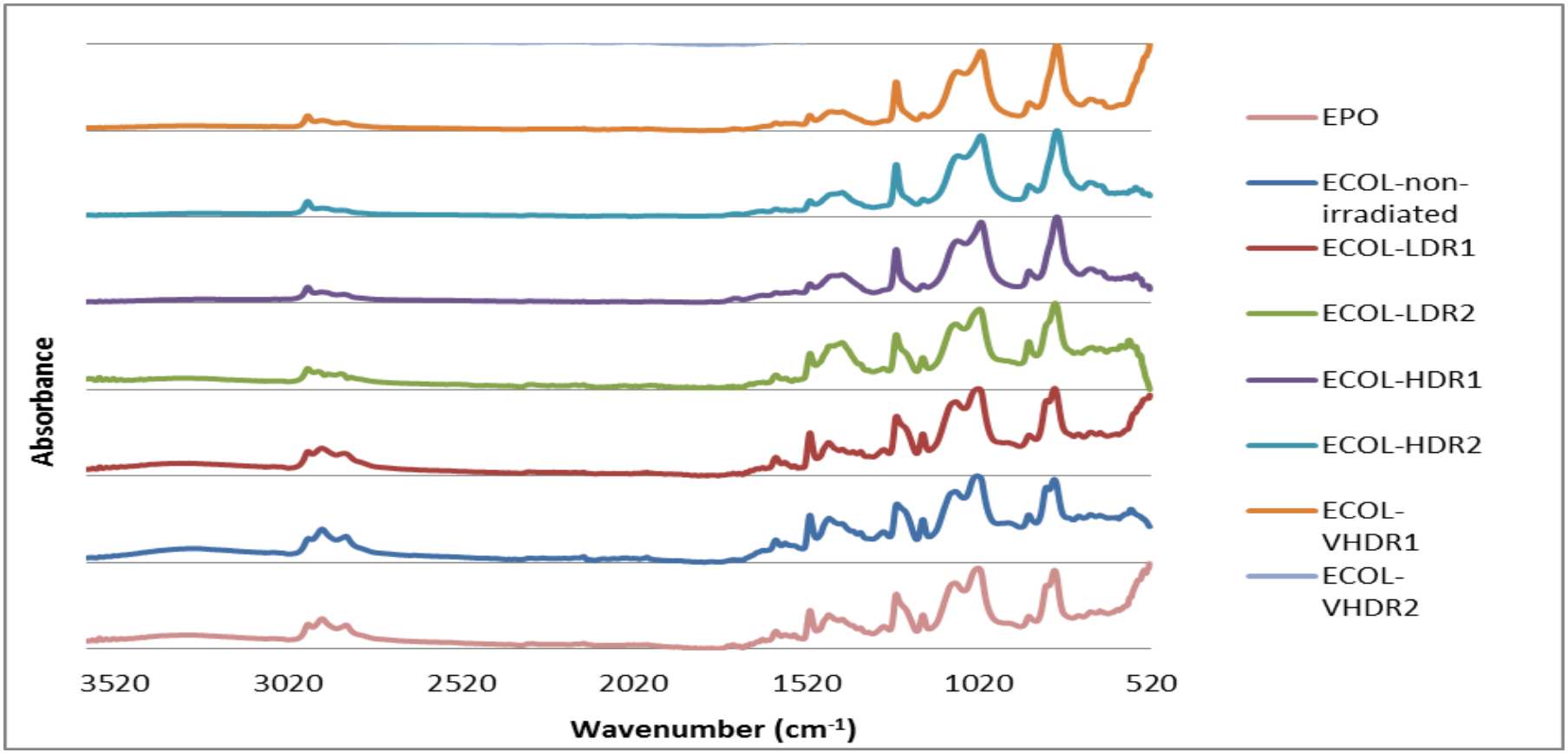

Figure 3.40: FTIR spectrum of ECOL-2,5 samples

(Samples were cured at 60 °C)

3.2.3 Dynamic Mechanical Analysis (DMA)

Various analytical methods have been used to characterize the reaction process of the curing of thermosets, such as Dynamic Mechanical Analysis (DMA) and Differential Scanning Calorimetry (DSC). DMA was carried out to determine the improvement of the mechanical properties after the adding of the boron particles into the polymer matrix.

DMA is the technique used to measure damping which is the measure of the energy dissipation of the material and stiffness by using the properties of the materials as a function of time, temperature, atmosphere, stress and frequency.

The results of the DMA tests indicate that there is an increase in T_g for the CAT and COT-reinforced filled epoxies with reference to unreinforced neat epoxy (Table 3.13). It is clear that the reinforcement is affecting the crosslinking process. The increasing in T_g is consistent with adding nano-reinforcement particles in other host materials that induce to the production of glassy-state polymeric systems [135-137].

The results of the DMA tests indicate that there was not any significant change in T_g for the ANB and COL-reinforced filled epoxies with reference to unreinforced neat epoxy (Table 3.14). It appears that the reinforcement is not affecting the crosslinking process significantly. The increase in T_g is consistent with the increasing in irradiation dose remarkably.

All boron minerals caused an increase on T_g of epoxy-boron samples. Because of the highly crystalline structure of boron minerals they are rigid materials. Therefore, when the mobility of the chains close to reinforcement particles is reduced, these results could be predictable.

Table 3.14: T_g comparison of neat-epoxy as a function of absorbed doses and non-irradiated epoxy-boron samples (Samples were cured at 60 °C)

Sample	T_g (°C)
EPO-Non Irradiated	50.03
EPO-LDR-3	51.63
EPO-HDR-3	69.80
EPO-VHDR-3	69.66
ECOL-2.5-Non	50.04
EANB-2.5-Non	51.19
ECAT-2.5-Non	53.85
ECOT-2.5-Non	54.10

The tan δ peak position for neat epoxy samples, which is a measure of the glass transition temperature (T_g), shifted to higher temperatures with irradiation (Figure 3.41). This is typically attributed in epoxies to an increase in the degree of crosslinking and following decrease in the molecular weight between crosslinks [135-138].

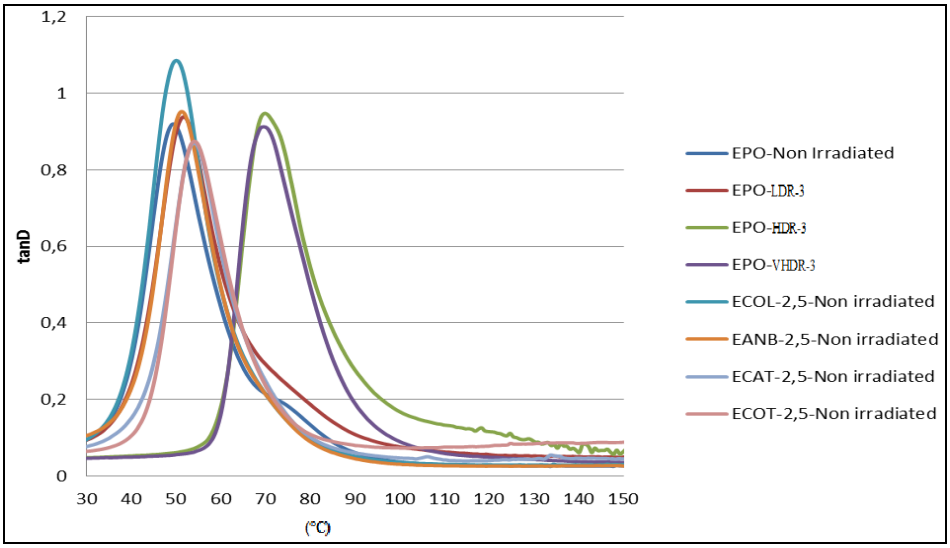

Figure 3.41: DMA results comparison of neat-epoxy as a function of absorbed doses and non-irradiated epoxy-boron samples

(Samples were cured at 60 °C)

3.2.4 Thermogravimetric Analysis (TGA)

TGA is one of the basic analysis methods to determine weight loss of the material function of increasing temperature in a controlled environment. TGA analysis was done in N_2 atmosphere with LECO TGA701 Thermogravimetric Analyzer.

The results of the TGA analysis are shown in Figure 3.42 and 3.43. A weight loss of about 100 % was observed for epoxy due to thermal degradation.

Thermal stability of anhydrous borax was up to 900 °C then a weight loss occurred after 110 °C due to moisture. The weight loss of calcined tincal started around 100 °C and after 150 °C, it was decreased with a constant ratio up to 600-650 °C. The theoretical water and OH- content of calcined tincal is 15 % by weight, but the loss percentage of its initial weight was 20 % so that moisture could contribute this extra weight loss.

The weight loss of concentrated tincal started at 75 °C which was related to loss of lattice water in its structure. The theoretical water and OH- content of concentrated tincal is 47.2 %, but the loss of its initial weight was 47.2 % by weight so that it could keep some OH- groups.

Colemanite showed quite differences when compared with other minerals. Thermal stability was up to 390 °C and then it started to lose its weight. This result stated that the polymeric structure of colemanite gave some extra stability itself. The weight was decreased to 62.3 % of its initial value and which meant it lost water more than its theoretical water and OH- content which is 21.9 % by weight.

It is significantly observed that the weight of COT and CAT increased due to the buoyancy effect of the gas flow in TGA. The reason was the increasing force of the gas made an impact on sample crucibles with the increase of velocity of gas flow at high temperatures.

From the weight loss of the composite samples, neat epoxy and neat minerals, it is clear that the weight loss of the composites was due to the degradation of the epoxy. Therefore, the total weight loss is proportional to the weight fraction of the epoxy [139]. Only the decomposition temperature shifted to the right which is about 10 °C increasing because of the boron minerals effects.

The same trends were observed for mineral composites. No significant influence of boron minerals on degradation was observed. Only the maximum decomposition temperature T_{max} is higher for ECAT-2.5-Non irradiated and EANB-2.5-Non irradiated.. Also the decomposition percentage of EPO-LDR-3 was higher than EPO-HDR-3 at the beginning of the progress.

The difference of final percentage of weight loss between the mineral composites came from the different water content in the mineral composition.

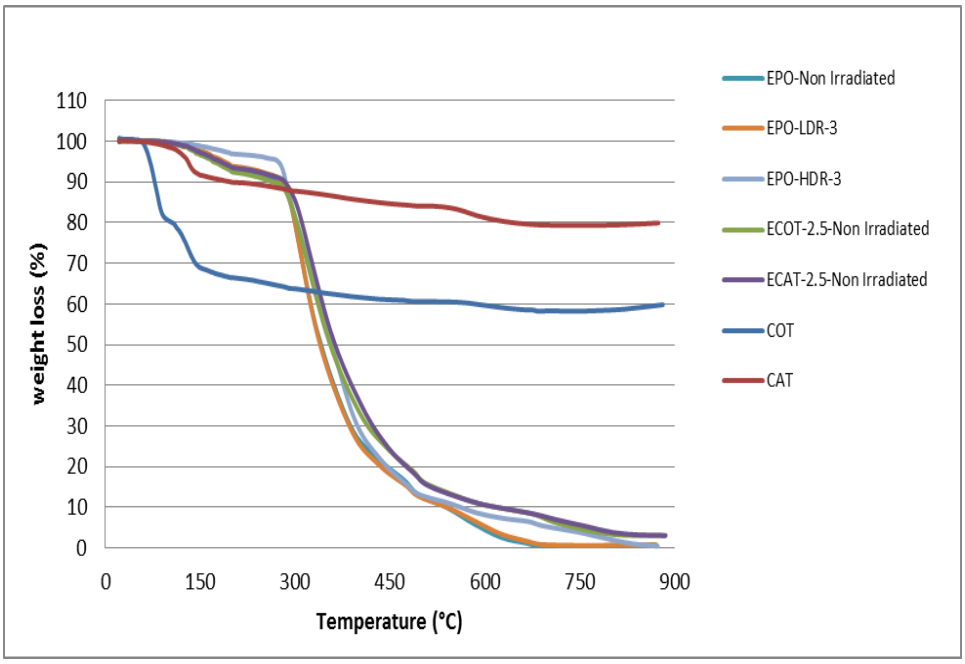

Figure 3.42: TGA curves of neat-epoxy as a function of absorbed doses, neat calcined tincal, neat concentrated tincal, ECAT-2.5-non-irradiated and ECOT-2.5-non-irradiated samples

(Samples were cured at 60 °C)

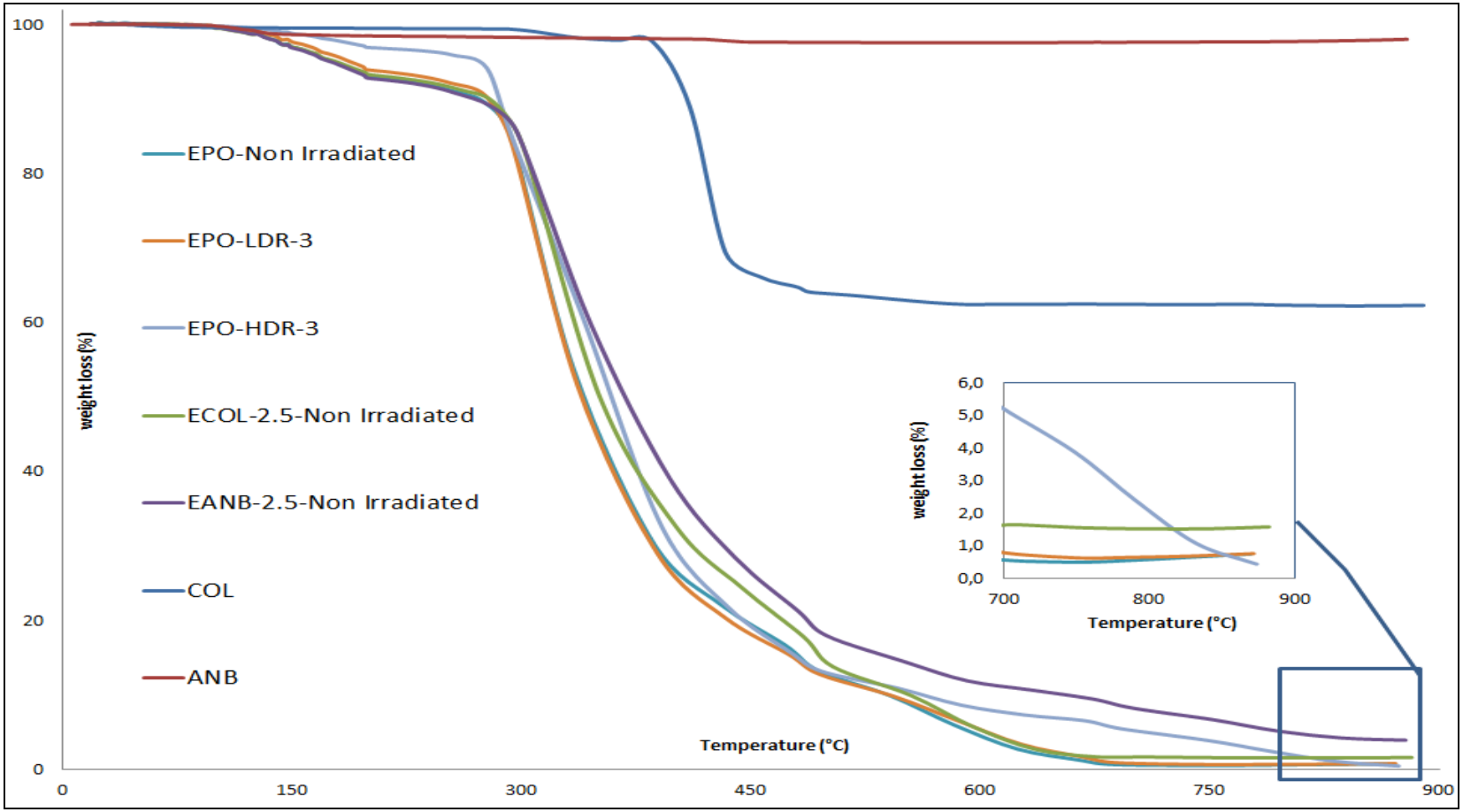

Figure 3.43: TGA curves of neat-epoxy as a function of absorbed doses, neat calcined tincal, neat concentrated tincal, EANB-2.5-non-irradiated and ECOL-2.5-non-irradiated samples (Samples were cured at 60 °C)

3.2.5 Scanning Electron Microscopy (SEM)

FE-SEM is a type of microscope that scans a focused beam of high-energy electrons over a surface to generate various signals at the surface of solid specimens which produces images of the sample. The electrons in the beam interact with atoms in the solid specimens, producing a variety of signals to be detected and that reveal information about the sample's surface topography and composition. FE-SEM analysis were done with Zeiss Supra 55.

FE-SEM was used to observe the morphology of the samples. FE-SEM images of the composite samples were acquired to verify the dispersion of boron minerals to evaluate the interface between the filler and epoxy (Figures 3.44 - 3.53).

The epoxy-boron samples showed smooth and ripples-full morphology that implies the brittle property of the composites used in the study. There were many irregular granules that uniformly distributed in the composites which were boron minerals.

Even the surface of the neat epoxy had cracks, this came from the curing where the interfacial weakness occurred between epoxy and boron minerals. Also, the fracture surfaces of the epoxy-boron samples increased while the irradiation doses were increased. Presumedly, this came from the oxidation reaction during the irradiation where free radicals occurred.

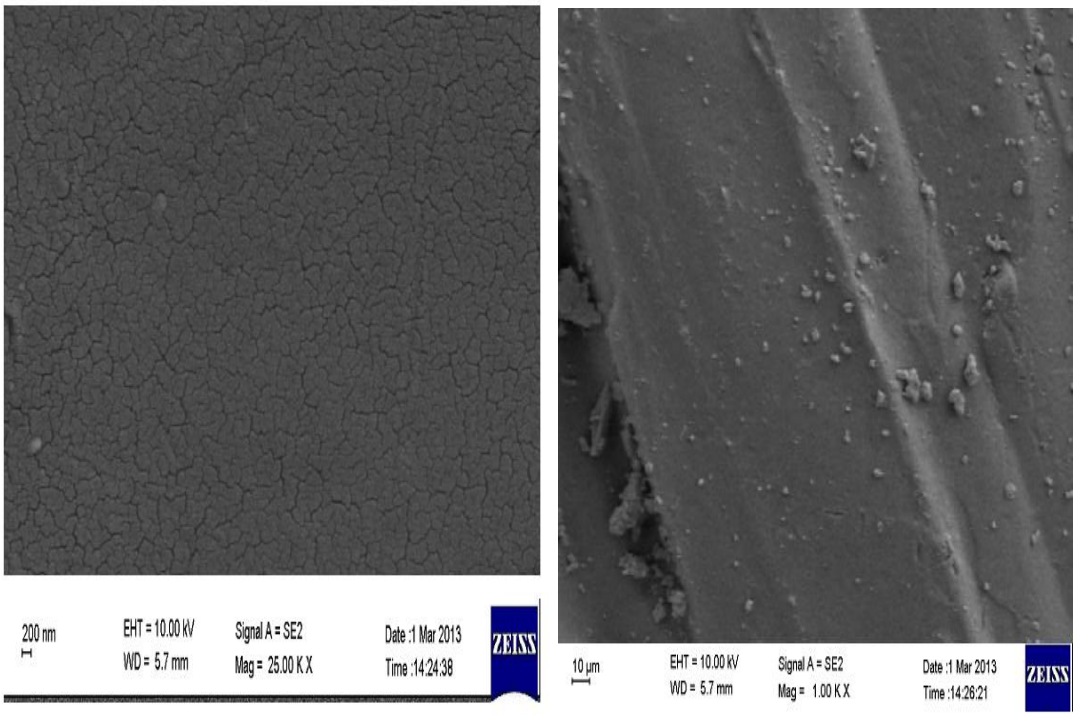

Figure 3.44: FE-SEM images of non-irradiated neat-epoxy sample

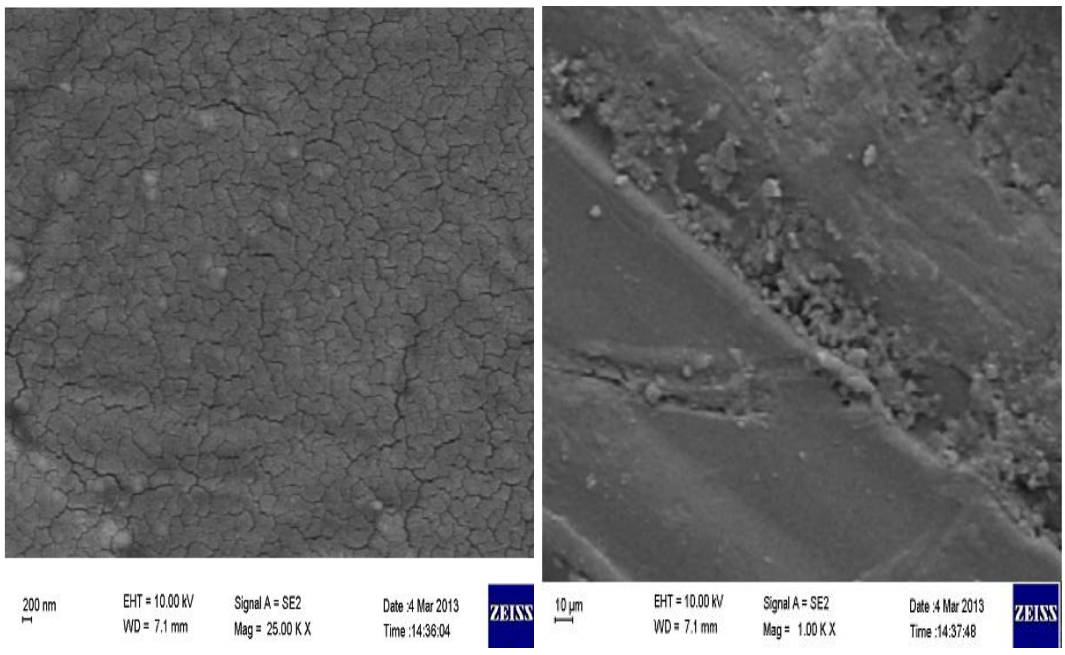

Figure 3.45: FE-SEM images neat-epoxy sample irradiated with 50 kGy by LDR

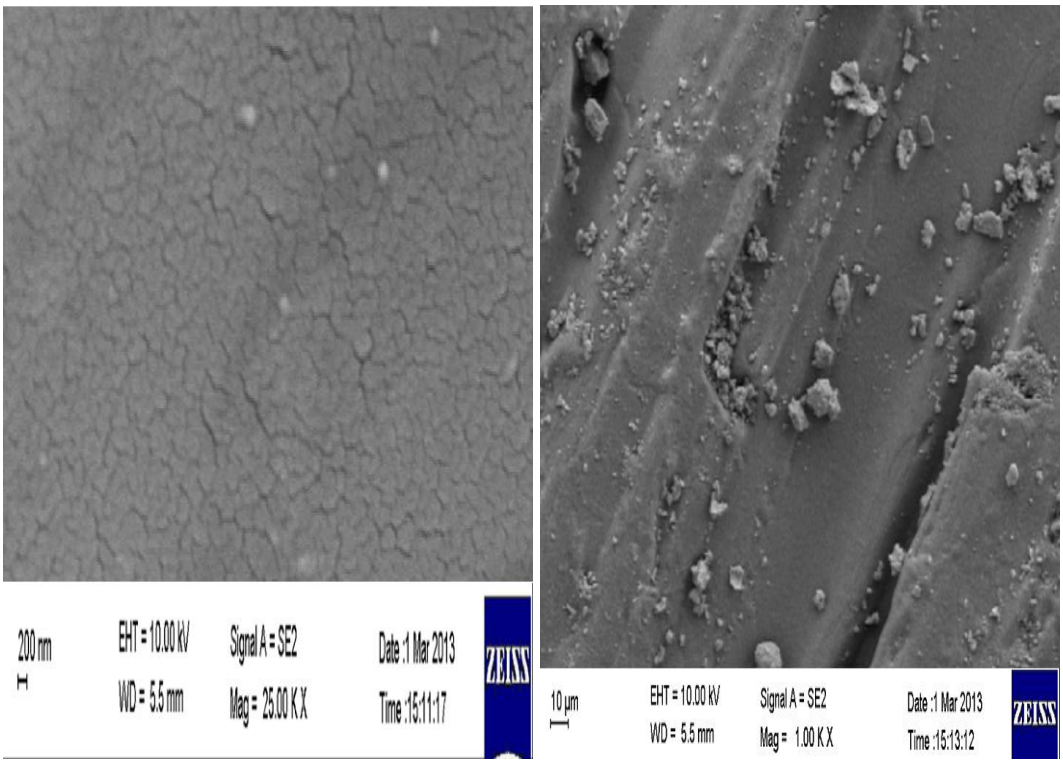

Figure 3.46: FE-SEM images of non-irradiated ECOT-1 sample

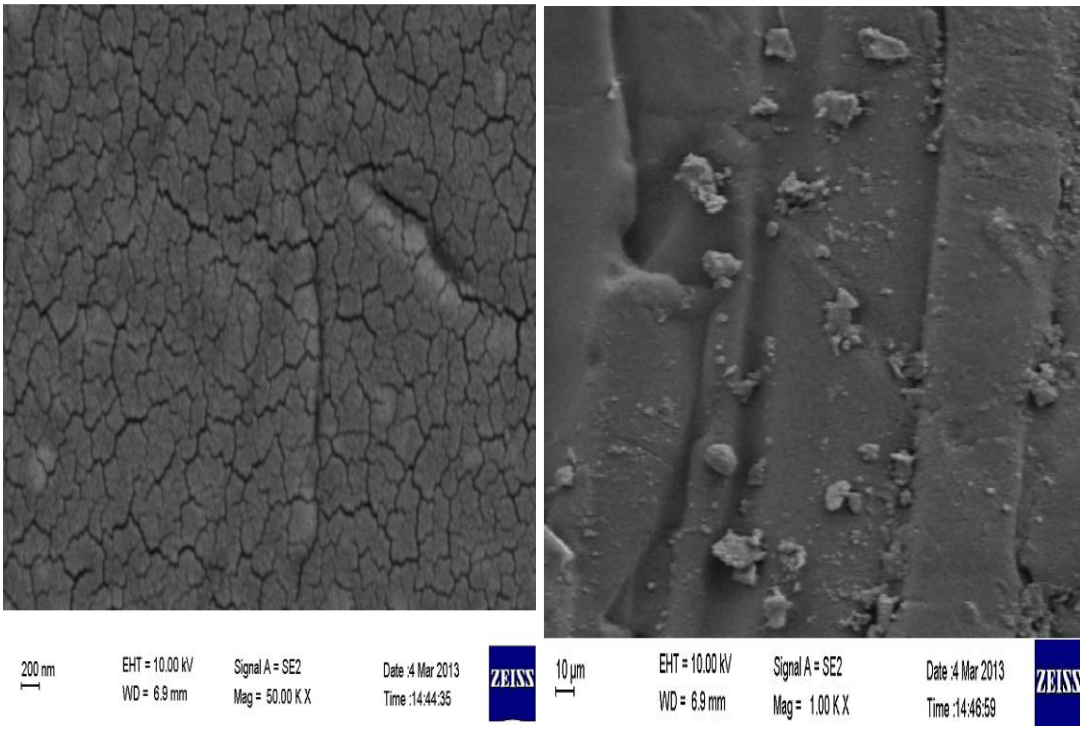

Figure 3.47: FE-SEM images of ECOT-1 sample irradiated with 50 kGy by LDR

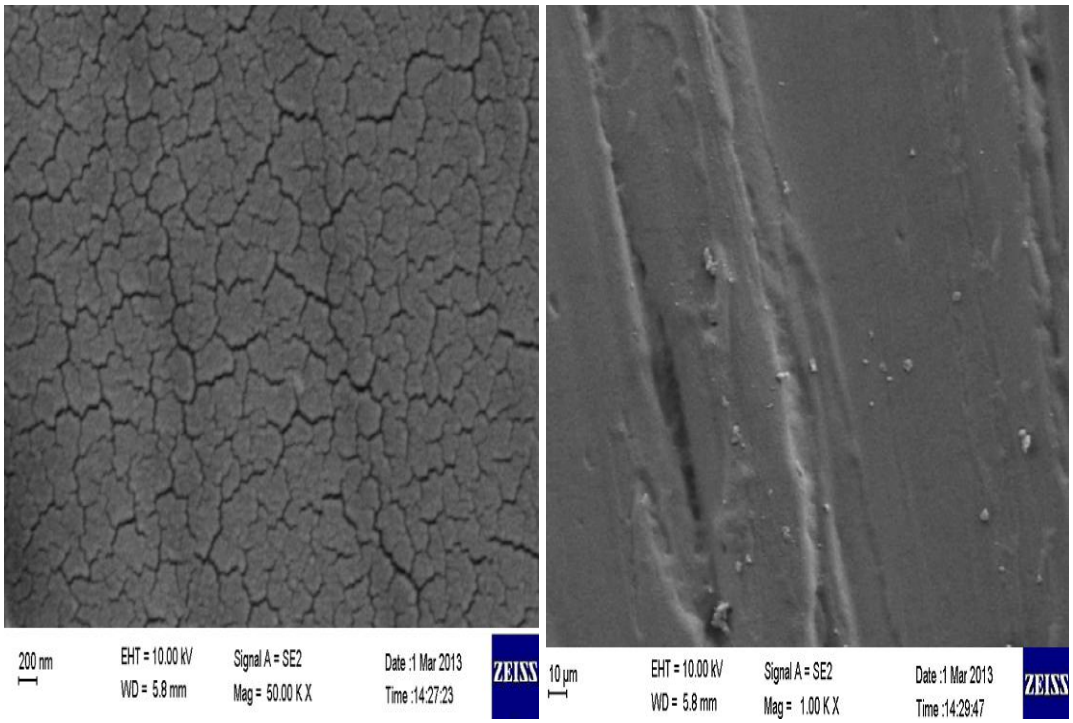

Figure 3.48: FE-SEM images of non-irradiated ECOT-5 sample

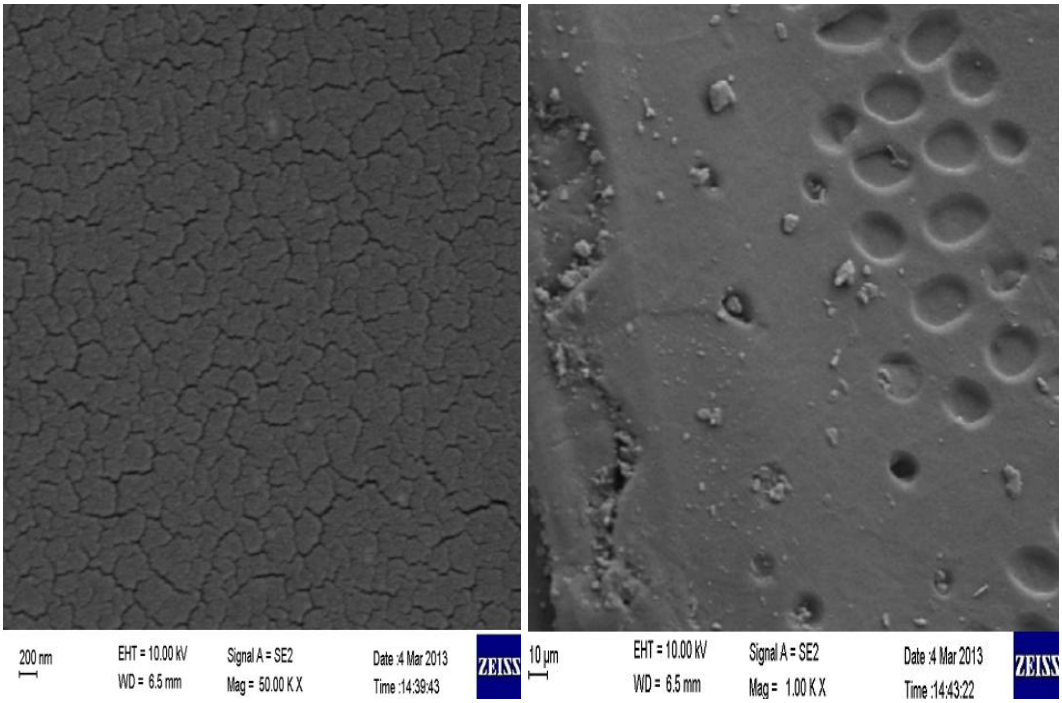

Figure 3.49: FE-SEM images of ECOT-5 sample irradiated with 50 kGy by LDR

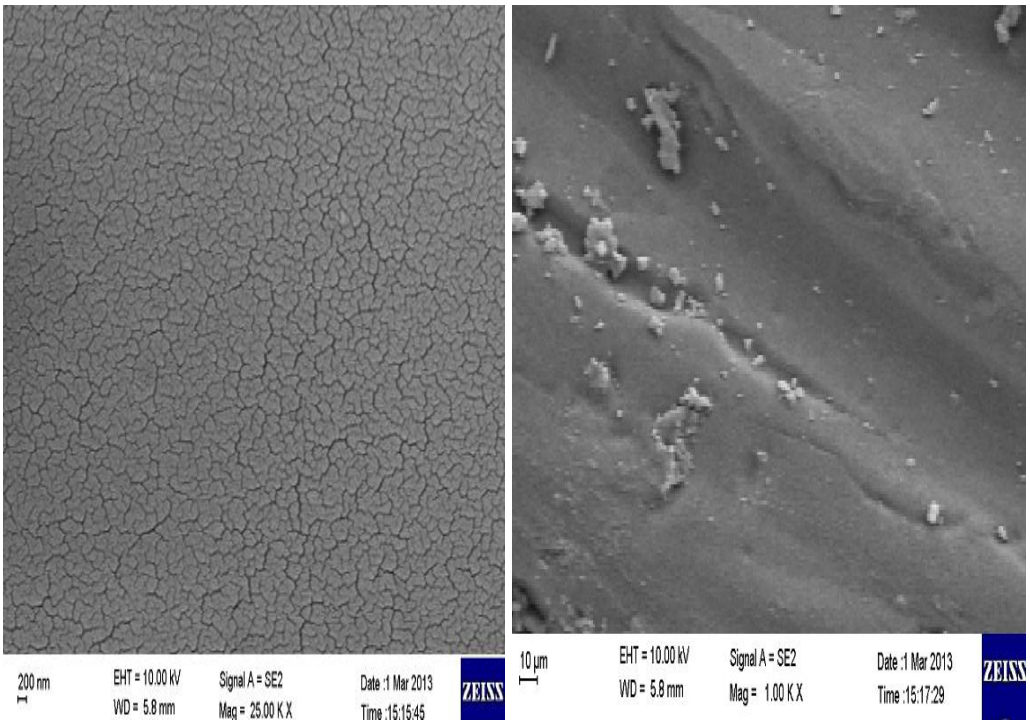

Figure 3.50: FE-SEM images of non-irradiated EANB-1 sample

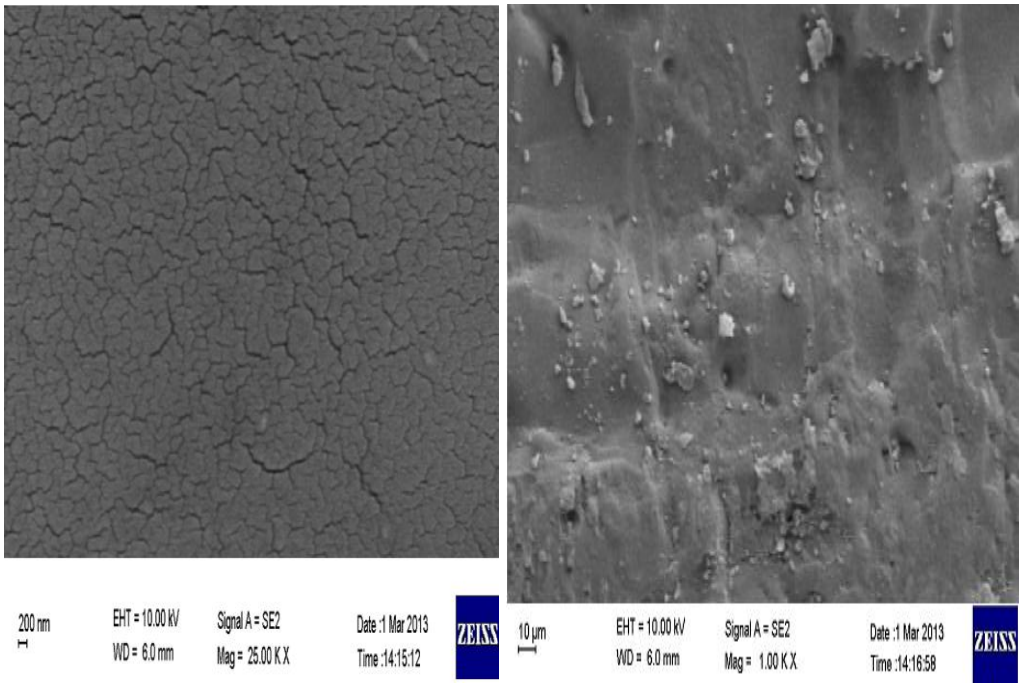

Figure 3.51: FE-SEM images of EANB-1 sample irradiated with 50 kGy by LDR

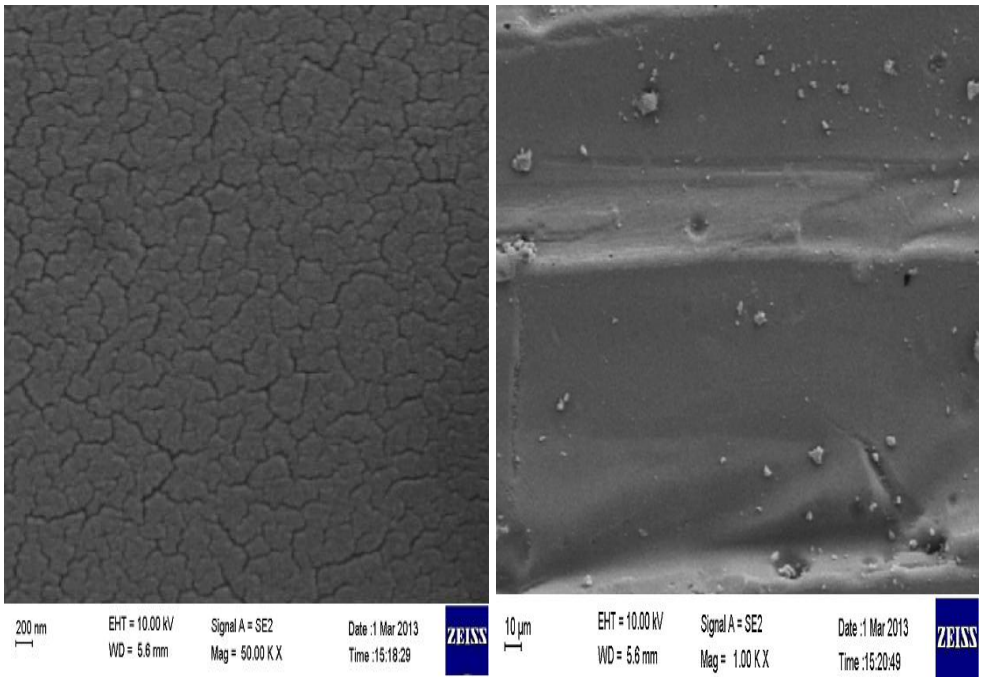

Figure 3.52: FE-SEM images of non-irradiated EANB-5 sample

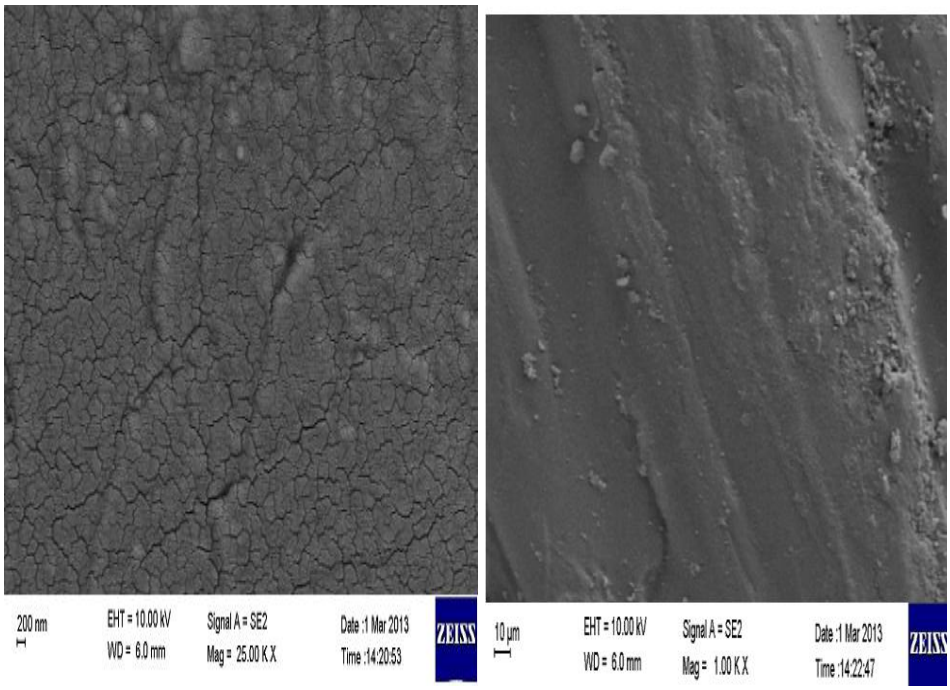

Figure 3.53: FE-SEM images of EANB-5 sample irradiated with 50 kGy by LDR

Figures 3.54 was used to the dispersion of boron minerals and Concentrated Tincal produce more agglomeration than Anhydrous Borax.

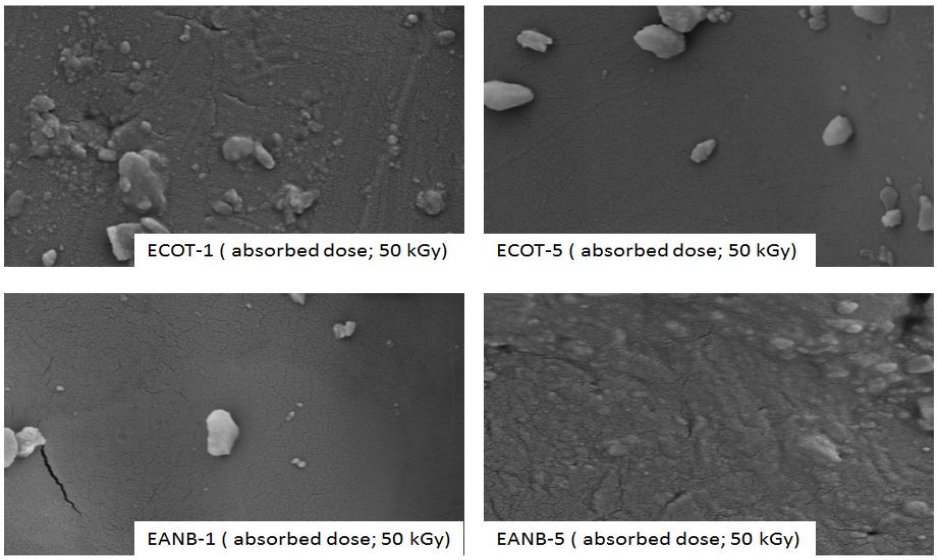

Figure 3.54: Effect of Filler Ratio on Mechanical Properties of Epoxy-Boron Composites

From Table 3.15, it is clear that, the decrease in tensile strength is due to agglomeration which caused non-homogeneous distribution at high fillers loading. This gives more stiffness to the epoxy-boron composites. Agglomeration caused weak adhesion between epoxy and boron fillers which caused decrease of tensile strength. Only concentrated tincal showed an increase of tensile strength which might be lower by adding more fillers [140-143].

Table 3.15: Effect of Filler Ratio on Mechanical Properties of Epoxy-Boron Composites

Tensile Strength (MPa)			
ECAT-1	34	ECAT-5	16
ECOT-1	19	ECOT-5	22
ECOL-1	33	ECOL-5	18
EANB-1	15	EANB-5	9

CHAPTER 4

CONCLUSIONS

Taking into account the respective advantages of epoxy and boron, , it was aimed to produce composite shielding materials against both gamma and neutron radiation where the effect of boron on the mechanical and thermal properties of epoxy were studied in terms of mineral type, mineral loading concentration and irradiation dose in air and under vacuum. The results for epoxy-boron composites can be summarized as;

The changes in mechanical or thermal properties could not be considered by itself only depending on the change of irradiation dose, or just only depending on the change of boron concentration.

The mechanical behavior of epoxy-boron samples showed a periodical behavior consists of three stages as ‘‘increment-decrement-increment’. This situation was related to the competition reaction between chain scission and crosslinking during irradiation by γ –rays. With the increase of irradiation dose, thermal stability and mechanical properties of composites decreased firstly, then increased slightly, and declined sharply at the end. Therefore, it could be said that the epoxy-boron composites could not be used against high absorbed doses.

Related to tensile test results, the highest tensile strength (33 MPa at 2500 kGy by HDR) and the highest Young’s modulus (1095 MPa at 500 kGy by LDR) were achieved for ECOL-1 sample. Higher peaks after reinforcement by boron minerals showed chain scission as a result of degradation was partially blocked and

this could be related to positive effect of boron minerals on shielding against radiation.

If the peaks of the epoxy showed higher intensities by increasing absorbed dose, it can be caused from prevention of formation of crosslinks. On the other side, the decrease in intensities of some peaks indicates the degradation. It was noticed that when the absorbed dose was raised the relative intensities of the band at 813, 1185 and 1252 cm^{-1} increased and those of the band at 806 cm^{-1} decreased. Such changes are supposed to be connected with the rotational isomerism.

All boron minerals caused an increase on T_g of epoxy-boron samples. Because of the highly crystalline structure of boron minerals they are rigid materials. Therefore, when the mobility of the chains close to boron particles is reduced, these results could be predictable. T_g shifting to higher temperatures with irradiation is attributed in epoxies to an increase in the degree of crosslinking and following decrease in the molecular weight between crosslinks.

From the weight loss of the composite samples, neat epoxy and neat minerals, it is clear that the weight loss of the composites was due to the degradation of the epoxy. Therefore, the total weight loss is proportional to the weight fraction of the epoxy. Only the decomposition temperature shifted to the right which is about 10 °C increasing because of the boron minerals effects. This is attributed in boron minerals due to lack of chemical bonding between epoxy chains and boron minerals.

The FE-SEM results showed that the composite failure was caused by the brittle fracture of the polymer matrix. Higher amount of boron minerals in the epoxy samples caused agglomeration. There were many irregular granules that uniformly distributed in the composites which were boron minerals. The epoxy-boron samples showed smooth and ripples-full morphology that implies the brittle property of the composites used in the study. Formation of fractures occurred because of the poor adhesion between epoxy matrix and boron minerals during curing.

REFERENCES

1. Potter, W.G., Epoxide Resins, Spinger-Verlog New York Publishing / London Iliffe Books Publishing, England (1970)

2. Lee, H., Neville, K., Epoxy Resins: Their Applications and Technology, McGraw-Hill Book Company Publishing, USA (1957)

3. Prime, R.B., Chapter 6 "Thermosets" in Thermal Characterization of Polymeric Materials (E. A. Turi, ed.) Academic Press, USA (1997)

4. Pascault, J.P., Williams, R.J.J., Epoxy Polymers New Materials and Innovations, Wiley-VCH Publishing, Germany (2010)

5. Rykowska, I., Wasiak, W., "Properties, Threats, and methods of analysis of bisphenol A and its derivatives", Acta Chromatoghraphica, vol. 16, pp. 7-20 (2006)

6. Carraher Jr, C.E., Introduction to Polymer Chemistry, CRC Press, USA (2010)

7. Peters, S.T., Handbook of Composites, Chapmann & Hall, Great Britain (1998)

8. Xue, S., Pinnavaia, T.J., "Porous synthetic smectic clay for the reinforcement of epoxy polymers", Microporous and Mesoporous Materials, vol. 107, pp. 134–140 (2008)

9. Singh-Beemat, J., Iroh, J.O., "Characterization of corrosion resistant clay/epoxy ester composite coatings and thin films", Progress in Organic Coatings, vol. 74, pp. 173– 180 (2012)

10. Chen, Z.K., Yang, J.P., Ni, Q.Q., Fu, S.Y., Huang, Y.G., “Reinforcement of epoxy resins with multi-walled carbon nanotubes for enhancing cryogenic mechanical properties”, Polymer, vol. 50, pp. 4753–4759 (2009)

11. Yousif, B.F., Shalwan, A., Chin, C.W., Ming, K.C., “Flexural properties of treated and untreated kenaf/epoxy composites”, Materials and Design, vol. 40, pp. 378–385 (2012)

12. Exner, W., Arlt, C., Mahrholz, T., Riedel, U., Sinapius, M., “Nanoparticles with various surface modifications as functionalized cross-linking agents for composite resin materials”, Composites Science and Technology, vol. 72, pp. 1153–1159 (2012)

13. Yang, H., Wang, X., Yu, B., Song, L., Hu, Y., Yuen, R.K.K., “Effect of borates on thermal degradation and flame retardancy of epoxy resins using polyhedral oligomeric silsesquioxane as a curing agent”, Thermochimica Acta, vol. 535, pp. 71– 78 (2012)

14. Li, X., Ou, Y., Shi, Y., “Combustion behavior and thermal degradation properties of epoxy resins with a curing agent containing a caged bicyclic phosphate”, Polymer Degradation and Stability, vol. 77, pp. 383–390 (2002)

15. Wang, X., Hu, Y., Song, L., Xing, W., Lu, H., Lv, P., Jie, G., “Flame retardancy and thermal degradation mechanism of epoxy resin composites based on a DOPO substituted organophosphorus oligomer”, Polymer, vol. 51, pp. 2435-2445 (2010)

16. Peng, W., Huang, X., Yu, J., Jiang, P., Liu, W., “Electrical and thermophysical properties of epoxy/aluminum nitride nanocomposites: Effects of nanoparticle surface modification”, Composites: Part A, vol. 41, pp. 1201–1209 (2010)

17. Findik, F., Mrad, N., Johnston, A., “Strain monitoring in composite patched structures”, Composite Structures, vol. 49, pp. 331-338 (2000)

18. Findik, F., Unal, H., “Development of thermal residual strains in a single sided composite patch”, Composites: Part B, vol. 32, pp. 379-383 (2001)

19. Naik, N.K., Ramasimha, R., Arya, H., Prabhu, S.V., ShamaRao, N., “ Impact response and damage tolerance characteristic of glass-carbon/epoxy hybrid composite plates”, Composites: Part B, vol. 32, pp. 565-574 (2001)

20. Sayer, M., Bektaş, N.B., Sayman, O., “An experimental investigation on the impact behavior of hybrid composite plates”, Composite Structures, vol. 92, pp. 1256–1262 (2010)

21. Karakuzu, R., Erbil, E., Aktas, M., “Impact characterization of glass/epoxy composite plates: An experimental and numerical study”, Composites: Part B, vol. 41, pp. 388–395 (2010)

22. Al-Turaif, H., “Effect of nano TiO2 particle size on mechanical properties of cured epoxy resin”, Progress in Organic Coatings, vol. 69, pp. 241–246 (2010)

23. Gould, R.F., Irradiation of Polymers, American Chemical Society, USA (1967)

24. Korkut, T., Gencel, O., Kam, E., Brostow, W., “X-Ray, Gamma, and Neutron Radiation Tests on Epoxy-Ferrochromium Slag Composites by Experiments and Monte Carlo Simulations”, International Journal of Polymer Analysis and Characterization, vol. 18, pp. 224-231 (2013)

25. Clegg, D.W., Collyer A.A., Irradiation Effects on Polymers , Elsevier Science Publishing, USA (1991)

26. In Irradiation of Polymers; Advances in Chemistry; American Chemical Society, USA (1967), Avaliable at: (http://pubs.acs.org/doi/pdf/10.1021/ba-1967-0066.pr001) (Accessed September 25th 2012)

27. Humer, K., Bittner-Rohrhofer, K., Fillunger, H., Maix, R.K., Prokopec, R., Weber, H.W., "Radiation effects on the mechanical properties of insulators for fusion magnets", Fusion Engineering and Design, vol. 81, pp. 2433–2441 (2006)

28. Prokopec, R., Humer, K., Maix, R.K., Fillunger, H., Weber, H.W., Knaster, J., Savary, F., "Qualification of the resin for the ITER TF coil insulation", Fusion Engineering and Design, vol. 86, pp. 1436–1439 (2011)

29. Prokopec, R., Humer, K., Maix, R.K., Fillunger, H., Weber, H.W., "Characterization of advanced cyanate ester/epoxy insulation systems before and after reactor irradiation", Fusion Engineering and Design, vol. 85, pp. 227–233 (2010)

30. Bittner-Rohrhofer, K., Humer, K., Fillunger, H., Maix, R.K., Weber, H.W., Fabian, P.E., Munshi, N.A., "Radiation effects on the mechanical integrity of novel organic insulators for the ITER magnet coils", Journal of Nuclear Materials, vol. 329–333, pp. 1083–1087 (2004)

31. Wu, Z., Zhang, H., Yang, H., Chu, X., Song, Y., Wu, W., Liu, H., Li, L., "Properties of radiation stable, low viscosity impregnating resin for cryogenic insulation system", Cryogenics, vol. 51, pp. 229–233 (2011)

32. Shindo, Y., Takeda, T., Narita, F., Miura, M., Watanabe, S., Koizumi, N., Idesaki, A., Okuno, K., "Interlaminar shear properties of composite insulation systems for fusion magnets at cryogenic temperatures", Cryogenics, vol. 50, pp. 36–42 (2010)

33. Huang, Y., Liang, L., Xu, J., Zhang, W., "The design study of a new nuclear protection material", Nuclear Engineering and Design, vol. 248, pp. 22– 27 (2012)

34. Djouani, F., Zahra, Y., Fayolle, B., Kuntz, M., Verdu, J., “Degradation of epoxy coatings under gamma irradiation”, Radiation Physics and Chemistry, Radiation Physics and Chemistry, vol. 82 (1), pp. 54-62 (2014)

35. Wei, C., Pan, W., Sun, S., Liu, H., “Irradiation effects on a glycidylamine epoxy resin system for insulation in fusion reactor”, Journal of Nuclear Materials, vol. 429, pp. 113-117 (2012)

36. Zhang, C., Zhu, F., Wang, Z., Meng, L., Liu, Y., “Amino functionalization of multi-walled carbon nanotubes by gamma ray irradiation and its epoxy composites”, Polymer Composites, vol. 33, pp. 267-274 (2012)

37. Nishimura, A., Izumi, Y., Imaizumi, M., Nishijima, S., Hemmi, T., Shikama, T., “Neutron and gamma ray irradiation effects on interlaminar shear strength of insulation materials with cyanate ester-epoxy blended resin”, Fusion Engineering and Design, vol. 86 , pp. 1558-1561 (2011)

38. Crădun, E., Zaharescu, T., Jitaru, I., Ignat, M., Cătănescu, L., Zărnescu, G., “Radiation behaviour of nanocomposite epoxy material”, UPB Scientific Bulletin, Series B: Chemistry and Materials Science, vol.73 , pp. 75-86 (2011)

39. Mantsch, A., Craciun, E., Zaharescu, T., Jipa, S., Jitaru, I., “Gamma radiation effects on the stability of epoxy resin modified with titania nanoparticles”, Materiale Plastice, vol.48, pp. 50-53 (2011)

40. Kim, K.Y., Im, D.S., Choi, J.H., Lee, K.Y., “Degradation properties of the epoxy nanocomposite caused by a gamma-ray irradiation”, Annual Report - Conference on Electrical Insulation and Dielectric Phenomena, CEIDP, art. no. 5724022 (2010)

41. Craciun, E., Zaharescu, T., Jipa, S., Jitaru, I., "Qualification of epoxy resin by radiochemical ageing", Optoelectronics and Advanced Materials, Rapid Communications, vol.4, pp. 1819-1822 (2010)

42. Queiroz, D.P.R., Fraïsse, F., Fayolle, B., Kuntz, M., Verdu, J., "Radiochemical ageing of epoxy coating for nuclear plants", Radiation Physics and Chemistry, vol.79, pp. 362-364 (2010)

43. Hoffman, E.N., Skidmore, T.E., "Radiation effects on epoxy/carbon-fiber composite", Journal of Nuclear Materials, vol.392, pp. 371-378 (2009)

44. Korkut, T., Karabulut, A., Budak, G., Aygün, B., Gencel, O., Hançerlioğulları, A., "Investigation of neutron shielding properties depending on number of boron atoms for colemanite, ulexite and tincal ores by experiments and FLUKA Monte Carlo simulations", Applied Radiation and Isotopes, vol.70, pp. 341–345 (2012)

45. Gencel, O., Brostow, W., Martínez-Barrera, G., Gok, M.S., "Mechanical properties of polymer concretes containing different amount of hematite or colemanite", Polimery, vol.57, pp. 276-283 (2012)

46. Sukegawa, A.M., Anayama, Y., Okuno, K., Sakurai, S., Kaminaga, A., "Flexible heat resistant neutron shielding resin", Journal of Nuclear Materials, vol. 417, pp. 850–853 (2011)

47. Drobny, J.G., Radiation Technology for Polymers, CRC Press, USA (2003)

48. Carraher, C.E., Introduction to Polymer Chemistry, Taylor & Francis Group, USA (2007)

49. Carraher, C.E., Polymer Chemistry, Taylor & Francis Group, USA (2008)

50. Ivanov, V.S., Radiation Chemistry of Polymers, Koninklijke B.V., Netherlands (1988)

51. Davenas, J., Stevenson, I., Celette, N., Cambon, S., Gardette, J.L., Rivaton A., Vignoud, L., "Stability of polymers under Ionising Radiation: The Many Faces of Radiation Interactions with Polymers", Nuclear Instruments and Methods in Physics Research B, vol.191, pp. 653-661 (2002)

52. Garrett, D.E., Borates: Handbook of Deposits, Processing, Properties and Use, Academic Press, San Diego, USA (1998)

53. Boron Application Areas: Energy, Avaliable at: http://www.boren.gov.tr /en/boron/areas-of-application/energy (Accessed March 5th 2015)

54. Brandt, A.M., Niedzwiedzka, D.J., "On the application of dispersed fibres as reinforcement for concrete shields against radiation", High Performance Fiber Reinforced Cement Composites (HPFRCC7), Germany (2015)

55. Sears, V.F., "Neutron scattering lengths and cross sections", Neutron News, vol. 3, pp. 22-37 (1992)

56. Prasad, S.G., Parthasaradhi, K., Bloomer, W.D., Al-Najjar, W.H., "Aluminum, copper, tin and lead as shielding materials in the treatment of cancer with high-energy electrons", Radiat. Phys. Chem., vol.53, pp. 361–366 (1998)

57. Bor Ürünleri (2012), Avaliable at: http://www.etimaden.gov.tr /tr/0_sayfa_ortakSayfa.asp?hangisayfa=4_sayfa_a_4 (Accessed April 27th 2012)

58. J.C.J. Bart, Plastics Additives: Advanced Industrial Analysis, IOS Press, Netherlands (2006)

59. Smith, B.C., Fundamentals of Fourier Transform Infrared Spectroscopy, Taylor & Francis, Florida, USA (2011)

60. Mravljak, M., Šernek, M., "The Influence of Curing Temperature on Rheological Properties of Epoxy Adhesives", Drvna Industrija, vol.62, pp.19-25 (2011)

61. Lapique, F., Redford, K., "Curing effects on viscosity and mechanical properties of a commercial epoxy resin adhesive", Int. J. Adhes. Adhes., vol.22, pp. 337-346 (2002)

62. Li, R., "Time-temperature superposition method for glass transition temperature of plastic materials", Mater. Sci. Eng., vol.A278, pp.36-45 (2000)

63. Tamulevich, T.W., Moore, V., "The Significance of Glass Transition Temperature on Epoxy Resins for Fiber Optic Applications (1980)", Epoxy Technology Inc. http://www.epotek.com/SSCDocs/whitepapers/Tech%20 Paper%2011.pdf. Accessed 15 September 2010

64. "Epoxy Coatings Guide", The Sherwin-Williams Company, Avaliable at: https://protective.sherwin-illiams.com/pdf/Epoxy%20Coatings%20Guide.pdf, (Accessed Jul 15th 2015)

65. van Driel, W.D., Fan, X.J., Solid State Lighting Reliability: Components to Systems , Springer Science & Business Media, USA (2013)

66. Hüner, Ü., "Effect of Water Absorption on the Mechanical Properties of Flax Fiber Reinforced Epoxy Composites", Advances in Science and Technology Research Journal, vol. 9, pp. 1-6 (2015)

67. Dutta, S.S., "Water absorption and dielectric properties of Epoxy insulation", M.Sc. Thesis, Norwegian University of Science and Technology, Norway (2008)

68. Mijovic, J., Zhang, H., "Local dynamics and molecular origin of polymer network-water interactions as studied by broadband dielectric relaxation spectroscopy, FTIR and molecular simulations", Macromolecules, vol.36, pp.1279 (2003)

69. Soles, C.L., Yee, A.F., "A discussion of the molecular mechanisms of moisture transport in epoxy resins", Journal of Polymer Science Part B: Polymer Physics, vol.38, pp.792 (2000)

70. Li, S., Liang, L., Li, J., Liu, N., A.Alim, M., "Characterization of water absorbed epoxy insulating coating material used in ZnO varistors by dielectric measurements", Materials Letters, vol. 60, pp. 114 – 119 (2006)

71. Li, J., Li, S., Alim, M.A., Chen, G., "The Degradation of Epoxy Resin-Coated ZnO Varistors at Elevated Temperatures and Ambient Humidity Conditions", Act. Passive Electron. Compon., vol. 26, pp. 235-243 (2003)

72. Salamone, J.C., Polymeric Materials Encyclopedia, CRC Press, Boca Raton, (2006)

73. Zou, C., Fothergill, J.C., Rowe, S.W., "The effect of water absorption on the dielectric properties of epoxy nanocomposites," IEEE T. Dielect. El. In., vol. 15, pp. 106—117 (2008)

74. Ezoe, M., Tada, M., Nakanisi, M., Proceedings of the 5th Int. Conf. On Prop. and Appl. of Dielect. Mat., p. 376 (1997)

75. Kumazawa, T., Oshi, M., Todoki, M., Watanabe, T., Proc. of the 5th Int. Conf. on Prop. and Appl. of Dielect. Mat., p. 491 (1997)

76. Kärner, H.C., Schütz, A., Proc. of the 4th Int. Conf. on Prop. and Appl.of Dielect. Mat., p. 344 (1994)

77. McMaster, M.G., Soane, D.S., “Water sorption in epoxy thin films,” IEEE Transactions on Composites, Hybrids and Manufacturing Technology, vol. 12, pp. 373–386 (1989)

78. Nogueira, P., Ramirez, C., Torres, A., Abad, M.J., Cano, J., Lopez-bueno, I., Barral, L., “Effect of water sorption on the structure and mechanical properties of an epoxy resin system”, Journal of Applied Polymer Science, vol. 80, pp. 71-80 (2001)

79. Cotugno, S., Larobina, D., Mensitieri, G., Musto, J., Ragosta, G., “A novel spectroscopic approach to investigate transport processes in polymers: the case of water-epoxy system”, Polymer, vol. 42, pp. 6431-6438 (2001)

80. Blanco, I., Cicala, G., Costa, M., Recca, A., “Development of an epoxy system characterized by low water absorption and high thermomechanical performances”, Journal of Applied Polymer Science, vol. 100, pp. 4880–4887 (2006)

81. Ji, W., Hu, J., Zhang, J., Cao, C., “Reducing the water absorption in epoxy coatings by silane monomer incorporation”, Corrosion Science, vol. 48, pp. 3731–3739 (2006)

82. Xiao, G.Z., Shanahan, M.E.R., “Swelling of DGEBA/DDA epoxy resin during hygrothermal ageing”, Polymer, vol. 39, pp. 3253-3260 (1998)

83. Calebrese, C., Hui, L., Schadler, L.S., Nelson, J.K., “A Review on the Importance of Nanocomposite Processing to Enhance Electrical Insulation”, International Power Modulator and High Voltage Conference, Atlanta (2010)

84. Roy, M., “An Examination of the potential for nanocomposites in the formulation of HV cable insulation”, PhD Thesis, Rensselaer Polytechnic Institute (2009)

85. Singh, N.L, Shah, N., Singh, K.P, Desai, C.F., "Electrical and thermal behavior of proton irradiated polymeric blends", Radiat Meas., vol. 40, pp. 741–745 (2005)

86. Marletta, G., "Chemical reactions and physical property modifications induced by keV ion beams in polymers", Nucl Inst Meth Phys Res B., vol. 46, pp. 295 (1990)

87. Nasef, M., Dahlan, M., Khairal, M., "Electron irradiation effects on partially fluorinated polymer films: Structure-property relationships", Nucl Inst and Meth B., vol. 201, pp. 604–614 (2003)

88. Mailhot, B., Morlat-Therias, S., Ouahioune, M., Gardette, J.L., "Study of the Degradation of an Epoxy/Amine Resin, 1 Photo- and Thermo-Chemical Mechanisms", Macromol. Chem. Phys., vol. 206, pp. 575–584 (2005)

89. Rivaton, A., Moreau, L., Gardette, J.L., "Photo-oxidation of phenoxy resins at long and short wavelengths-I. Identification of the Photoproducts" and "Photo-oxidation of phenoxy resins at long and short wavelengths-II. Mechanisms of formation of the photoproducts", Polym. Degrad. Stab., vol. 58, pp. 321-333 (1997)

90. Monney, L., Bole, J., Dubois, C., Chambaudet, A., "Trapping and identification of volatile photo-products of a photo-oxidised epoxy matrix", Polym. Degrad. Stab. 1999, vol. 66, pp. 17-22 (1999)

91. Zhou, W., Wang, Z.L., Scanning Microscopy for Nanotechnology, Springer, USA (2006)

92. Nouh, S.A., El-Hussieny, H., Morsy, A., "Radiation Induced Changes in some SSNTDs", Radiat. Effec. Defec. Soli., vol. 159, pp. 115-124 (2004)

93. Maxwell, I.D., Pethrick, R.A., "Low-temperature rearrangements of amine cured epoxy-resins", J. Polymer Degradation Stability, vol. 5, pp. 275-301 (1983)

94. Musto, P., Ragosta, G., Russo, P., Mascia, L., "Thermal-oxidative degradation of epoxy and epoxy-bismaleimide networks: kinetics and mechanism Macromol. Chem. Phys., vol. 202, pp. 3445-3458 (2001)

95. Anderson, B.J., "Thermal stability of high temperature epoxy adhesives by thermogravimetric and adhesive strength measurements", Polymer Degradation and Stability, vol.96, pp. 1874-1881 (2011)

96. Petrie, E.M., Handbook of Adhesives and Sealents, New York: McGraw-Hill, (2007)

97. Petrie, E.M., Epoxy Adhesive Formulations, New York: McGraw-Hill (2006)

98. Mravljak, M., Šernek, M., "The Influence of Curing Temperature on Rheological Properties of Epoxy Adhesives", Drvna Industrija, vol. 62, pp. 19-25 (2011)

99. Epoxy Technology, Tech Tip 23: T_g - Glass Transition Temperature for Epoxies (2012)

100. Carbas, R.J.C., Marques, E.A.S., Lopes, A.M., da Silva, L.F.M., "Effect of Cure Temperature on the Glass Transition Temperature of an Epoxy Adhesive", 15th International Conference on Experimental Mechanics, Porto/Portugal (2012)

101. da Silva, L.F.M., Öchsner A., Adams, R.D., Handbook of Adhesion Technology, Springer (2011)

102. Varley, R.J., Hodgkin, J.H., Simon, G.P., "Toughening of trifunctional epoxy system. V. Structure-property relationships of neat resin", Journal of Applied Polymer Science, vol. 77, pp. 237 (2000)

103. Ziaee, S., Palmese, G.R., “Effects of temperature on cure kinetics and mechanical properties of vinyl–ester resins”, Journal of Polymer Science: Part B: Polymer Physics, 37, 725 (1999)

104. Gan, S., Gilham, J.K., Prime, R.B., “A methodology for characterizing reactive coatings: time-temperature-transformation (TTT) analysis of the competition between cure, evaporation and thermal degradation for an epoxy-phenolic”, Journal of Applied Polymer Science, vol. 37, pp. 803 (1989)

105. Menczel, JD., Prime, R.B., “Thermal analysis of polymers: fundamentals and applications”, 1st ed. New Jersey: John Wiley & Sons, Inc. (2009)

106. Wenguo, N., Heng, L., Chunsheng, Z., Le, L., Dong C., Zhenzhen, D., “The effects of cure temperature history on the stability of polyimide films”, Journal of Semiconductors, vol. 34, no. 6 (2013)

107. Montoya, A., Effect of Cure Process on Glass Transition Temperature , NASA Technical Information Paper (2003)

108. Sinclair, J.W., “Effect of Cure Temperature on Epoxy Resin Properties,” J. Adhesion, vol. 38, pp. 219 (1992)

109. Suryanarayana, D., Wu, T.Y., Varcoe, J.A., “Encapsulants Used in Flip-Chip Packages”, Proc. of 43rd ECTC Conference (1993)

110. Wang, D.W., Papathomas, K.I., “Encapsulant for Fatigue Life Enhancement of Controlled Collapse Chip Connection”, Proc. of 43rd ECTC Conference (1993)

111. Comstock, B., “Die Attach Epoxy’s Role in Thin Package delamination,” Semiconductor International, vol. 162 (1993)

112. Kashani, P., Minaie, B., "An ex-situ state-based approach using rheological properties to measure and model cure in polymer composites", Journal of Reinforced Plastics and Composites, vol. 30, pp. 123-133 (2011)

113. Epoxy Technology, Tech Tip 23: T_g - Glass Transition Temperature for Epoxies (2012)

114. Lee, H.T., Levi, D.W., "Effect of curing temperature on thermal degradation of an epoxide resin", J. Appl. Polymer Sci., vol. 13, pp. 1703-1705 (1969)

115. Hemmerich, K.J., "Polymer Materials Selection for Radiation-Sterilized Products", Medical Plastics, MDDI Medical Device and Diagnostic Industry News Products and Suppliers (http://www.mddionline.com; 2000)

116. Barrera, G.M., Villarruel, U.T., Santiago, E.V., Lopez, S.H., Brostow, W., "Compressive Strength of Gamma-Irradiated Polymer Concrete", Polymer Composites, vol. 29, pp. 1210–1217 (2008)

117. Chang, L., Zhang, Y., Liu, Y., Fang, J., Luan, W., Yang, X., Zhang, W., "Preparation and characterization of tungsten/epoxy composites for γ-rays radiation shielding", Nuclear Instruments and Methods in Physics Research B, vol. 356–357, pp. 88-93 (2015)

118. Vignoud, L., David, L., Sixou, B., Vigier, G., "Influence of electron irradiation on the mobility and on the mechanical properties of DGEBA/TETA epoxy resins", Polymer, vol. 42, pp. 4657–4665 (2001)

119. Yu, Q., Chen, P., Gao, Y., Ma, K., Lu, C., Xiong, X., "Effects of electron irradiation in space environment on thermal and mechanical properties of carbon fiber / bismaleimide composite", Nucl. Instr. Meth. Phys. Res. Sect. B, vol. 336, pp. 158–162 (2014)

120. Fouchal, F., Knight, J.A.G., Dickens, P., Garrington,N., "Online Monitoring of Epoxy Resin Cure using Infrared Spectroscopy", International Solid Freeform Fabrication Symposium, 441 (2001)

121. Çetin, B., Ünal, H.İ., Erol, Ö., "Synthesis, Characterization and Electrokinetic Properties of Polyindene/Colemanite Conducting Composite", Clays and Clay Minerals, vol. 60, pp. 300-314 (2012)

122. Budak, A., Gönen, M., "Extraction of Boric Acid from Colemanite Mineral by Supercritical Carbon Dioxide", Journal of Supercritical Fluids, vol. 92, pp. 183-189 (2014)

123. Frost, R.L., Xi, Y., Scholz, R., Belotti, F.M., Filho, M.C., "Infrared and Raman Spectroscopic Characterization of the Borate Mineral Colemanite – $CaB_3O_4(OH)_3.H_2O$ – Implications for the Molecular Structure", Journal of Molecular Structure, vol. 1037, pp 23-28 (2013)

124. Park, E.H., Jeong, S.U., Jung, U.H., Kim, S.H., Lee, J., Nam, S.W., Lim, T.H., Park, Y.J., Yu, Y.H., "Recycling of Sodium Metaborate to Borax", International Journal of Hydrogen Energy, vol. 32, pp. 2982-2987 (2007)

125. Pavlyukevich, Y. G., Levitskii, I. A., Mazura, N. V., "Use of Colemanite in Glass Fiber Production", Glass and Ceramics, vol. 66, pp. 345-349 (2009)

126. Peak, D., Luther III, G.W. Sparks, D.L., "ATR-FTIR Spectroscopic Studies of Boric Acid Adsorption on Hydrous Ferric Oxide", Geochimica et Cosmochimica Acta, vol. 67, pp. 2551-2560 (2003)

127. Weir, C.E., "Infrared Spectra of the Hydrated Borates", Journal of Research of the National Bureau of Standards – A. Physics and Chemistry, vol. 70A, pp. 153-164 (1966)

128. Rosu, L., Cascaval, C.N., Ciobanu, C., Rosu, D., Ion, E.D Morosanu, C., Enachescu, M., “Effect of UV radiation on the semi-interpenetrating polymer networks based on polyurethane and epoxy maleate of bisphenol A”, J. Photochem. Photobiol. A: Chem., vol. 169, pp. 177–185 (2005)

129. Rosu, D., Cascaval, C.N., Rosu, L., “Effect of UV radiation on photolysis of epoxy maleate of bisphenol A”, J. Photochem. Photobiol. A: Chem., vol. 177, pp. 218–224 (2006)

130. Avram, M., Mateescu, Gh.D., Infrared Spectroscopy Applications in Organic Chemistry, J. Wiley & Sons, New York (1972)

131. Simitzis, J., Zoumpoulakis, L., Soulis, S., “Effect of composition and polyesterification catalysts on the optical properties of cured polyesters”, Polym. Int., vol. 51, pp. 308–318 (2002)

132. Rami, N., Meghraoui, H., Ziraoui, R., El khoukhi, T., Mouhib, M., El Harfi, A., “Influence of gamma irradiation on the chemical and physical properties of DGEDDS / PDA and DGEDDS / MDA epoxy resins”, J. Mater. Environ. Sci., vol.1, pp. 277-288 (2010)

133. Hong, S.G., Wu, C.S., "DSC AND FTIR Analysis of the curing behaviors of epoxy dicy/solvent open systems", Thermochimica Acta, vol. 316, pp. 67 (1998)

134. Dominguez-Rosado, E., Pichtel, J., “Chemical characterization of fresh, used and weathered motor oil via GC/MS, NMR and FTIR techniques”, Proc. Indiana Acad. Sci., vol. 112, pp.109 (2003)

135. Gershon, A.L., Bruck, H.A., Hopkins, A.R., Segal, K.N., “Curing Effects of Single-Wall Carbon NanoTube Reinforcement on Mechanical Properties of Filled Epoxy Adhesives”, Composites Part A: Applied Science and Manufacturing, vol. 41, pp.729 (2010)

136. Rittigstein, P., Priestley, R D., Broadbelt, L. J., Torkelson, J. M., "Model Polymer Nanocomposites Provide Understanding of Confinement Effects in Real Nanocomposites" , Nature Materials, vol. 6, pp. 278 (2007)

137. Ramanathan, T., Abdala, A.A., Stankovich, S., Dikin, D.A., Alonso, M.H., Piner, R.D., "Functionalized graphene sheets for polymer nanocomposites", Nat Nano., vol. 3, pp. 327 (2008)

138. Lin, C.T., Lee, H.T., Chen, J.K., "Synthesis and characterization of molybdenum/phenolic resin composites binding with aluminum nitride particles for diamond cutters", Applied Surface Science, vol. 284, pp. 297 (2013)

139. Yee, R.Y., Stephens, T.S., "A TGA technique for determining graphite fiber content in epoxy composites", Thermochimica Acta, vol. 272, pp. 191 (1996)

140. Gao, Y., Liu, L., Zhang, Z., "Mechanical Performance of Nano-CaCO3 Filled Polystyrene Composites", Acta Mechanica Solida Sinica, vol. 22, pp. 555–562 (2009)

141. Agubra, V.A., Owuor, P.S., Hosur, M.V., "Influence of Nanoclay Dispersion Methods on the Mechanical Behaviour of E-Glass/Epoxy Nanocomposites", Nanomaterials, vol. 3, pp. 550-563 (2013)

142. Lam, C.K., Cheunga, H.Y., Lau, K.T., Zhou, L.M., Hob, M.W., Hui, D., "Cluster Size Effect in Hardness of Nanoclay/Epoxy Composites", Composites: Part B, vol. 36, pp. 263–269 (2005)

143. Yasmin, A., Daniel, I,M., "Mechanical and Thermal Properties of Graphite Platelet/Epoxy Composites", Polymer, vol. 45, pp. 8211–8219 (2004)

APPENDIX A

CHEMICAL COMPOSITION OF EPOXY COMPONENTS USED IN THIS STUDY

	Adriapox Special	Indurente A37
Chemical Composition	1,6 ESANDIOLDIGLICIDETERE	MXDA (M-PHENYLENEBIS (METHYLAMINE)
		N-Aminoethylpiperazine
	REACTION PRODUCT: BISPHENOL A-(EPICHLORHYDRIN)	ALFA-(2-Aminometlyethyl)-Poly[oxy(methyl-1,2-ethanediyl)]
		4 4'-isopropylidenediphenol (bisphenol A)

APPENDIX B

CONTENTS OF BORON MINERALS USED IN THIS STUDY

Table B.1: Contents of Etibor-68 (Anhydrous Borax)

Content	Unit	Amount
B_2O_3	%	68.00 (min.)
Na_2O	%	30.27 (min.)
SO_4	ppm	200 (max.)
Cl	ppm	105 (max.)
Fe	ppm	150 (max.)
Insolubles in Water	ppm	920 (max.)

Table B.2: Contents of Calcined Tincal

Content	Unit	Amount
B_2O_3	%	52.00 (min.)
Na_2O	%	23.00 (min.)
SO_4	%	0.15 (max.)
Fe	%	0.11 (max.)
SiO_2	%	3.00 (max.)
CaO	%	3.25 (max.)
MgO	%	3.00 (max.)

Table B.3: Contents of Concentrated Tincal

Content	Unit	Amount
B_2O_3	%	29.00
Na_2O	%	12.80
As	ppm	9
SiO_2	%	2.50
CaO	%	2.80
MgO	%	2.70

Table B.4: Contents of Ground Colemanite

Content	Unit	Amount
B_2O_3	%	40.00 ± 0.50
CaO	%	27.00 ± 1.00
SiO_2	%	4.00-6.50
SO_4	%	0.60 (max.)
As	ppm	35 (max.)
Fe_2O_3	%	0.08 (max.)
Al_2O_3	%	0.40 (max.)
MgO	%	3.00 (max.)
SrO	%	1.50 (max.)
Na_2O	%	0.35 (max.)
L.O.I.	%	24.60 (max.)

CURRICULUM VITAE

PERSONAL INFORMATION

Surname, Name: BABUÇCUOĞLU, Yurdaer
Nationality: Turkish (T.C.)
Date and Place of Birth: 2 March 1980, Çankırı
Marital Status: Married
Phone: +90 542 532 95 79
e-mail: yurdaer@hotmail.com.tr

EDUCATION

Degree	Institution	Year of Graduation
MS	METU – Chemical Engineering	2007
BS	Anadolu Uni. – Business Administration	2010
BS	Gazi Uni. – Chemical Engineering	2004
High School	Gazi Anatolian High School, Ankara	1998

WORK EXPERIENCE

Year	Place	Enrollment
2005-Present	Maden Tetkik ve Arama Genel Md.	Chemical Engineer
2002 June	Petkim	Intern.Engineering Stdnt.
2001 June	Petkim	Intern.Engineering Stdnt.

FOREIGN LANGUAGES: English

ORAL PRESENTATIONS

1. Babuçcuoğlu, Y., Akgün, A.M., Demirtaş, G., and Yüksel, B., "Türkiye ve Dünya Maden Aramacılığında MTA Analiz Laboratuvarlarının Yeri ve Önemi", VI. Geochemistry Symposium, Mersin Turkey, 2014.
2. Akgün, A.M., Babuçcuoğlu, Y., Babuçcuoğlu, A., and Arslan, Y., "Burdur Gölü Toprak Yapısının Kaplıca Toprakları ile Element İçeriği Açısından Benzerliği", XIII. National Spectroscopy Congress, Burdur Turkey, 2013.
3. Babuçcuoğlu, Y., and Akgün, A.M., "Jeokimyasal Aramalarda Analiz Yöntemleri", I. Symposium of Geosciences, Isparta Turkey, 2012.
4. Babuçcuoğlu, Y., and Akgün, A.M., "Dünyada ve Türkiye'de Jeokimyasal Analiz Çalışmaları", ES-AN 2012, Trabzon Turkey, 2012.

POSTER PRESENTATIONS

1. Bahadır Coşkun, A., Babuçcuoğlu, A., Akgün, A.M., and Babuçcuoğlu, Y., "Investigation of Mineralogical Matrix Effect on XRF Analysis of Geological Samples", 6th Black Sea Basin Conference on Analytical Chemistry, Trabzon Turkey, 2013.
2. Akgün, A.M., Kaplan, E., Babuçcuoğlu, Y., Arslan, Y., and Kendüzler, E., "Determination of Some Heavy Metals in Soil Samples", VIII. Aegean Analytical Chemistry Days, İzmir Turkey, 2012.
3. Akgün, A.M., Babuçcuoğlu, Y., Babuçcuoğlu, A., and Arslan, Y., "Jeokimyasal Örneklerde Çözme Yöntemlerinin Karşılaştırılması", ES-AN 2012, Trabzon Turkey, 2012.
4. Akgün, A.M., Babuçcuoğlu, Y, and Arslan, Y., "Jeokimyasal Analiz Sürecinde Dere Sedimanı Örnekleri içerisindeki Bazı Elementlerin Derişimlerinin Zaman Bağlı Olarak Değişimlerinin ICP-OES Tekniği ile İncelenmesi", XII. National Spectroscopy Congress, Antalya Turkey, 2011.

HOBBIES

Basketball, Movies, Comics, Music